



저작자표시-비영리-변경금지 2.0 대한민국

이용자는 아래의 조건을 따르는 경우에 한하여 자유롭게

- 이 저작물을 복제, 배포, 전송, 전시, 공연 및 방송할 수 있습니다.

다음과 같은 조건을 따라야 합니다:



저작자표시. 귀하는 원저작자를 표시하여야 합니다.



비영리. 귀하는 이 저작물을 영리 목적으로 이용할 수 없습니다.



변경금지. 귀하는 이 저작물을 개작, 변형 또는 가공할 수 없습니다.

- 귀하는, 이 저작물의 재이용이나 배포의 경우, 이 저작물에 적용된 이용허락조건을 명확하게 나타내어야 합니다.
- 저작권자로부터 별도의 허가를 받으면 이러한 조건들은 적용되지 않습니다.

저작권법에 따른 이용자의 권리는 위의 내용에 의하여 영향을 받지 않습니다.

이것은 [이용허락규약\(Legal Code\)](#)을 이해하기 쉽게 요약한 것입니다.

[Disclaimer](#)

Doctoral Thesis

**Studies of Lipophilic Complexes of
Mangan Family (VIIB) Radionuclides**

February 2019

Graduate School of Seoul National University

College of Medicine

Nuclear Medicine

Banka Vinay Kumar

의학박사학위논문

**Studies of Lipophilic Complexes of
Mangan Family (VIIB) Radionuclides**

망간족 방사성 핵종의 친유성착체 연구

2019 년 2 월

서울대학교 대학원
의과대학 핵의학 전공

Banka Vinay Kumar

Studies of Lipophilic Complexes of Mangan Family (VIIB) Radionuclides

(Academic Advisor: Jae Min Jeong, Ph.D.)

Submitting a Doctoral Thesis in Medicine

October 2018

Graduate School of Seoul National University

College of Medicine

Nuclear Medicine

Banka Vinay Kumar

Confirming the Doctoral Thesis Written by

Mr. Banka Vinay Kumar

February 2019

Chair _____ **(Seal)**

Vice Chair _____ **(Seal)**

Examiner _____ **(Seal)**

Examiner _____ **(Seal)**

Examiner _____ **(Seal)**

망간족 방사성 핵종의 친유성착체 연구

지도교수 정재민

이 논문을 의학박사 학위논문으로 제출함

2018 년 10 월

서울대학교 대학원
의과대학 핵의학 전공
Banka Vinay Kumar

Banka Vinay Kumar 의 의학박사 학위논문으로
인준함

2019 년 2 월

위원장	_____	(인)
부위원장	_____	(인)
위원	_____	(인)
위원	_____	(인)
위원	_____	(인)

Abstract

Studies of Lipophilic Complexes of Mangan Family (VIIB) Radionuclides

Banka Vinay Kumar

Department of Nuclear Medicine

College of Medicine

The Graduate School

Seoul National University College of Medicine

Technetium (Tc) and rhenium (Re) belongs to transition metals VIIB group in the period table. Both elements coordinated with ligands to form complex with similar structural geometry due to similar chemical characteristic. Radionuclide ^{99m}Tc utilized for diagnostic, whereas ^{188}Re used for theranostic purposes in the field of nuclear medicine. Furthermore, both radionuclide can be easily produced from generator in high specific activity.

A lipiodol solution of ^{188}Re -4-hexadecyl-2,2,9,9-tetramethyl-4,7-diaza-1,10-decanedithiol (HTDD) has been successfully developed for liver cancer therapy; however, its preparation requires a multi-step synthesis. So we synthesized a new compound, 4-hexadecyl-4,7-diaza-1,10-decanedithioacetate (AHDD), without gem dimethyl groups to address these issues. AHDD and AHTDD was formulated into a

kits. AHDD or AHTDD with acetyl groups is stable in air and easily breaks thiol ester bonds in the labeling step to form rhenium-188-HDD or rhenium-188-AHDD. The AHDD kit was labeled with ^{188}Re was significantly higher efficiency ($98.8 \pm 0.2\%$). After extraction with lipiodol, the overall yield of ^{188}Re -HDD/lipiodol was showing higher as $90.2 \pm 2.6\%$ than that of ^{188}Re -HDD/lipiodol ($p < 0.01$). A comparative biodistribution study of ^{188}Re -HTDD and ^{188}Re -HDD was performed in normal mice after intravenous injection. The lungs were identified as the main uptake site due to capillary-blockage. ^{188}Re -HDD/lipiodol showed a significantly higher lung uptake than that of ^{188}Re -HTDD/lipiodol ($p < 0.05$). Hence concluded, the newly synthesized ^{188}Re -HDD/lipiodol showed improved radiolabeling yield and biodistribution results compared to ^{188}Re -HTDD/lipiodol, and may therefore be more suitable for liver cancer therapy.

Technetium $^{99\text{m}}\text{Tc}$ -Exametazime ($^{99\text{m}}\text{Tc}$ -HMPAO) is currently used as a radiopharmaceutical for determining regional cerebral blood flow imaging by SPECT. The HMPAO ligand exists in two diastereomeric forms: d,l and meso which showed different properties in vivo. In addition, the later studies indicated that brain uptake of $^{99\text{m}}\text{Tc}$ -complexes formed from separated d- and l-enantiomers differed. Separation of enantiomers is difficult by fractional crystallizations method. Usually, the substance is obtained in low chemical yield in a time consuming procedure. Furthermore, the final product still contains some amounts of the meso-form. So we have developed new efficient route for synthesis of R,R-HMPAO and S,S-HMPAO enantiomeric compounds in 6-steps. Nucleophilic substitution ($\text{S}_{\text{N}}2$)

of 2,2-dimethylpropane-1,3-diamine reacting either with (**S**-) **1a** or (**R**-) **1b** Methyl-2-chloropropanoate to produce compound **2a** R,R-isomer or **2b** S,S-isomer derivatives. **2a** or **2b** protected with a Benzylchloroformate (Cbz) followed by multiple steps Weinreb amide and methylation reaction using Grignard reagent, oxime formation with ketone group and finally deprotecting Cbz group through hydrogenolysis which gives S, S-HMPAO (**7a**) or R, R-HMPAO (**7b**). Enantiomeric compounds synthesized with excellent yield, high purity and which does not contain any undesired product such as meso- and diastereomers as compared with other HMPAO routes. R,R HMPAO and S,S HMPAO kits containing 10 μ g SnCl₂·2H₂O concentration was labeled with ^{99m}Tc showing higher radiolabeling efficiency (90%) than other different SnCl₂·2H₂O concentration of HMPAO, also comparatively showing good radiolabeling with commercially available kit

Keywords:

Radionuclide, diagnosis, theranostic, generator, ¹⁸⁸Re, Rhenium, Hepatic Carcinoma, Lipiodol, N₂S₂, AHDD, HDD, HTDD, ^{99m}Tc-d,l-HMPAO, ^{99m}Tc-exametazime, brain SPECT, R, R-HMPAO, S, S-HMPAO, meso-HMPAO

Student number: 2012-31334

Contents

Abstract	i
Contents.....	iv
List of Tables	vii
List of Figures.....	viii
List of Schemes	xi
General introduction.....	1
1-1. General Chemistry of Rhenium and Technetium.....	2
1-2. Diagnostic and Therapeutic Radionuclides.....	3
1-3. Production and Nuclear Properties of Medical Technetium &Rhenium Radionuclides.....	6
Chapter.1: Development of 4-hexa decyl-4,7-diaza-1,10- decanedithiol (HDD) kit for the preparation of the liver cancer therapeutic agent Re-188-HDD/ lipiodol	
2-1. Introduction	9
2-2. Materials and Methods	24
2-2-1 General.....	24
2-2-2 Chemical synthesis	26
2-2-3 Kit formulation.....	30

2-2-4	Radiolabeling.....	31
2-2-5	Biodistribution study.....	33
2-3	Results.....	34
2-3-1	Chemical synthesis.....	34
2-3-2	Radiolabeling.....	35
2-3-3	Biodistribution study	39
2-4	Discussion	45
2-5	Conclusion	48

Chapter.2: New efficient route for synthesis of *R,R*-HMPAO and *S,S*-HMPAO enantiomeric compounds for preparation of Technetium ^{99m}Tc Exametazime

3-1	Introduction	49
3-2	Materials and Methods	57
3-2-1	General	57
3-2-2	Chemical synthesis of <i>S, S</i> HMPAO	58
3-2-3	Chemical synthesis of <i>R, R</i> HMPAO	64
3-2-4	Chemical synthesis of <i>Meso</i> HMPAO	71
3-2-5	Kit formulation.....	74
3-2-6	Radiolabeling.....	76
3-3	Results	78
3-3-1	Chemical synthesis.....	78
3-3-2	Radiolabeling.....	80

3-4 Discussion.....	90
3-5 Conclusion.....	94
References	95
Appendix	109
Spectral data	
¹ H NMR Spectra.....	110
¹³ C NMR Spectra	116
Mass Spectra.....	119
Abstract in Korean	126

List of Tables

Table.1 Therapeutic radionuclide with β –ray emission

Table.2 Diagnostic radionuclide for γ -scintillation camera or SPECT

Table 3. Examples of radioisotopes used for HCC transarterial metabolic radiotherapy.

Table 4. Reported conditions of ^{188}Re -SSS/lipiodol for optimal radiolabeling efficiencies.

Table 5. Reported conditions of Rhenium chelating agents for optimal radiolabeling efficiencies.

Table.6 Radiolabeling efficiency and final yield of AHDD and AHTDD kits.

Table 7. Biodistribution of ^{188}Re -HDD /lipiodol in normal Balb/c male mice at 30 min, 1, 3, and 24 h after injection

Table 8. Biodistribution of ^{188}Re -HTDD /lipiodol in normal Balb/c male mice at 30 min, 1, 3, and 24 h after injection

Table 9. List of radiopharmaceuticals for routine imaging of regional cerebral blood flow

Table 10. Radiolabeling efficiency of $^{99\text{m}}\text{Tc}$ -*R,R* HMPAO and $^{99\text{m}}\text{Tc}$ -*S,S* HMPAO

Table 11. Radiolabeling efficiency of $^{99\text{m}}\text{Tc}$ -*dl* HMPAO and $^{99\text{m}}\text{Tc}$ -*Meso* HMPAO

List of Figures

Figure 1. ^{99}Mo - $^{99\text{m}}\text{Tc}$ and $^{188}\text{W}/^{188}\text{Re}$ transportable generator system

Figure 2. Decay scheme of ^{99}Mo to $^{99\text{m}}\text{Tc}$ production

Figure 3. Decay scheme for ^{188}Re production

Figure 4. Lipiodol- An iodinated and esterified lipid of poppy seed oil

Figure 5. Embolic agents injected through the hepatic artery

Figure 6. Chemical structures of ^{188}Re labeled SSS based bifunctional chelating agent

Figure 7. Chemical structures of ^{188}Re labeled N_2S_2 based bifunctional chelating agents

Figure 8. Rabbits with TAE. **(A)** ROIs were drawn for whole body and tumor in rabbits of each group. **(B)** In CT (top) and SPECT (bottom) images, lipiodol (white arrow) and matching radioactivity (black arrow) were effectively localized and visualized in hepatic tumors.

Figure 9. First human images of ^{188}Re -HTDD/ Lipiodol Therapy

Figure 10. Kit formulation of AHDD and AHTDD precursor

Figure 11. Procedure for the preparation of a lipiodol solution of ^{188}Re -labeled agents

Figure 12. Radiolabeling efficiencies of ^{188}Re -HDD/lipiodol and ^{188}Re -HTDD/lipiodol prepared using the AHDD and AHTDD kits, respectively, were evaluated by ITLC-SG/acetone and ITLC-SG/ saline. Radioactivity was detected by a Radio-TLC scanner. Radio-chromatograms of **(A)** ^{188}Re -HDD from ITLC-

SG/acetone, (B) 188Re-HDD from ITLC-SG/saline, (C) 188Re-HTDD from ITLC-SG/ acetone, and (D) 188Re-HTDD from ITLC-SG/saline

Figure 13. Biodistribution of (A) 188Re-HDD/lipiodol and (B) 188Re-HTDD/lipiodol in normal BALB/c male mice at 0.5, 1, 3, and 24 h after injection.

Figure 14. Biodistribution of 188Re-HDD/lipiodol and 188Re-HTDD/lipiodol in normal BALB/c male mice at (A) 0.5 h (B) 1 h (C) 3 h, and (D) 24 h after post-injection. p values are of comparisons between 188Re-HDD and 188Re-HTDD labeled agents (t test): (***) p < 0.005, (*) p < 0.05, n = 4 at each time point.

Figure 15. Diastereomers of HMPAO

Figure 16. Flow-chart of the d,l-HMPAO purification process

Figure 17. Recrystallization process for R, R HMPAO and S, S HMPAO isomer

Figure 18. Flow-chart of the HMPAO kit formulation process

Figure 19. Radiolabeling TLC conditions of ^{99m}Tc-HMPAO isomers

Figure 20. Radiolabeling efficiencies of ^{99m}Tc-R,R HMPAO with various concentration of SnCl₂·2H₂O solution (0.5-16μg) were evaluated by ITLC-SG/Butanone, ITLC-SG/Saline and Whatman's No-1 paper/ 50% Acetonitrile in water. Radioactivity was detected by a Radio-TLC scanner

Figure 21. Radiolabeling efficiencies of ^{99m}Tc-S,S HMPAO with various concentration of SnCl₂·2H₂O solution (0.5-16μg) were evaluated by ITLC-SG/Butanone, ITLC-SG/Saline and Whatman's No-1 paper/ 50% Acetonitrile in water. Radioactivity was detected by a Radio-TLC scanner

Figure 22. Labeling efficiency of ^{99m}Tc-R,S HMPAO and ^{99m}Tc-S,S HMPAO at various concentration of SnCl₂·2H₂O solution

Figure 23. Radiolabeling efficiencies of ^{99m}Tc -*dl* HMPAO with various concentration of SnCl_2 (1.0-8.0 μg) were evaluated by ITLC-SG/Butanone, ITLC-SG/Saline and Whatman's No-1 paper/ 50% Acetonitrile in water. Radioactivity was detected by a Radio-TLC scanner

Figure 24. Radiolabeling efficiencies of ^{99m}Tc -*Meso* HMPAO with various concentration of $\text{SnCl}_2 \cdot 2\text{H}_2\text{O}$ solution (0.5-8.0 μg) were evaluated by ITLC-SG/Butanone, ITLC-SG/Saline and Whatman's No-1 paper/ 50% Acetonitrile in water. Radioactivity was detected by a Radio-TLC scanner.

Figure 25. Radiolabeling efficiencies of ^{99m}Tc -*dl* HMPAO (Ceretek™) were evaluated by ITLC-SG/Butanone, ITLC-SG/Saline and Whatman's No-1 paper/ 50% Acetonitrile in water. Radioactivity was detected by a Radio-TLC scanner

List of Synthetic Scheme

Scheme 1. Synthesis of N, N'-dibutyloxycarbonyl-bis-(2-hydroxyethyl)-ethylene diamine (**1**); N, N'-di (tert-butoxycarbonyl)-4, 7-diaza-1, 10-decanedithioacetate (**2**); N, N'-4,7-diaza-1,10-decanedithioacetate (**3**); N, N'-4-hexadecyl-4, 7-diaza-1, 10-decanedithioacetate (**4**).

Scheme 2. Radiolabeling synthesis of AHDD and AHTDD with ¹⁸⁸Re.

Scheme 3. Chemical synthesis of *S, S* HMPAO isomer

dimethyl 2,2'-((2,2-dimethylpropane-1,3-diyl)bis(azanediyl))(2*S*,2'*S*)-dipropionate (**2a**); dimethyl 2,2'-(6,6-dimethyl-3,9-dioxo-1,11-diphenyl-2,10-dioxa-4,8-diazaundecane-4,8-diyl)(2*S*,2'*S*)-dipropionate (**3a**); dibenzyl (2,2-dimethylpropane-1,3-diyl)-bis(((*S*)-1-(methoxy-(methyl)-amino)-1-oxopropan-2-yl)-carbamate) (**4a**); dibenzyl (2,2-dimethyl propane-1,3-diyl)-bis(((*S*)-3-oxobutan-2-yl)-carbamate) (**5a**); dibenzyl (2,2-dimethylpropane-1,3-diyl)-bis(((*S,E*)-3-(hydroxyimino)-butan-2-yl)carbamate) (**6a**); (2*E*,2'*E*,3*S*,3'*S*)-3,3'-((2,2-dimethyl-propane-1,3-diyl)-bis-(azanediyl))-bis(butan-2-one) dioxime (**7a**).

Scheme 4. Chemical synthesis of *R, R* HMPAO

dimethyl 2,2'-((2,2-dimethylpropane-1,3-diyl)bis(azanediyl))(2*R*,2'*R*)-dipropionate (**2b**); dimethyl 2,2'-(6,6-dimethyl-3,9-dioxo-1,11-diphenyl-2,10-dioxa-4,8-diazaundecane-4,8-diyl)(2*R*,2'*R*)-dipropionate (**3b**); dibenzyl (2,2-dimethyl

propane-1,3-diyl)-bis(((*R*)-1-(methoxy-(methyl) amino)-1-oxopropan-2-yl)carbamate) (**4b**); dibenzyl (2,2-dimethyl propane-1,3-diyl)-bis(((*R*)-3-oxobutan-2-yl) carbamate) (**5b**); dibenzyl (2,2-dimethylpropane-1,3-diyl)-bis(((*R,E*)-3-(hydroxyimino) butan-2-yl)carbamate) (**6b**); (*2E,2'E,3R,3'R*)-3,3'-((2,2-dimethyl propane-1,3-diyl)-bis(azanediy)) bis(butan-2-one) dioxime (**7b**).

Scheme 5. 4,8-diaza-3,6,6,9-tetra-methylundecane 3,8-diene-2, 10-diene bisoxime (**1**); (*RR, SS*)-4, 8-diaza-3,6,6,9-tetra-methyl-undecane-2, 10-dione bisoxime (*d,l*-HMPAO) (**2**).

Scheme 6. Radiolabeling of *R,R*-HMPAO, *S,S*-HMPAO, *Meso*-HMPAO and *dl*-HMPAO with ^{99m}Tc

1. General introduction

Nuclear medicine is an independent medical specialty that involves administration of radioactive drugs (radiopharmaceuticals) for the purpose of medical imaging and therapy [1]. In terms of nuclear chemistry, the radiopharmaceuticals contain radioactive elements (radionuclides) that emit particular types of nuclear radiation (α , β , γ) over a particular duration of time (half-life) and with a specific energy level and length of body tissue penetration [2]. The potential use of radionuclides in medical diagnostic imaging and therapeutic nuclear medicine has been recognized for many decades [3]. Current research shows that approximately over 10,000 medical facilities worldwide use radionuclides in medical diagnostic imaging and therapy.

Cancerous and benign tumors have received considerable attention due to severity and increasing death rates. Similarly, rhenium (Re) and technetium (Tc) have been researched due to potential therapeutic nuclear medicine application of rhenium radionuclides ^{188}Re and the potential application of technetium radionuclide $^{99\text{m}}\text{Tc}$ in medical diagnostic imaging [6, 7].

Rhenium based radiopharmaceuticals involve both ^{186}Re and ^{188}Re radionuclides and they are both γ and β -emitting agents. Due to their favorable nuclear properties, minimized side effects, and favorable pharmacokinetic and pharmacodynamic properties, they are widely applied in therapeutic nuclear medicine for different disease treatment in which both cancerous and benign tumors are emphasized [8]. In addition, the ^{188}Re radionuclides based radiopharmaceuticals have shown value for a variety of applications in oncology, rheumatology and interventional

radiology/cardiology [8]. Technetium based radiopharmaceuticals involve a ^{99m}Tc radionuclide, which is a γ -emitter and finds applications in nuclear medicine, specifically in medical diagnostic imaging [6]. The use of ^{99m}Tc radionuclide in medical diagnostic imaging began in 1961, with the thyroid being the first imaged organ [6].

1-1. General Chemistry of Rhenium and Technetium

The chemistry of rhenium (Re) and technetium (Tc) are similar to each other. Hence, the chemistry of rhenium can successfully be used for modeling the technetium chemistry and vice versa [9]. Similar physical properties of rhenium and technetium, particularly displaying the same photo-emission energy, are of interest in nuclear medicine. These enable monitoring of biodistribution of radiopharmaceuticals based on these metals using the same γ -ray camera [2, 10]. Another advantage is that the analogous rhenium and technetium radiopharmaceuticals are expected to share the same biodistribution pattern in the patient [2, 11].

Rhenium (Re) and technetium are located in Group VII on the Periodic Table with the atomic numbers 43 (technetium) and 75 (rhenium) and are perhaps the most versatile of all the transition metals [12]. Due to their location in the middle of the d-block of transition metals, they exhibit the properties of both early and later transition metals. Consequently, they display a variety of coordination compounds in all oxidation states from -1 to +7 [12]. Rhenium and technetium compounds in the +2 and +6 oxidation states show instability and consequently, are rare in literature [2, 13]. Rhenium and technetium based radiopharmaceuticals are typically in +5 and +1 oxidation states due to considerable stability [2, 13]. In addition,

technetium and rhenium based radiopharmaceuticals in +1 and +5 oxidation states have shown respectable biodistribution (pharmacokinetics) in medical imaging and therapeutic nuclear medicine compared to other oxidation states [14-16].

1-2. Diagnostic and Therapeutic Radionuclides

Radioisotopes emitting penetrating gamma rays are used for diagnostic (imaging) where the radiation has to escape the body before being detected by a specific device Single-photon emission computed tomography (SPECT). The most common Diagnostic radionuclide for γ -scintillation camera or SPECT are: gallium-67 (^{67}Ga), krypton-81m ($^{81\text{m}}\text{Kr}$), technetium-99m ($^{99\text{m}}\text{Tc}$), indium (^{111}In), iodine-123 (^{123}I), thallium (^{201}Tl) (Table 2).

The potential use of radionuclides in therapy has been recognized for many decades. A number of radionuclides, such as phosphorous-32 (^{32}P), scandium-47, copper-64, copper-67, strontium-89 (^{89}Sr), and yttrium-90 (^{90}Y), rhodium-105 (^{105}Rh), silver-111 (^{111}Ag), tin-117m ($^{117\text{m}}\text{Sn}$), iodine-131 (^{131}I), promethium-149 (^{149}Pm), Samarium-153 (^{153}Sm), holmium-166 (^{166}Ho), lutetium-177 (^{177}Lu), rhenium-186 (^{186}Re), rhenium-188 (^{188}Re) (Table 1) have been used successfully for the treatment of many benign and malignant disorders.

Table.1 Therapeutic radionuclide with β –ray emission

Radionuclide	Decay (days)	Max E_{β} (MeV)	γ -energy (MeV)	Production
^{32}P	14.3	1.71		Nuclear reactor
^{47}Sc	4.4	0.6	0.159 (68%)	Particle accelerator
^{64}Cu	0.5	0.57	0.511 (38%)	Particle accelerator
^{67}Cu	2.6	0.57	0.184 (48%) 0.092 (23%)	Particle accelerator
^{89}Sr	50.5	1.46		Nuclear reactor
^{90}Y	2.7	2.27		^{90}Sr (reactor) \rightarrow ^{90}Y
^{105}Rh	1.5	0.57	0.319 (19%) 0.306 (5%)	Nuclear reactor
^{111}Ag	7.5	1.05	0.342 (6%)	Particle accelerator
$^{117\text{m}}\text{Sn}$	13.6	0.13	0.158 (87%)	Nuclear reactor
^{131}I	8.0	0.81	0.364 (81%)	Nuclear reactor
^{149}Pm	2.2	1.07	0.286 (3%)	Nuclear reactor
^{153}Sm	1.9	0.8	0.103 (29%)	Nuclear reactor
^{166}Ho	1.1	1.6	0.81 (6.3%)	Nuclear reactor
^{177}Lu	6.7	0.50	0.113 (6.4%) 0.208 (11%)	Nuclear reactor
^{186}Re	3.8	1.07	0.137 (9%)	Nuclear reactor
^{188}Re	0.7	2.11	0.155 (15%)	

Table 2. Diagnostic radionuclide for γ -scintillation camera or SPECT

Radionuclide	Half-life	Decay mode	γ -energy (KeV)	Production
^{67}Ga	78.3 h	EC	93, 185, 300	Nuclear reactor
$^{81\text{m}}\text{Kr}$	13 s	IT	190	Particle accelerator
$^{99\text{m}}\text{Tc}$	6.02 h	IT	141	Particle accelerator
^{111}In	67.3 h	EC	173, 247	Particle accelerator
^{123}I	13 h	EC	159	Nuclear reactor
^{201}Tl	73 h	EC	135, 167	$_{90}\text{Sr}$ (reactor) \rightarrow $_{90}\text{Y}$

EC: Electron capture; **IT:** Isomeric transition

1-3. Production and Nuclear Properties of Medical Technetium and Rhenium Radionuclides

Both are generate produced radionuclides, which makes it more readily and economically available than the other radioisotopes. Similarly to Tc-99m, the radionuclide Re-188 is produced in high-specific activity through the generator system (Figure 1)

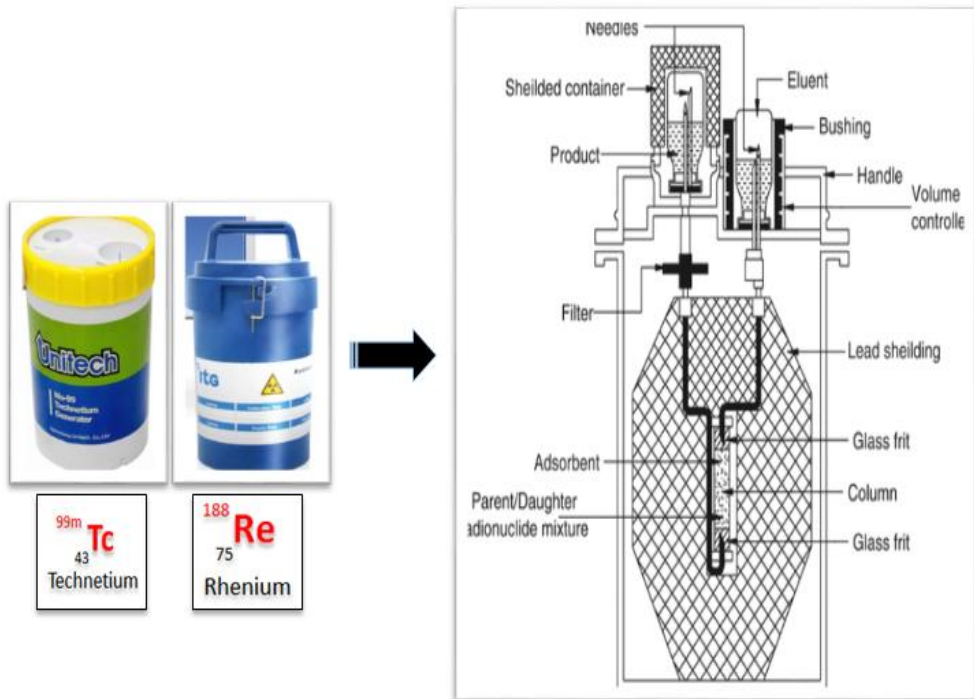


Figure 1. ^{99}Mo - $^{99\text{m}}\text{Tc}$ and $^{188}\text{W}/^{188}\text{Re}$ transportable generator system

Technetium radionuclide ^{99m}Tc is then produced from a molybdenum radionuclide (^{99}Mo) [25]. During that process, the long half-life of ^{99}Mo (66 hours) in the form of a molybdate ion, $^{99}\text{MoO}_4^{2-}$, is introduced to the reactor, and the short half-life of ^{99m}Tc (6.02 hours) is progressively produced from the decay of the parent ^{99}Mo and it is formed as pertechnetate ion, $^{99m}\text{TcO}_4^-$, with β and γ ray emissions [6, 26]. ^{99m}Tc has 6.02 hours of half-life and emits γ particles of 140.5Kev energy, and its shorter half life is of interest in medical imaging [26] (**Figure 2**). The production of ^{99m}Tc radionuclides occur in the molybdenum-technetium (^{99}Mo - ^{99m}Tc) generator system; it is based on the principle that the short-lived radioactive daughter, ^{99m}Tc , is easily and repeatedly isolated from the long-lived parent radionuclide, ^{99}Mo [26, 27].

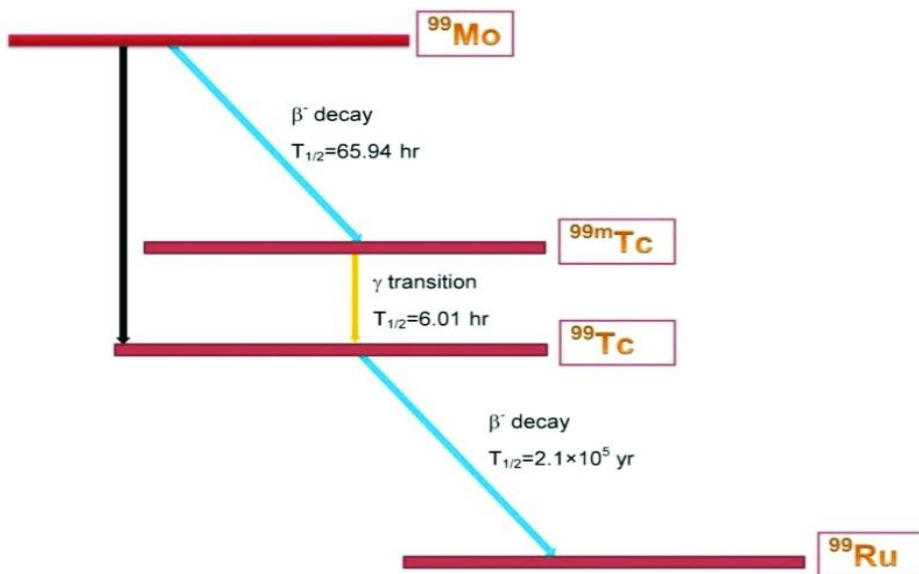


Figure 2. Decay scheme of ^{99}Mo to ^{99}Tc production

^{188}Re radionuclide is obtained in high specific activity from a commercially available tungsten-188 / Rhenium-188 ($^{188}\text{W} / ^{188}\text{Re}$) generator system, and has 17 hours half-life, and emits β particles of 2.12 Mev energy and γ particles of 155 Kev energy (**Figure 3**) [19]. As result, ^{188}Re radionuclide is produced from a generator with the parent radioisotope ^{188}W (W = Tungsten) which originates in a nuclear reactor by double neutron capture of ^{186}W to produce ^{188}W [22]. The production of ^{188}Re radionuclide applies beta (β) decay of ^{188}W radionuclide generator and the reaction has half lif of 69.4 days. The production of ^{188}Re radionuclide is shown in the following nuclear reaction scheme [21]:

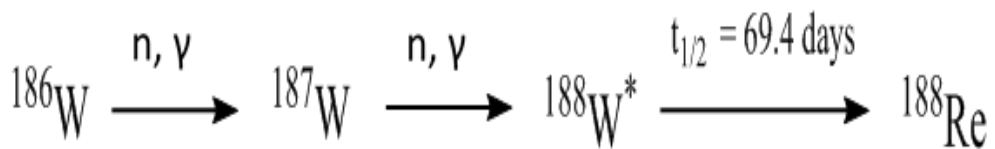


Figure 3. Decay scheme for ^{188}Re production

Chapter.1: Development of 4-hexadecyl-4,7-diaza-1,10-decanedithiol (HDD) kit for the preparation of the liver cancer therapeutic agent Re-188-HDD/ lipiodol

2-1. Introduction

Various radioisotopes have been used for hepato cellular carcinoma (HCC) trans arterial radiotherapy(1-5) (Table 1), among them rhenium-188 (^{188}Re) is most commonly used(6), because ^{188}Re is a high energy β -emitting radioisotope obtained from the $^{188}\text{W}/^{188}\text{Re}$ - generator (**Figure 1, 2**), which has shown utility for a variety of therapeutic applications in nuclear medicine, oncology, and interventional radiology/cardiology(7). ^{188}Re decay is accompanied by a 155 keV predominant energy γ -emission, which could be detected by γ -cameras, for imaging, biodistribution, or absorbed radiation dose studies. It has an attractive physical properties (**Table 3**) and its potential low cost associated with a long-lived parent make it an interesting option for clinical use(6).

The clinical efficacy, for several therapeutic applications, of a variety of ^{188}Re -labeled agents is demonstrated. The high energy of the β -emission of ^{188}Re is particularly well suited for effective penetration in solid tumors. Its total radiation dose delivered to tissues is comparable to other radionuclides used in therapy. Furthermore, radiation safety and shielding requirements are an important subject of matter. In the case of bone metastases treatment, therapeutic ratios are presented in order to describe the efficacy of ^{188}Re usage.

Table 3. Examples of radioisotopes used for HCC transarterial metabolic radiotherapy

Radio elements	Half-life (days)	$E_{\beta\text{-max}}$ (MeV)	Maximum range in tissues (mm)	E_{γ} (KeV)
^{131}I	8.05	6.06	2	364
^{186}Re	3.7	1.7	5	137
^{188}Re	0.7	2.1	10	155
^{90}Y	2.67	2.2	12	None
^{166}Ho	1.1	1.85	8.7	80.6

Lipiodol.

Lipiodol is an iodinated and esterified lipid of poppy seed oil that has been used as a contrast agent for the detection of liver cancer (**Figure 4**) (8-11). When injected through the hepatic artery it accumulates in the liver cancer because of its high viscosity (**Figure 5**). This property of lipiodol has encouraged many researchers to use it as a radioisotope carrier. Other carriers such as microspheres can also be used. However, lipiodol is the most effective and convenient carrier because of its excellent targeting ability as well as its capacity to be accurately monitored by X-ray.



Figure 4. Lipiodol- An iodinated and esterified lipid of poppy seed oil

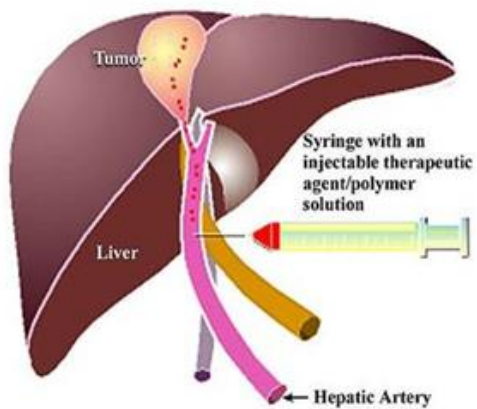


Figure 5. Embolic agents injected through the hepatic artery

There have been many attempts to label lipiodol with therapeutic radioisotopes, including ^{166}Ho , ^{131}I , ^{90}Y , ^{186}Re and ^{188}Re (5-9)

^{131}I -labelled lipiodol is commercially available and is currently used in many countries. However, its high cost and high external radiation dose due to its high energy gamma radiation limits its general use (6, 10-12). Among the metallic beta emitters, ^{188}Re became the most important candidate for labelling lipiodol because of its convenience and economy. Early attempts to label lipiodol with ^{188}Re were not very successful, since ^{188}Re is obtained as an aqueous solution and lipiodol is available as an oil. Direct chemical reaction is precluded because they are not miscible. If a bichelating agent were to be linked with lipiodol in order to facilitate labelling with ^{188}Re , the chemical properties of the resulting conjugate would be changed. In addition, its chemistry would be difficult to characterize since lipiodol is not composed of a single substance.

^{188}Re -DEDC-lipiodol.

Radiolabeling yields (> 95%) have been considerably improved by labeling lipiodol through rhenium(V)-Nitride-bis(diethylthiocarbamate) (DEDC) complex (12). This method involves the reaction of $[\text{}^{188}\text{Re}][\text{ReO}_4]^-$ with N-methyl S-methyl dithiocarbamate (DTCZ), as donor of nitrido nitrogen atoms, sodium oxalate and SnCl_2 to afford a mixture of two intermediate compounds. When this mixture is reacted with the sodium salt of a dithiocarbamate ligand (L) of the type $\text{Na}[\text{R}_2\text{N}-\text{C}(=\text{S})\text{S}]$ ($\text{R} = \text{CH}_3, \text{CH}_3\text{CH}_2, \text{CH}_3\text{CH}_2\text{CH}_2$), the formation of the bis-substituted, neutral complexes $[\text{}^{188}\text{Re}][\text{Re}(\text{N})(\text{L})_2]$ is easily obtained in high yield (> 95%). The $\text{Re}(\text{V})$ nitrido precursor was prepared in high yields using a lyophilized kit

formulation and the resultant complex being highly lipophilic is quantitatively extracted into lipiodol. It was found that the $^{188}\text{Re-N-DEDC-lipiodol}$ was highly stable in physiological solution and in rat's blood. It selectively gets accumulated in the tumor with high target to non-target ratios (13). Furthermore, results of transchelation experiments showed that these compounds were inert toward transchelation by cysteine and glutathione (12).

The results of the initial clinical trials showed that this could be a useful radiopharmaceutical for the therapy of unresectable hepatocellular carcinoma.

$^{188}\text{Re-EDD/Lipiodol}$.

$^{99\text{m}}\text{Tc-ECD}$ (Ethyl cyteinate dimer) is a known brain perfusion imaging agents and it is an approved drug. Ethyl cyteinate dimer (ECD) was labelled with ^{188}Re instead of $^{99\text{m}}\text{Tc}$ and then extracted by Lipiodol to form a new agent $^{188}\text{Re-ECD/Lipiodol}$ (79.77 ± 3.0), and it found to be stable in human serum at 37°C for at least 2 days (**Figure 6**) (14). Radiolabeling conditions of $^{188}\text{Re-ECD/lipiodol}$ were presented in Table 3. $^{188}\text{Re-ECD/Lipiodol}$ showed high accumulation in the hepatoma (1 h: 11.19 ± 4.11 ; 24 h: 7.30 ± 2.20 ; 48 h: 3.55 ± 1.03) was observed in hepatoma-bearing Sprague-Dawley (SD) rats after injection through the hepatic artery.

$^{188}\text{Re(III)-SSS-lipiodol}$.

SSS-lipiodol [SSS = $(\text{S}_2\text{CPh})(\text{S}_3\text{CPh})_2$] is an another N_2S_2 based bifunctional chelating agent developed and labeled with ^{188}Re with a very high radiochemical yields ($87 \pm 9.1\%$) (**Figure 6**), showed a clear advantage over the previously mentioned radiolabeling techniques for ^{188}Re . Radiolabeling conditions of $^{188}\text{Re-}$

SSS lipiodol were presented in **Table 4**. The radiochemical purity ($93 \pm 3.4 \%$), is satisfactory and the radiolabeling is stable for at least 48 h *in-vitro*. ^{188}Re -SSS lipiodol was injected to the hepatic artery of healthy pigs and they were sacrificed at 1, 24 and 48 h post-injection, for *ex-vivo* γ -counting. *Ex-vivo* γ -counting confirmed the predominantly hepatic uptake and revealed weak lung and intestinal uptake. There was very weak urinary elimination ($2.3 \pm 0.5\%$ at 48 h) and a slightly higher level of intestinal elimination ($4.8\% \pm 1.9\%$ at 48 h). The autoradiographic studies showed ^{188}Re -SSS lipiodol to be located mainly in sinu-soids, like ^{131}I -lipiodol. The main difference is represented by very weak urinary elimination and more marked intestinal elimination (15).

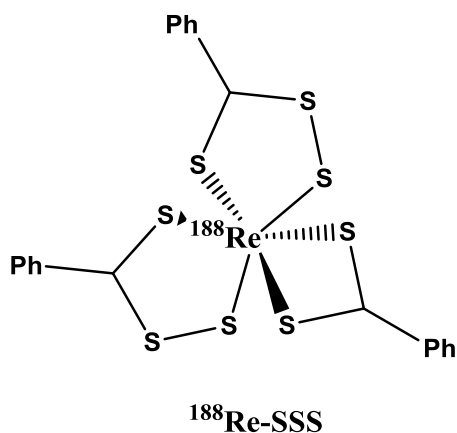


Figure 6. Chemical structures of ^{188}Re labeled SSS based bifunctional chelating agent

A comparative evaluation of ^{188}Re -SSS-lipodol with ^{131}I -lipiodol in rats bearing hepatocarcinoma, was performed. This study shows that, in HCC-bearing rats, treatment by ^{131}I -lipiodol is more effective compared with the ^{188}Re -SSS lipiodol/ ^{131}I -lipiodol mixture or ^{188}Re -SSS lipiodol alone, because it is the only treatment that makes it possible to obtain a prolonged improvement of survival. This study also shows that treatment by ^{188}Re -SSS lipiodol alone is ineffective with the HCC-tumour model used here, which is built up of a single, small tumour (16).

Table 4. Reported conditions of ^{188}Re -SSS/lipiodol for optimal radiolabeling efficiencies

Materials	Conditions
Ligand sodium dithiobenzoate (mg)	20
Sodium gluconate (mg)	30
Ascorbic acid (mg)	40
Potassium oxalate (mg)	0.8
Physiological serum (mL)	0.5
Perrhenate activity (mL)	0.5
RT stirring (min)	15
Heating (°C)/ time (min)	100/30
Final yield (%)	87% ± 9.1
Radiochemical purity (%)	93% ± 3.4
Reference	(15)

However, this may not be extendable to HCC in humans as the tumors are fairly large. The International Atomic Energy Agency (IAEA) conducted a multi-country Phase I/II clinical trial involving 185 patients in eight countries using ^{188}Re -HTDD/Lipiodol in which three complete responses and 19 partial responses were reported (17, 18). The overall results of the clinical studies with ^{188}Re -HTDD/Lipiodol demonstrated that it is a clinically useful agent (17, 18). However, potential liver leakage of activity has been a concern and there are more developments to improve the radiolabeling yields and the *in vivo* stability of the ^{188}Re -SSS lipiodol radiopharmaceutical.

Bifunctional chelating agents for ^{188}Re Labeling.

Several N_2S_2 based bifunctional chelating agents, 2,2,9,9-tetramethyl-4,7-diaza-1,10-decanedithiol (TDD) (8), 4-Octyl-2,2,9,9-tetramethyl-4,7-diaza-1,10-decanedithiol (ODD) (19), 4-Dodecyl-2,2,9,9-tetramethyl-4,7-diaza-1,10-decanedithiol (DDD) (19), 4-hexadecyl-2,2,9,9-tetramethyl-4,7-diaza-1,10-decanedithiol (HTDD) (20), 4-hexadecyl-2,2,9,9-tetramethyl-4,7-diaza-1,10-decanedithioacetate (HTDD-A) (9) and 4-hexadecyl-4,7-diaza-1,10-decanedithiol (HDD) (21), have been developed for ^{188}Re labeling (**Figure 7**).

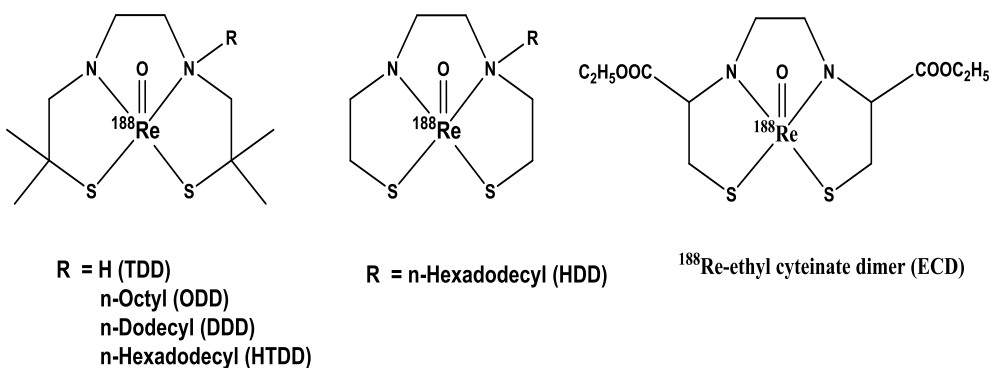


Figure 7. Chemical structures of ^{188}Re labeled N_2S_2 based bifunctional chelating agents

^{188}Re -lipiodol for Hepatic Carcinoma (HCC)

Hepatic carcinoma is a most prevalent cancer worldwide and although most cases still occur in developing countries in South-East Asia and Africa (22) (23) (24) (25). Almost 700,000 new cases are diagnosed yearly throughout the world and unfortunately the prognosis remains poor since more than 500,000 deaths are ascribed to HCC each year (25). Thus the development of therapeutic radiopharmaceuticals for its management if intercepted early, is an active field of radiopharmaceuticals research for many researchers. ^{131}I labelled lipiodol is a commercially available radiopharmaceutical for the treatment of hepatocarcinoma(5, 26-29) (30). Lipiodol or ethiodized oil, contains iodine combined with ethyl esters of fatty acids and is used as a contrast agent in myelography. The inactive iodine of

lipiodol are exchanged with ^{131}I , followed by solvent extraction of the labeled product for preparation of the radiopharmaceutical.

There are several reports describing the preparation of ^{188}Re -lipiodol starting with Kim *et al.* suspending ^{188}Re sulphur colloid in lipiodol (31). A N_2S_2 (diaminedithiol) based chelating agent 2,2,9,9-tetramethyl-4,7-diaza-1,10-decane dithiol(8) (TDD, Figure 6) was synthesized and labeled with technetium ($^{99\text{m}}\text{Tc}$ -TDD) or rhenium (^{188}Re -TDD) in high yields ($72.0 \pm 5.0 \%$), and found to be stable in room temperature and in human serum at 37°C for up to 48 h (19). ^{188}Re -TDD showed high accumulation in the hepatoma (5 min: 33.1 ± 24.1 ; 60 min: 13.5 ± 10.6 ; 24 h: 3.02 ± 2.78) was observed in hepatoma-bearing Sprague-Dawley (SD) rats after injection through the hepatic artery (19). However, ^{188}Re -TDD tumor retention is not enough to treat liver cancer. Therefore a new form of TDD, 4-hexadecyl-2,2,9,9-tetramethyl-4,7-diaza-1,10-decanedithiol (HTDD) (20) was developed to improve tumor retention by introducing a long alkyl chain and it is labeled with ^{188}Re in high yields ($65.0 \pm 7.0 \%$). A comparative study between ^{188}Re -TDD and ^{188}Re -HTDD were performed in VX2 carcinoma (liver) bearing rabbits (**Figure 8**). The residences times of radioactivity in the liver were 10.2 ± 1.0 h in the ^{188}Re -TDD and 17.6 ± 0.8 h in the ^{188}Re -HTDD ($p = 0.034$) (8). A comparative study between ^{188}Re -HTDD and ^{131}I -lipiodol was conducted in patients (Ghent University hospital, Belgium). This study showed that ^{188}Re -HDD/lipiodol yielded smaller cytotoxic effect and a lower radiation exposure for an expected higher tumor-killing effect. Dosimetry-guided transarterial radionuclide therapy with ^{188}Re -HTDD/lipiodol in a patient with unresectable hepatocellular carcinoma was evaluated. This study

showed that transarterial radionuclide therapy with ^{188}Re -HTDD/lipiodol appears to be a safe, effective and promising therapeutic option in cases of unresectable hepatocellular carcinoma with portal vein thrombosis (32, 33). The maximum tolerated activity to be safely injected in the patient was calculated to be about 8.325 GBq (225 mCi) with the lungs being the dose limiting organ. Two doses of the radiopharmaceutical resulted in the complete disappearance of a large volume tumor and the patient was disease free for 18 months. A large scale clinical trial involving 93 patients in India and Vietnam using ^{188}Re -HDD-lipiodol were conducted (34). Similarly, 35 treatments in 28 patients with ^{188}Re -HDD-lipiodol activity ranging from 4.81-7.03 GBq(130-190 mCi) has been reported (35, 36). The studies confirmed that the patients tolerated the dose and no severe complications were reported. Response assessment showed partial response in 1, stable disease in 28 and disease progression in 2 treatments. There was a significant reduction in AFP (An alpha-fetoprotein) levels measured in patients six weeks after treatment. Radiolabeling procedure and radiolabeling conditions of ^{188}Re - N_2S_2 based derivatives were presented in Table 5.

The above mentioned Lipiodol labeled with ^{188}Re via bifunctional chelating agents has been prepared; however it was found that this approach had drawbacks such as low radiolabeling efficiency, low stability and a complicate procedure for preparation (3, 37). ^{188}Re -4-hexa-decyl-2,2,9,9-tetra-methyl-4,7-diaza-1,10-decanedithiol (HTDD)/ lipiodol was later developed to address these limitations; owing to its high labeling yield and simple preparation, ^{188}Re -HTDD/lipiodol was successfully introduced for clinical application (20, 38, 39). Multi-center clinical

application of ^{188}Re -HTDD/lipiodol was initiated by the International Atomic Energy Agency (IAEA) (**Figure 9**) (40-42).

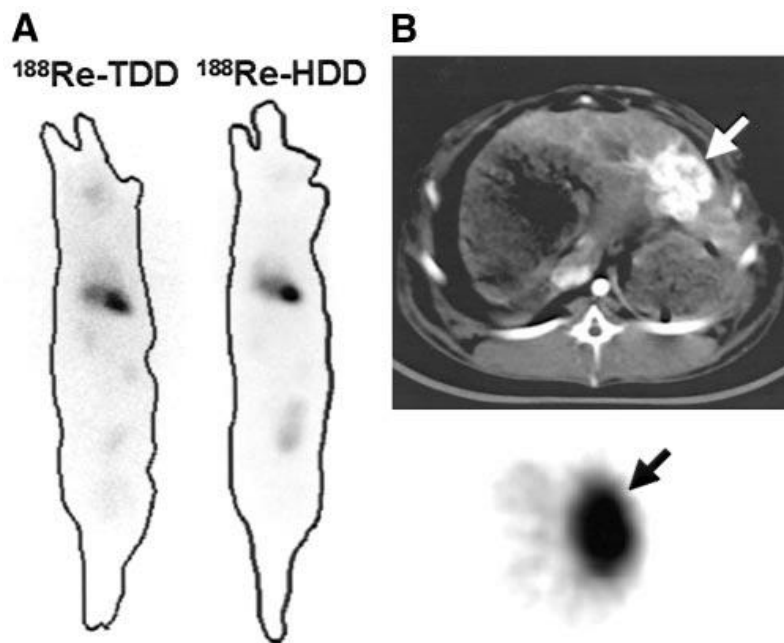


Figure 8. Rabbits with TAE. (A) ROIs were drawn for whole body and tumor in rabbits of each group. (B) In CT (top) and SPECT (bottom) images, lipiodol (white arrow) and matching radioactivity (black arrow) were effectively localized and visualized in hepatic tumors.

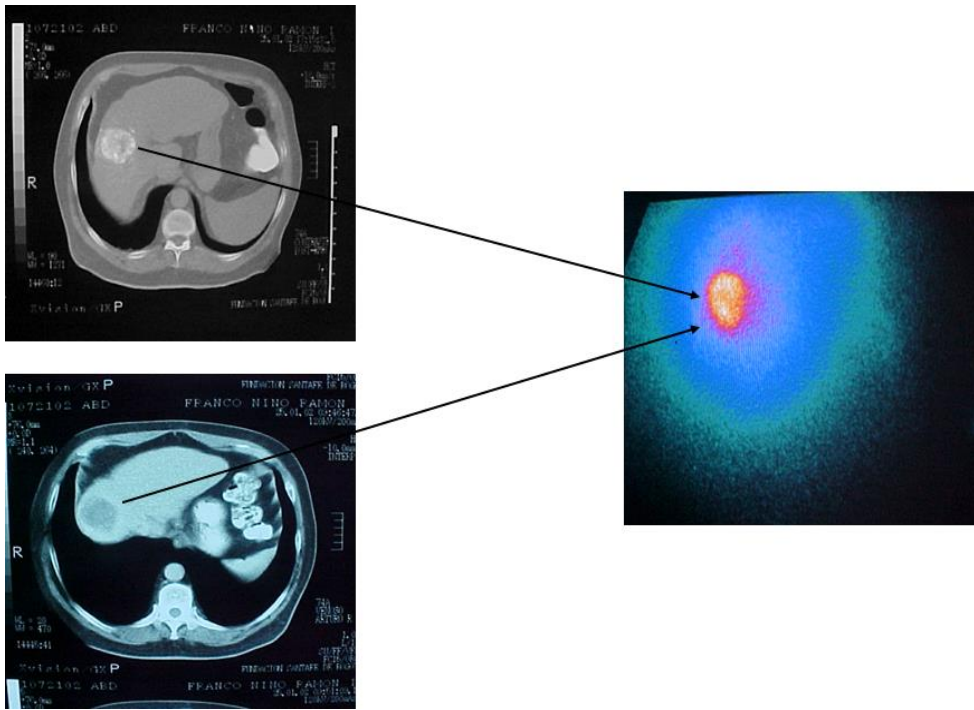


Figure 9. First human images of ^{188}Re -HTDD/ Lipiodol Therapy
Courtesy- Dr Patricia Bernal, Santa fe de Bogota, Bogota, Colombia

Table 5. Reported conditions of Rhenium chelating agents for optimal radiolabeling efficiencies

Conditions	TDD	ODD	DDD	HTDD	HTDD-A	HDD	ECD
Precursor Weight (mg)	1	1	1	1	3	1	1
SnCl ₂ · 2H ₂ O (mg)	10	3	3	10	10	6	15
Tartaric acid (mg)	200	30	30	40	20	20	10
Mannitol (mg)				20	10	10	-
¹⁸⁸ ReO ₄ ⁻ (mL)	3	3	3	3	3	3	1-2
Heating Time (min)	15 ~ 30	60	60	60	60	60	30
Lipiodol (mL)	1-3	3	3	3	3	3	3
Labeling efficiency (%)	88	60-80	60-80	83.4±3.2	60-80	98.8±0.2	79.7
Final yield (%)	72.0±5.0	50-70	50-70	82.1±0.6	50-70	90.2±2.6	
Reference	(8)	(19)	(19)	(9) (43)	(9)	(43)	(14)

To address the major challenges for HTDD kit formulation, namely the instability of sulfhydryl groups and the hygroscopic nature of HTDD, an AHTDD kit, in which the reactive sulfhydryl groups were protected with acetyl groups, has been developed successfully(44).

However, its preparation requires multi-step synthesis and is time consuming; in addition, labeling yield was not very satisfactory. To overcome these problems, we synthesized 4-hexadecyl-4,7-diaza-1,10-decanedithioacetate (AHDD); this compound does not contain gem dimethyl groups, which might lead to a higher labeling yield and an improved biodistribution (**Scheme 1**). In this study, the design, synthesis, and formulation of AHDD kit are presented along with a comparative radiolabeling and Biodistribution studies of ^{188}Re -HDD/liiodol and ^{188}Re -HTDD/liiodol in mice.

2-2. Materials and methods

2-2-1. General

A $^{188}\text{W}/^{188}\text{Re}$ -generator was purchased from Enviro Korea (Daejeon, Korea). ^1H - and ^{13}C -NMR spectra were recorded on a Bruker Avance 600 FT NMR spectrometer (600 MHz for ^1H , 150 MHz for ^{13}C ; Bruker Ltd., Germany). Chemical shifts (δ) were reported in ppm downfield from tetra methyl silane and multiplicities were indicated by s (singlet), d (doublet), t (triplet), m (multiplet), br (broad), and bs (broad singlet). Electrospray ionization positive mode mass spectra (ESI+-MS) were acquired on a Waters ESI ion trap spectrometer (Milford, MA, USA). The samples were diluted 100 times with methanol and directly injected into the injection port. Data were reported in the form of m/z versus intensity. HRMS were acquired on a LTQ-Orbitrap Velos ion trap spectrometer (Thermo Scientific, France). The gamma scintillation counter was a Packard Cobra II (Perkin Elmer, MN, USA). Radio-thin layer chromatography (TLC) was counted using a Bio-Scan AR-2000 System imaging scanner from Bioscan (Washington, DC, USA). Instant TLC-silica gel (ITLCSG) plates were purchased from Varian, Agilent Technologies (Lake Forest City, CA, USA). 1-iodohexadecane was purchased from Tokyo Chemical Industry (Japan). All other chemicals were purchased from Sigma-Aldrich (St. Louis, MO, USA). The animal studies were performed at the Seoul National University Hospital, Seoul, Korea, which is fully accredited by AAALAC International (2007, Association for Assessment and Accreditation of Laboratory Animal Care International). In

addition, the National Research Council guidelines for the care and use of laboratory animals (revised in 1996) were observed throughout.

2-2-2. Chemical synthesis

2-2-2-1. N, N'-dibutyloxycarbonyl-bis-(2-hydroxyethyl)-ethylene diamine (2)

Di-tert-butyl dicarbonate (22.0 g, 0.10mol) and saturated aqueous sodium bicarbonate solution (17.0mL) were slowly and successively added to a stirred solution of N,N'-bis-(2-hydroxyethyl)-ethylene diamine (**1**) (5.0 g, 0.03 mol) in chloroform(125 mL). The mixture was stirred at room temperature for 5 h. After monitoring the reaction by ESI+-MS, the organic layer was separated, washed with water (100 mL × 2), dried over MgSO₄, and evaporated to dryness under reduced pressure. The white crystals obtained were washed with two 50 mL portions of hexane on a filter, recrystallized from ethyl acetate and dried under vacuum to obtain compound **2**. Yield: 10.5 g, 89.3%. ¹H-NMR (CD₃OD, 600 MHz): δ (in ppm) = 1.45 (m, 18H, 2C (CH₃)₃), 3.31-3.32 (m, 4H, NCH₂CH₂N), 3.42 (bs, 4H, 2NCH₂-CH₂O), 3.63 (bs, 4H, 2NCH₂CH₂O). ¹³C-NMR (CD₃OD, 150 MHz): δ (in ppm) = 157.60, 157.51, 81.47, 81.32, 61.42, 61.22, 51.36, 50.88, 47.71, 47.28, 28.90. Mass spectrum (ESI+), m/z = 349.3 [M + H]⁺ observed.

2-2-2-2. N, N'-di (tert-butoxycarbonyl)-4, 7-diaza-1, 10-decane dithioacetate (3)

Triphenylphosphine (PPh₃) (15.508 g, 0.059 mol) was dissolved in dry tetrahydrofuran (THF, 300 mL), and the solution was cooled to 0 °C. Diisopropylazodicarboxylate (DIAD) (12.0 g, 0.059 mol) was added to the solution at 0 °C and stirred for a further 45 min at the same temperature; during this procedure, a precipitate formed. Meanwhile, **2** (4.5 g, 0.01 mol) and thioacetic acid

(4.6 g, 0.06 mol) were dissolved in dry THF (75 mL) and the resulting solution was added to the above suspension dropwise for 5 min. The mixture was stirred at 0 °C for 1 h and then at room temperature for 15 h. The suspension became a clear yellow solution. After monitoring the reaction by TLC (n-hexane: ethyl acetate, 8:2, v/v) and ESI+-MS, the solution was evaporated to dryness under reduced pressure, and the crude product was purified by silica gel column chromatography (n-hexane: ethyl acetate) to obtain compound **3**. Yield: 4.4 g, 73.3%. ¹H-NMR (CDCl₃, 600 MHz): δ (in ppm) = 1.46 (s, 18H, 2C(CH₃)₃), 2.33 (s, 6H, SC(O)CH₃), 2.99-3.03 (m, 4H, CH₂S), 3.34-3.36 (m, 8H, NCH₂). ¹³C-NMR (CDCl₃, 150 MHz): δ (in ppm) = 195.35, 195.01, 155.22, 155.11, 80.13, 79.94, 47.16, 46.27, 45.84, 45.29, 30.60, 28.37, 27.64, 27.24, 27.13. Mass spectrum (ESI+), m/z=465.4 [M+H]⁺ observed.

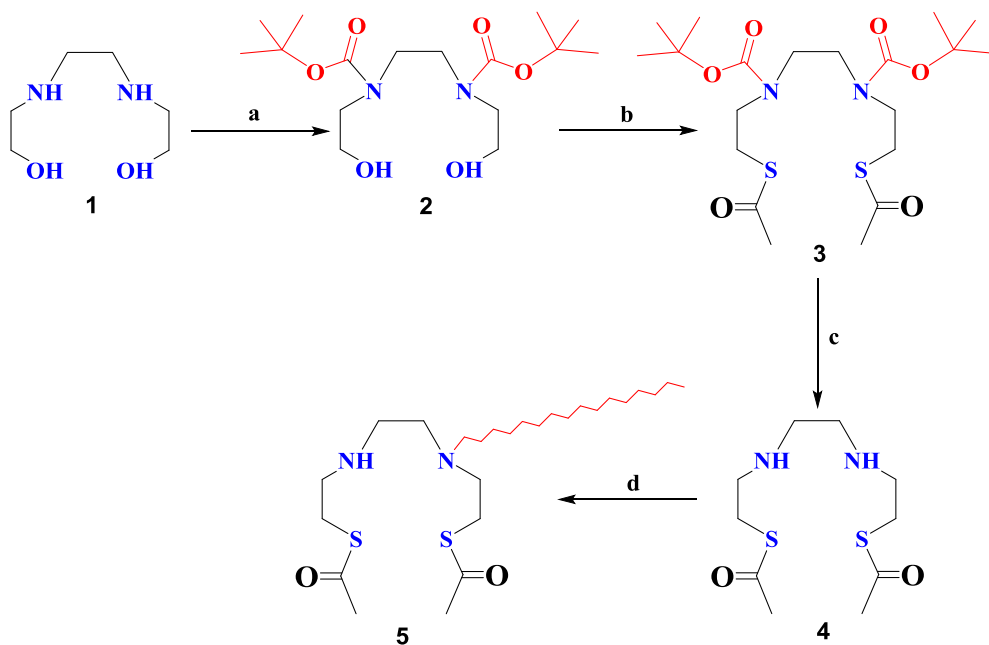
2-2-2-3. N, N'-4,7-diaza-1,10-decanedithioacetate (4)

Anhydrous trifluoroacetic acid (20 mL) was added to a solution of **2** (1.33 g, 2.86 mmol) in 20 mL of dichloromethane with stirring in lot wise (10 and 10 mL) at room temperature for 1 h. After monitoring the reaction by ESI+-MS, the solvent was evaporated under reduced pressure to obtain compound **4**. Yield: 0.61 g, 94.8%. Mass spectrum (ESI+), m/z = 265.3 [M + H]⁺ observed. Proceeded to the next step without purification.

2-2-2-4. N, N'-4-hexadecyl-4, 7-diaza-1, 10-decanedithioacetate (5)

1-Iodohexadecane (1.2 g, 0.003 mol) was added dropwise to a stirred solution of 3 (0.6 g, 0.002 mol) and K₂CO₃ (2.2 g, 0.015 mol) in a mixture of acetonitrile (6 mL) and chloroform (6 mL) in a 2-necked round bottom flask fitted with a condenser, and then stirred at room temperature overnight. The reaction mixture was heated to 50 °C and stirred up to 8 h. The reaction was monitored by TLC and ESI+-MS. The solution was filtered through celite to remove the K₂CO₃ and concentrated under reduced pressure. The resulting crude product was purified over silica gel column chromatography (n-hexane: ethyl acetate, 6:4, v/v) to obtain compound 5. Yield: 0.77 g, 69.7%. ¹H-NMR (CDCl₃, 600 MHz): δ (in ppm) 0.86-0.89 (t, 3H, J = 6.82 Hz CH₃), 1.25 (bs, 30H, -N-(CH₂)₁₅), 1.49-1.55 (m, 8H, NCH₂), 1.97 (s, 6H, SC(O) CH₃), 3.19-3.22 (m, 4H, CH₂S). ¹³C-NMR (CDCl₃, 150 MHz): δ (in ppm) = 169.95, 41.35, 31.92, 29.69, 29.35, 23.38, 22.85, 22.68, 14.11, 11.33. Mass spectrum (ESI+), m/z = 489.3[M + H]⁺ observed, high resolution mass spectrometry (HRMS) [M + H]⁺: observed 489.354, calculated 489.357.

Scheme1. Chemical synthesis of HDD



Reagents and conditions: (a) t-Boc, CHCl_3 , aqueous NaHCO_3 solution, RT 5 h; (b) PPh_3 , THF, DIAD, Thioacetic acid, 0 °C, RT 15 h; (c) CHCl_2 , TFA(1:1), RT stirring, 1 h; (d) 1-iodohexadecane, K_2CO_3 , chloroform-acetonitrile mixture, overnight RT stirring, ~50 °C for 8 h.

2-2-3. Kit formulation

AHDD and AHTDD kits were prepared for radiolabeling with ^{188}Re according to a previously published method (39). The kits were prepared by freeze drying in 10-mL vials containing 1 mg of AHDD or AHTDD, 6mg of $\text{SnCl}_2 \cdot 2\text{H}_2\text{O}$, 20 mg of tartaric acid, and 10 mg of mannitol. The vials were stored in a refrigerator around -30°C until use (**Figure 10**).

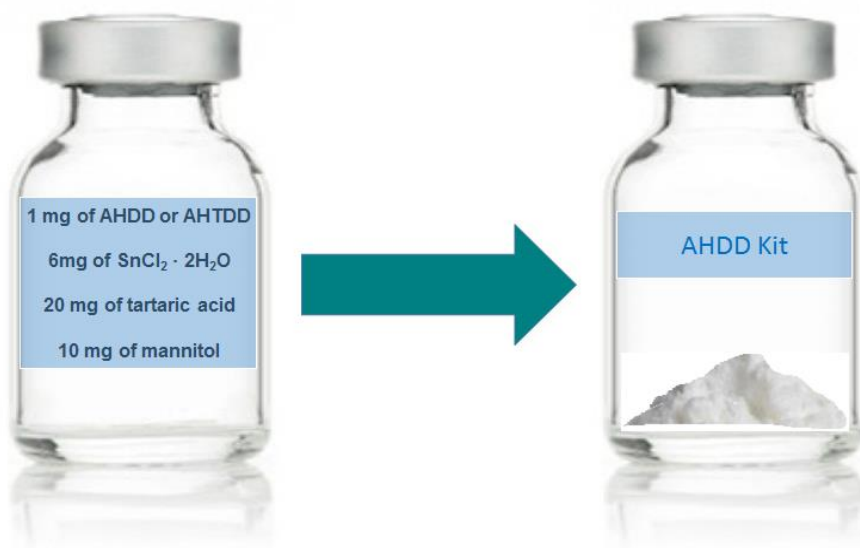


Figure 10. Kit formulation of AHDD and AHTDD precursor

2-2-4. Radiolabeling

^{188}Re -perrhenate was eluted from a $^{188}\text{W}/^{188}\text{Re}$ -generator using normal saline solution according to previously published methods (45, 46). To label the HDD or HTDD, 3.0 mL aliquot of eluted ^{188}Re perrhenate (82 MBq) was added to the AHDD or AHTDD kit (**Scheme 2**). The mixture was shaken vigorously to dissolve the contents. The pH of the solution ranged between 2 and 2.3. The solution was heated in a boiling water bath for 1 h. Lipiodol (3 mL) was added to the solution and thoroughly mixed to extract the radiolabeled ^{188}Re -HDD or ^{188}Re -HTDD into the lipiodol phase. The vial was then centrifuged at 3000 rpm for 10 min to separate the water and lipiodol phase. The lipiodol phase containing lipophilic ^{188}Re -HDD or ^{188}Re -HTDD was carefully collected using a syringe with a long needle (**Figure 11**). The radiochemical purity of the lipiodol extract was evaluated using ITLC-SG (10 × 100 mm) as a stationary phase and normal saline or acetone as a mobile phase.

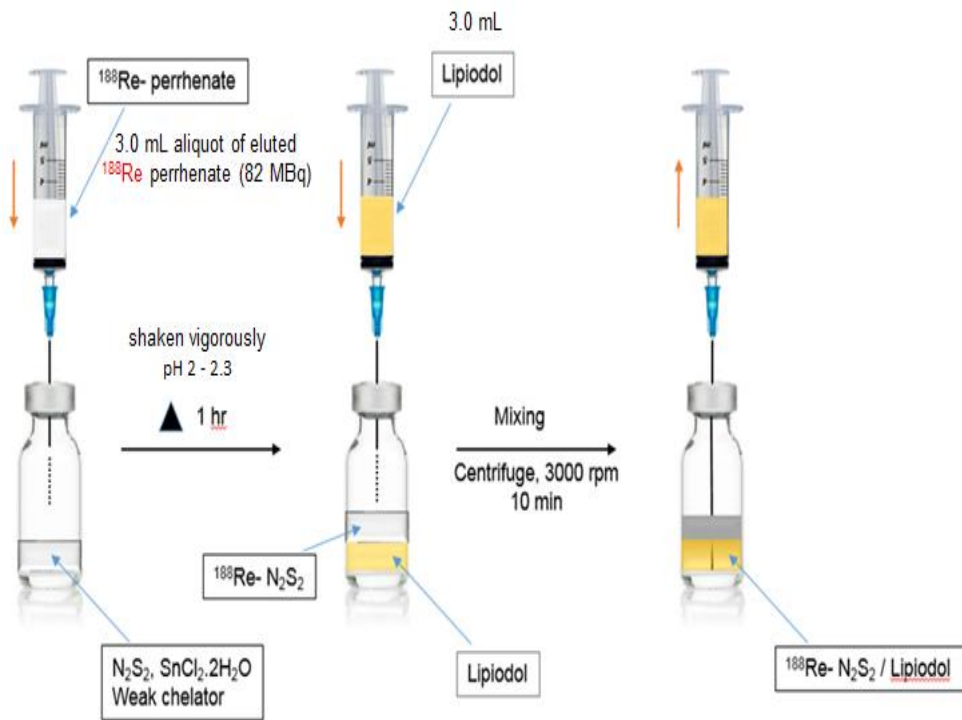


Figure 11. Procedure for the preparation of a lipiodol solution of ^{188}Re -labeled agents

2-2-5. Biodistribution study

All animal experiments were performed with the approval of the Institutional Animal Care and Use Committee of the Biomedical Research Institute at the Seoul National University Hospital which is a facility accredited by the Association for Assessment and Accreditation of Laboratory Animal Care (AAALAC) International. In addition, the National Research Council guidelines for the care and use of laboratory animals (revised in 1996) were observed throughout. For a comparative biodistribution study of lipiodol solutions of $^{188}\text{Re-HDD}$ and $^{188}\text{Re-HTDD}$, the radiolabeled agents (185 kBq/0.03 mL) were injected into normal BALB/c mice (male, 23.1 ± 1.3 g, $n = 4/\text{group}$) through the tail veins. Mice were sacrificed by cervical dislocation after 0.5, 1, 3, and 24 h. Blood and other organs such as the heart, lungs, liver, spleen, intestine, kidneys, and stomach, as well as muscle were rapidly separated and weighed; radioactivity was counted using a gamma scintillation counter. Results were expressed as the percentage of injected dose per gram of tissue (% ID/g). Student's t-test was performed to determine the significance between the lung uptakes of $^{188}\text{Re-HDD/lipiodol}$ and $^{188}\text{Re-HTDD/lipiodol}$.

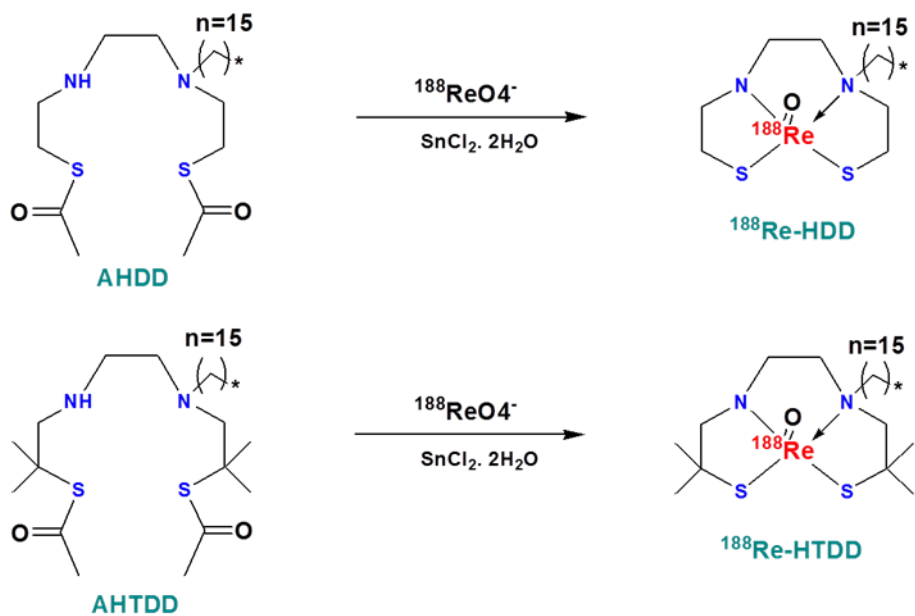
2-3. Results

2-3-1. Chemical synthesis

The cold precursor **5** was synthesized according to the described methods (**Scheme 1**) in four steps. tert- Butyloxycarbonyl protected diamine dialcohol compound (**2**) was prepared from commercially available N,N'-bis-(2-hydroxyethyl)-ethylene diamine (**1**) and Di-tert-butyl dicarbonate. The Boc protected compound **2** was displaced with thioacetates using PPh₃, DIAD, Thioacetic acid by Mitsunobu displacement type reaction to form compound (**3**). Both side deprotection of tert-Butyloxycarbonyl groups with anhydrous trifluoroacetic acid in dichloromethane was carried out to produce diamine-dithiol moiety (**4**); subsequent conjugation with long alkyl chain 1-iodohexadecane in solvent mixture of chloroform-acetonitrile using potassium carbonate as base led to the synthesis of final N₂S₂ chelator (**5**) which can used for complexing with radioactive substance. The crude intermediate **3** and final product **5** were purified by silica gel column chromatography with yields of 73.3 and 69.7%, respectively. All intermediates and the final compound were fully characterized by NMR techniques (¹H, ¹³C), Low resolution and high resolution mass spectroscopy.

2-3-2. Radiolabeling

AHDD and AHTDD kit (containing 1 mg of AHDD or AHTDD, 6mg of $\text{SnCl}_2 \cdot 2\text{H}_2\text{O}$, 20 mg of tartaric acid, and 10 mg of mannitol) were prepared. ^{188}Re -perrhenate was added, heated for 1hr and extracted lipiodol to form ^{188}Re -HDD/lipiodol or ^{188}Re -HTDD/lipiodol (**Scheme 2**). The radiochemical purity of the lipiodol extract was determined using ITLC-SG (10× 100mm) as a stationary phase and normal saline or acetone as a mobile phase. The Rf value of ^{188}Re -HDD/lipiodol was found to be either 1.0 by ITLC-SG/acetone or 0.0 by ITLC-SG/normal saline (**Figure 12**). From these results, AHDD kit was labeled with ^{188}Re with significantly higher efficiency than that of AHTDD kit ($p < 0.01$) (**Table 4**). The overall yield of ^{188}Re -HDD/ lipiodol after extraction with lipiodol also was significantly higher than that of ^{188}Re -HTDD/lipiodol ($p < 0.01$) (**Table 6**).



Scheme 2. Radiolabeling of AHDD and AHTDD with ^{188}Re

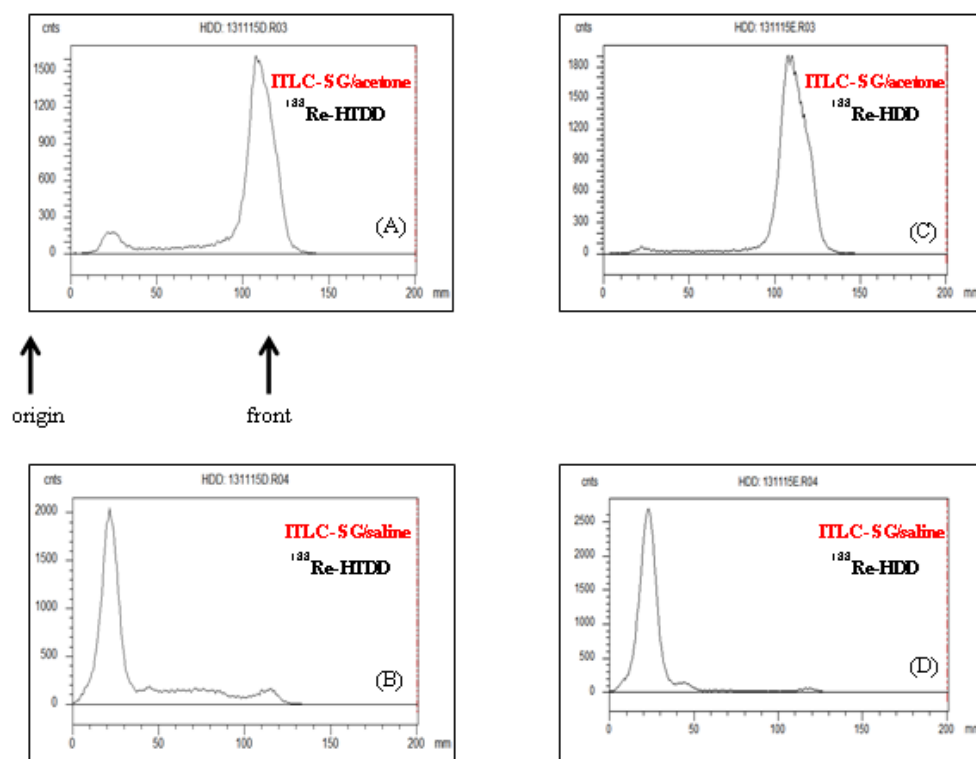


Figure 12. Radiolabeling efficiencies of ^{188}Re -HDD/lipiodol and ^{188}Re -HTDD/lipiodol prepared using the AHDD and AHTDD kits, respectively, were evaluated by ITLC-SG/acetone and ITLC-SG/ saline. Radioactivity was detected by a Radio-TLC scanner. Radio-chromatograms of (A) ^{188}Re -HDD from ITLC-SG/acetone, (B) ^{188}Re -HDD from ITLC-SG/saline, (C) ^{188}Re -HTDD from ITLC-SG/acetone, and (D) ^{188}Re -HTDD from ITLC-SG/saline.

Table 6. Radiolabeling efficiency and final yield of AHDD and AHTDD kits

Precursor	Labeling efficiency (%)	Final Yield (%)
AHDD	98.8 ±0.2	90.2 ±2.6
AHTDD	83.4 ±3.2	82.1 ±0.6

The values represents mean ± standard deviation (n = 4).

Statistical analysis was performed by using Student's t-test.

2-3-3. Biodistribution study

The comparative biodistribution data of lipiodol solutions of ^{188}Re -HDD and ^{188}Re -HTDD at 0.5, 1, 3, and 24 h were obtained using normal BALB/c male mice (n = 4/group) after intravenous injection of each radiolabeled agent (185 kBq/0.03 mL) (Table 7, 8; Figure 13, 14). The lungs showed the highest uptake in both the ^{188}Re -HDD and ^{188}Re -HTDD among the organs evaluated due to capillary embolism (Figure 13). In all studied cases and at all investigated time points, ^{188}Re -HDD/lipiodol showed a significantly higher lung uptake than ^{188}Re -HTDD/lipiodol ((p < 0.05): 230.87 ± 13.45 vs. $187.18 \pm 23.7\%$ ID/g at 0.5, 254.41 ± 27.68 vs. $166.83 \pm 38.57\%$ ID/g at 1 h, 217.50 ± 46.29 vs. $133.39 \pm 36.03\%$ ID/g at 3 h, and 128.96 ± 20.14 vs. 84.71% ID/g at 24 h) (Figure 14). Stomach tissue showed the second highest uptake; moreover, ^{188}Re -HTDD/lipiodol showed a significantly higher uptake than ^{188}Re -HDD/ lipiodol at all time points ((p < 0.05): 25.10 ± 4.85 vs. $10.73 \pm 2.37\%$ ID/g at 0.5, 35.36 ± 13.45 vs. $16.45 \pm 3.86\%$ ID/g at 1 h, 29.73 ± 3.24 vs. $18.69 \pm 6.20\%$ ID/g at 3 h, 3.60 vs. $4.25 \pm 1.49\%$ ID/g at 24 h) (Figure 14), which indicated the higher in vivo stability of ^{188}Re -HDD/lipiodol. In addition, ^{188}Re -HTDD/lipiodol showed higher liver uptakes than ^{188}Re -HDD/lipiodol at 0.5, 1 and 3 h ((p < 0.05): 15.79 ± 1.23 vs. $11.80 \pm 1.66\%$ ID/g at 0.5, 15.57 ± 0.89 vs. $14.36 \pm 1.11\%$ ID/g at 1 h, 17.76 ± 3.14 vs. $12.70 \pm 1.72\%$ ID/g at 3 h) (Figure 14). For both agents, intestinal uptake gradually increased with time (5.42 ± 0.27 vs. $3.13 \pm 0.24\%$ ID/g at 0.5, 5.87 ± 0.77 vs. $4.20 \pm 0.37\%$ ID/g at 1 h, 10.18 ± 0.66 vs. $7.00 \pm 1.40\%$ ID/g at 3 h, 10.65 vs. $8.94 \pm 5.56\%$ ID/g at 24 h). This is caused by a slow excretion through the hepatobiliary tract due to the lipophilic nature of the

agents and high solubility in lipiodol. The blood activity of ^{188}Re - HTDD/lipiodol was higher than that of ^{188}Re -HDD/lipiodol at 0.5 h, 1 h and 3 h ($p < 0.05$): 9.36 ± 0.67 vs. $4.59 \pm 0.13\%$ ID/g at 0.5, 7.77 ± 0.36 vs. $5.17 \pm 0.87\%$ ID/g at 1 h, 7.30 ± 0.77 vs. $4.99 \pm 0.61\%$ ID/g at 3 h, 2.46 vs. $2.01 \pm 0.25 \%$ ID/g at 24 h) (**Figure 14**). The other organs showed low uptakes, and no significant differences between the two agents were found.

Table 7: Biodistribution of ¹⁸⁸Re-HDD /lipiodol in normal Balb/c male mice at 30 min, 1, 3, and 24 h after injection

Tissue	30 min	1 hr	3 hr	24 hr
Blood	4.59 ± 0.13	5.17 ± 0.87	4.99 ± 0.61	2.01 ± 0.25
Muscle	1.00 ± 0.09	0.91 ± 0.10	0.89 ± 0.16	0.40 ± 0.08
Heart	10.27 ± 3.23	8.72 ± 2.99	8.82 ± 4.17	3.24 ± 1.61
Lung	230.86 ± 13.45	254.41 ± 27.68	217.50 ± 46.29	128.96 ± 20.14
Liver	11.80 ± 1.66	14.36 ± 1.11	12.70 ± 1.72	9.25 ± 1.17
Spleen	2.82 ± 0.41	4.08 ± 0.97	4.66 ± 1.25	9.49 ± 4.72
Stomach	10.73 ± 2.37	16.45 ± 3.86	18.69 ± 6.20	4.25 ± 1.49
Intestine	3.13 ± 0.24	4.20 ± 0.37	7.00 ± 1.40	8.94 ± 5.56
Kidney	7.9283 ± 1.27	9.45 ± 1.07	9.64 ± 1.85	5.82 ± 1.45

(%ID/g Tissue: mean ± SD)

Table 8: Biodistribution of ¹⁸⁸Re-HTDD /lipiodol in normal Balb/c male mice at 30 min, 1, 3, and 24 h after injection

Tissue	30 min	1 hr	3 hr	24 hr
Blood	9.36 ± 0.67	7.77 ± 0.36	7.30 ± 0.77	2.46
Muscle	1.32 ± 0.23	0.95 ± 0.12	1.08 ± 0.28	0.29
Heart	7.16 ± 2.35	6.66 ± 3.05	8.52 ± 2.59	2.80
Lung	187.18 ± 23.70	166.83 ± 38.57	133.39 ± 36.03	84.71
Liver	15.79 ± 1.23	15.57 ± 0.89	17.76 ± 3.14	7.73
Spleen	4.11 ± 0.33	3.99 ± 0.61	4.03 ± 0.72	3.02
Stomach	25.10 ± 4.85	35.36 ± 13.45	29.73 ± 3.24	3.60
Intestine	5.42 ± 0.27	5.87 ± 0.77	10.18 ± 0.66	10.65
Kidney	9.37 ± 0.90	8.58 ± 0.53	9.18 ± 0.60	4.23

(%ID/g Tissue: mean ± SD)

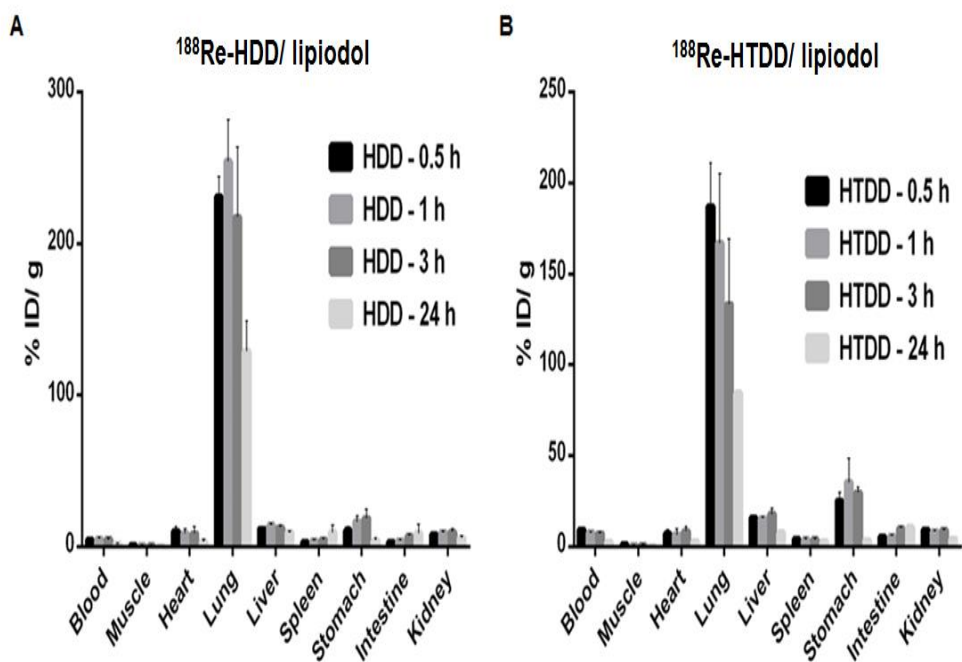


Figure 13. Biodistribution of (A) $^{188}\text{Re-HDD/lipiodol}$ and (B) $^{188}\text{Re-HTDD/lipiodol}$ in normal BALB/c male mice at 0.5, 1, 3, and 24 h after injection.

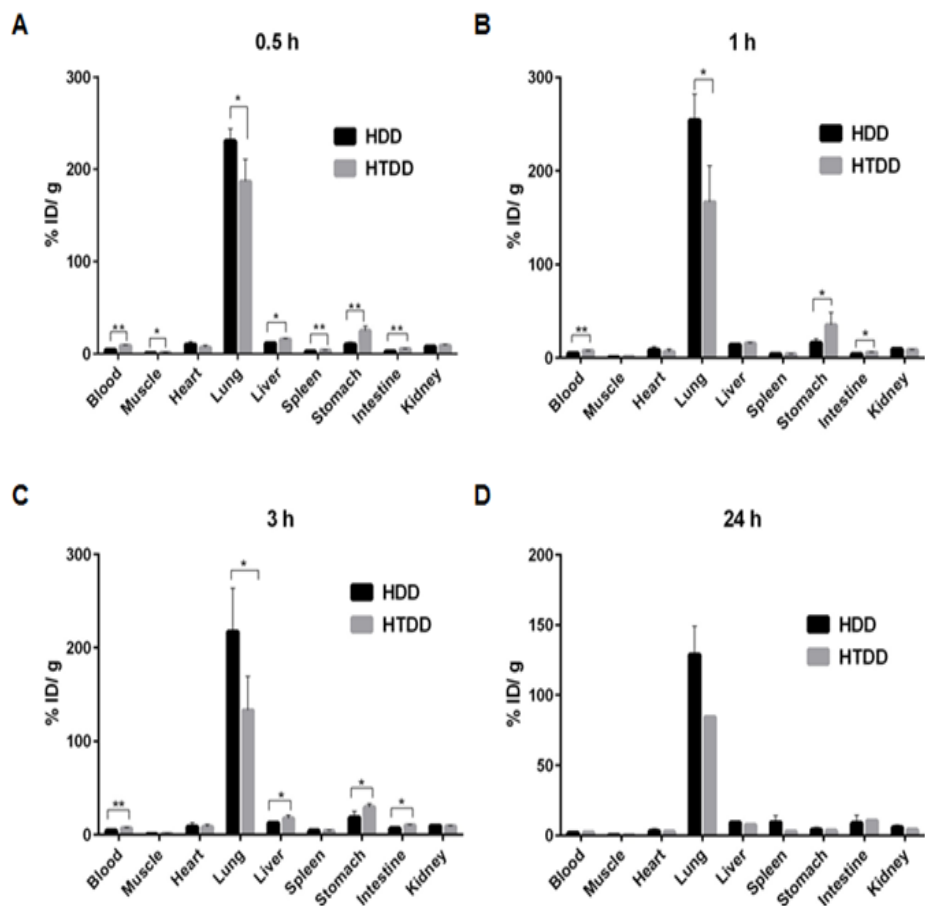


Figure 14. Biodistribution of ^{188}Re -HDD/liiodol and ^{188}Re -HTDD/liiodol in normal BALB/c male mice at (A) 0.5 h (B) 1 h (C) 3 h, and (D) 24 h after post-injection. p values are of comparisons between ^{188}Re -HDD and ^{188}Re -HTDD labeled agents (t test): (**) p < 0.005, (*) p < 0.05, n = 4 at each time point.

2-4. Discussion

^{188}Re -HDD/lipiodol has been employed for the treatment of liver cancer patients. ^{188}Re is a promising candidate for a therapeutic radioisotope. It has appropriate β - and γ -rays for therapy and imaging and an adequate half-life of 17 h. In addition, it is conveniently provided by an in-house generator system. To take advantage of ^{188}Re in TAE, direct labeling of lipiodol was initially tried yet was not easy because of some chemical limitations (11). Because ^{188}Re is obtained in an aqueous form whereas lipiodol is available as an oil form, they are chemically immiscible. In addition, if a bifunctional chelating agent is linked with lipiodol for labeling, the chemical property of the resultant conjugate is altered (11).

Making a solution of ^{188}Re -labeled lipophilic agent with lipiodol is a practical method bypassing direct labeling of lipiodol (8). Nevertheless, in cases of solution form, tumor retention without dissociation and washout is an important concern. This was the actual situation encountered when ^{188}Re -TDD/lipiodol was first developed as a solution form. ^{188}Re -TDD showed high accumulation in the hepatoma was observed in hepatoma-bearing Sprague-Dawley (SD) rats after injection through the hepatic artery (19). However, ^{188}Re -TDD tumor retention is not enough to treat liver cancer.

Therefore a new form of TDD, 4-hexadecyl-2,2,9,9-tetramethyl-4,7-diaza-1,10-decanedithiol (HTDD) (20) was developed to improve tumor retention by introducing a long alkyl chain but, it was found that this approach had drawbacks

such as low radiolabeling efficiency, low stability and a complicate procedure for preparation (3, 37).

^{188}Re -HTDD/lipiodol was later developed to address these limitations; owing to its high labeling yield and simple preparation. ^{188}Re -HTDD/lipiodol was successfully introduced for clinical application (20, 38, 39). Multi-center clinical application of ^{188}Re -HTDD/lipiodol was initiated by the International Atomic Energy Agency (IAEA) (40-42).

However, the HTDD kit formulation is non-trivial due to the reactive nature of its sulfhydryl groups, the main issue being the fast deterioration during the formulation process. To address this, our group has developed AHTDD in 2002 (44). It was prepared through a 9-steps synthesis, bears gem dimethyl groups on both the ethylene bridges between nitrogen and sulfur atoms. Both the sulfhydryl groups were protecting with acetyl groups that could be easily removed by hydrolysis during radiolabeling without additional treatment.

A similar approach was formerly employed for the radiolabeling of Mercapto acetyl glycyglycyglycine (MAG3) with $^{99\text{m}}\text{Tc}$ (47). Benzoyl protected MAG3, which can be easily deprotected during radiolabeling procedure, was used for the kit formulation. However, some difficulties related to the multistep synthesis of the cold compound and low labeling yield remained unsolved.

We therefore developed an approach for a robust synthesis of AHDD, with no gem dimethyl groups and can be synthesized in only four steps (**Scheme 1**). The kit formulation was relatively straightforward as previously reported(44). The radiolabeled ^{188}Re -HDD/lipiodol and ^{188}Re -HTDD/lipiodol were prepared from the

AHDD and AHTDD kit, respectively. The AHDD kit was labeled with ^{188}Re with significantly higher efficiency than that of AHTDD kit ($p < 0.01$) (**Table 1**). The overall yield of ^{188}Re -HDD/ lipiodol after extraction with lipiodol also was significantly higher than that of ^{188}Re -HTDD/lipiodol ($p < 0.01$) (**Figure 12; Table 6**)

The comparative biodistribution study showed, as expected the lungs highest uptake of both lipiodol solutions of ^{188}Re - HDD and ^{188}Re -HTDD agents among the organs evaluated due to capillary embolism (**Figure 13, 14**). At all investigated time point's ^{188}Re -HDD/lipiodol showed a significantly higher lung uptake than ^{188}Re -HTDD/lipiodol. Stomach tissue showed the second highest uptake; moreover, ^{188}Re -HTDD/lipiodol showed a significantly higher uptake than ^{188}Re -HDD/ lipiodol at all time points, which indicated the higher in vivo stability of ^{188}Re -HDD/lipiodol. In addition, ^{188}Re -HTDD/lipiodol showed higher liver uptakes than ^{188}Re -HDD/lipiodol at 0.5, 1 and 3 h. For both agents, intestinal uptake gradually increased with time. This is caused by a slow excretion through the hepatobiliary tract due to the lipophilic nature of the agents and high solubility in lipiodol. The blood activity of ^{188}Re - HTDD/lipiodol was higher than that of ^{188}Re -HDD/lipiodol. The other organs showed low uptakes, and no significant differences between the two agents were found. Therefore, our results showed that ^{188}Re -HDD has more suitable biodistribution properties than ^{188}Re -HTDD/lipiodol for liver cancer therapy.

2-5. Conclusion

In conclusion, we synthesized a new AHDD precursor and formulated a kit for the preparation of ^{188}Re -HDD/lipiodol, which showed improved radiolabeling yield (90.2%) and biodistribution properties for liver cancer therapy compared to the previously reported AHTDD kit.

Chapter.2: New efficient route for synthesis of *R,R*-HMPAO and *S,S*-HMPAO enantiomeric compounds for preparation of Technetium ^{99m}Tc Exametazime

3-1. Introduction

Cerebral blood flow (CBF)

Cerebral blood flow (CBF) is the blood supply to the brain a given period of time.(48) In an adult, CBF is typically 750 millilitres per minute or 15% of the cardiac output equates to an average perfusion 50 to 54 millilitres of blood per 100 grams of brain tissue per minute.(49, 50) CBF is tightly regulated to meet the brain's metabolic demands.(49) Too much blood (a condition known as hyperemia) can raise intracranial pressure (ICP), which can compress and damage delicate brain tissue. Too little blood flow (ischemia) results if blood flow to the brain is below 18 to 20 ml per 100 g per minute, and tissue death occurs if flow dips below 8 to 10 ml per 100 g per minute. In brain tissue, a biochemical cascade known as the ischemic cascade is triggered when the tissue becomes ischemic, potentially resulting in damage to and the death of brain cells.

Functional magnetic resonance imaging (MRI), positron emission tomography (PET) and Single-photon emission computed tomography (SPECT) are neuroimaging techniques that can be used to measure CBF. These techniques are also used to measure regional CBF (rCBF) within a specific brain region.

Over the last decade, several new radiopharmaceuticals have been developed for routine imaging of regional cerebral blood flow using SPECT (**Table 9**) such as

selenium-75-labeled di-(piperidinoethyl) selenide (PIPSE) and di-(morpholinoethyl)selenide (MOSE) (51), 123I-p-iodo-N-isopropylamphet amine (IMP) (52), 123I-N,N-dimethyl-N'-(2-hydroxy-5-iodo-3-methylbenzyl)- 1,3-propanediamine (HIPDM) (53). and thallium-201 (201Tl) diethyldithiocarbamate (DDC) (54) have generated wide interest in possibilities for routine imaging of regional cerebral blood flow (rCBF) using rotating head single photon emission computed tomography (SPECT).

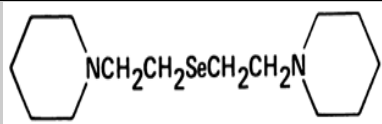
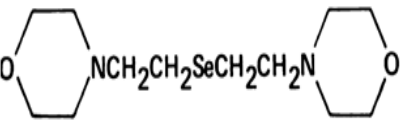
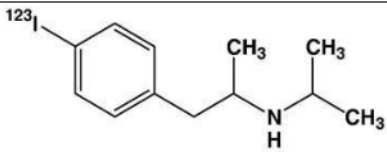
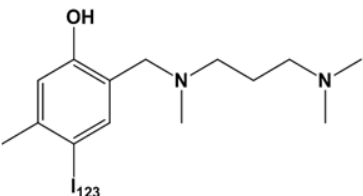
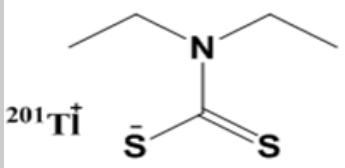
In particular, highly lipophilic radiopharmaceuticals are needed which pass the blood-brain barrier and has been the agent of choice for SPECT studies of rCBF (55).

First a new class of Se-75 labeled diamines that can take advantage of the pH gradient that exists between blood (pH -7.4) and brain (intracellular pH -7.0) has been developed. (51, 56) At high pH these compounds are neutral and lipid soluble and can freely diffuse into cells but at lower pH they become charged and can no longer diffuse out. The minimum concentration gradient is a function of the equilibria established by the local pH shift. Several of these compounds displayed high brain uptake and retention after intravenous injection in rats and monkeys. However, some of the gamma rays of Se-75 (260-410 keV) are too high for gamma camera imaging, and the long physical Half-life ($T_{1/2}$ =120 days) will give high patient radiation dose, both of which limit the clinical application of Se-75 labeled compounds. A more useful agent might be realized by substituting I-123 for the Se-75. Iodine-123 has superior physical properties; a shorter half-life ($T_{1/2}$ = 13.3 h) will

lower the radiation dose to patients, and a better gamma energy (159 keV) is more suitable for imaging with single photon imaging devices (53).

¹²³I-IMP has attracted much attention (57). Winchell (52, 58) developed which has a high extraction rate during the first pass and a constant brain activity between 20 and 60 mm after injection (59). ¹²³I-IMP has been studied intensively (60-65) but the agent is expensive and not readily available, which restricts its clinical use in the study of acute cerebral ischemia. Later developed thallium-201 diethyldithiocarbamate (²⁰¹Tl-DDC), a lipophilic agent which could possibly serve as an alternative to ¹²³I-IMP (54), but it also poor physical characteristics. However none of these radiopharmaceuticals is suitable for routine rCBF studies.

Table 9. List of radiopharmaceuticals for routine imaging of regional cerebral blood flow

Radionuclide	Structure	Chemical name
Selenium-75 (⁷⁵ Se)		Se-75- di-(piperidino ethyl) selenide (PIPSE)
Selenium-75 (⁷⁵ Se)		Se-75- di-(morpholino ethyl)selenide (MOSE)
Iodine-123 (¹²³ I)		123I-p-iodo-N-isopropyl amphetamine (IMP)
Iodine-123 (¹²³ I)		123I-N,N-dimethyl-N'-(2-hydroxy-5-iodo-3-methylbenzyl)- 1,3-propanediamine (HIPDM)
Thallium-201 (²⁰¹ Tl)		Diethyl dithiocarbamate (DDC)

As technetium-99m (^{99m}Tc) has none of these disadvantages. Several investigators have sought to develop new rCBF tracers based upon this radionuclide (66-68). The main biologic requirements for such a radiopharmaceutical are the abilities to cross the intact blood brain barrier (BBB) and to distribute in the brain proportionally to blood flow. Once in the brain, the tracer should retain a fixed regional distribution for a time sufficient to permit image acquisition. For a rotating gamma camera system, this is typically 20-30 min. To cross the BBB, the technetium complex has to be relatively small (<500 Daltons), lipophilic, and possess a net charge of zero. While the new tracers have the required chemical characteristics, and are capable of crossing the BBB, all display rapid efflux from brain tissue (66-68).

A diamine dithiol (DADT) derivative with an amine side chain was reported to provide a ^{99m}Tc -complex with improved brain retention (69). Following the discovery that the ^{99m}Tc -complex of propylene amine oxime (PnAO) is neutral and lipophilic (68) and demonstrates transient flow-related brain uptake in rats (70), dogs (71), and humans (72), a large number of derivatives of PnAO were synthesized at the Amersham International Laboratories.

The aim of this work was to obtain a ligand which not only transported ^{99m}Tc across the BBB, but allowed the radiotracer to be retained with a fixed distribution for a time sufficient to permit SPECT imaging. From that study, the synthesis of the active substance, ligand HMPAO (hexa methyl propylene amineoxime) has been first described by Novotnik et al. (73-78). As elucidated by Neirinckx et al. (75), HMPAO has two chiral centers producing the meso- (R,S), d- (R,R) and l- (S,S) diastereomers (**Figure-15**).

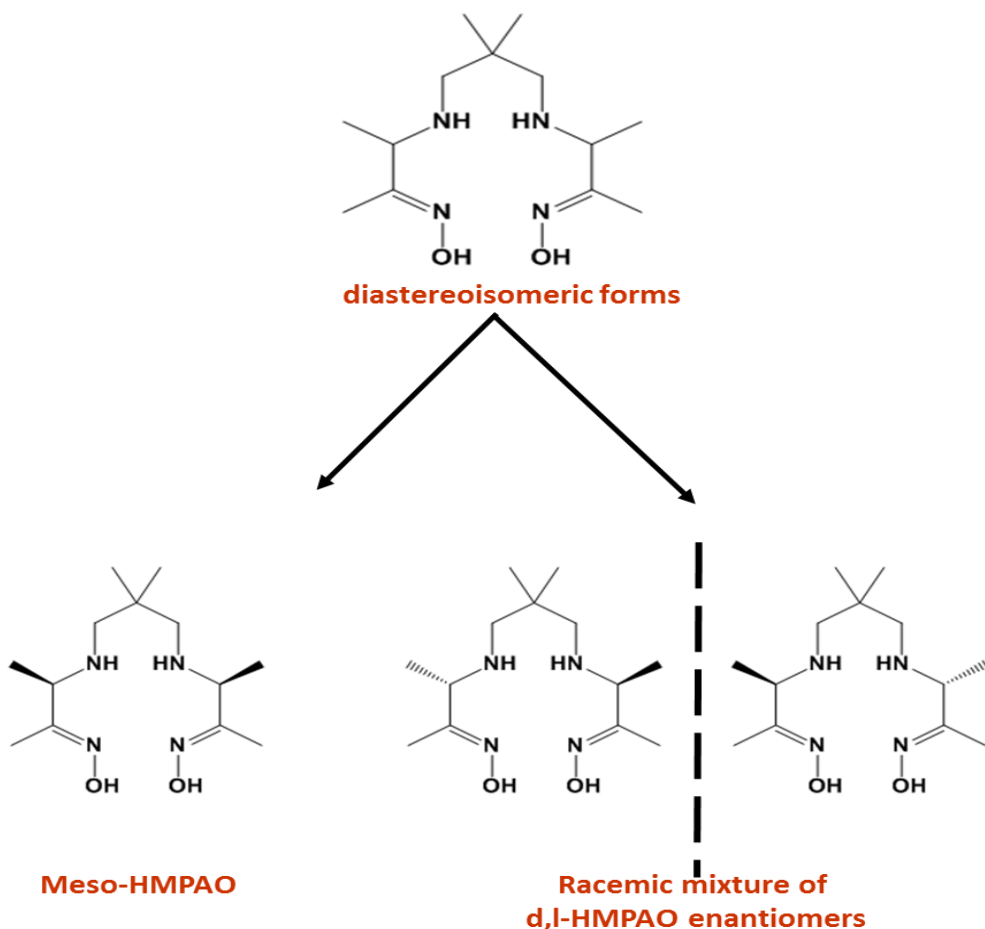


Figure 15. Diastereomers of HMPAO

It was originally confirmed that technetium-99m complexes of these two HMPAO diastereomers (*meso*- and *dl* racemate) showed different properties in vivo both in rats (75) and in humans (79). They rapidly and easily diffused across the blood-brain barrier (BBB) at normal flow rates and had similar brain uptake. However, the *dl*-complex revealed superior brain uptake and retention (4.1% after 8h post injection) compared to the complexes generated from *meso*-isomer (1.7%) and

stereoisomeric mixtures (1.9%) (79). Thus, the *meso*-diastereomer component decreased the radiopharmaceutical concentration in the brain. In addition, the later studies indicated that brain uptake of ^{99m}Tc -complexes formed from separated *d* (*R*)- and *l* (*S*)-enantiomers differed.

The previously various reported procedures for separation of *d*-HMPAO, *l*-HMPAO from mixture of *dl* and *meso* -HMPAO form involved the repeated fractional crystallizations of crude HMPAO from organic solvents (78) (**Figure-16**). This method is very time consuming and affords many fractions of varying crystallinity and diastereomeric composition. Hence, it results in the drastic reduction of the final synthesis yield of both *d*- & *l*-enantiomers and also still containing tracer amount of *meso* -HMPAO (80).

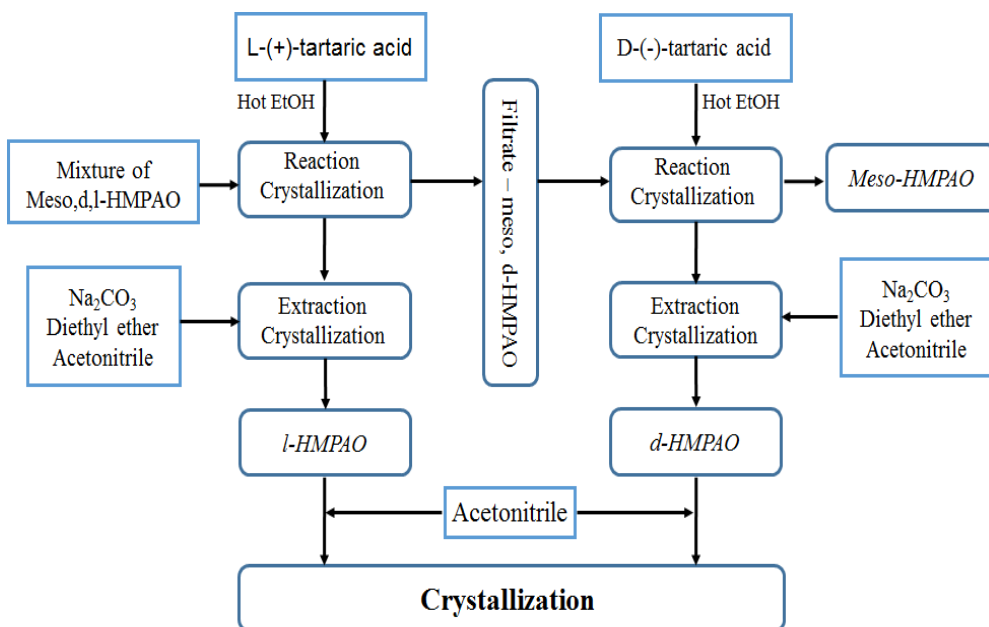


Figure 164. Flow-chart of the d,l-HMPAO purification process

The aim of this study was to develop new efficient route for synthesis of *R,R*-HMPAO and *S,S*-HMPAO enantiomeric compounds, which would provide product with the high yield and high purity. Also formulation, comparative radiolabeling using various stannous chloride concentrations of all isomers with commercially available kits.

3-2. Materials and methods

3-2-1. General

A $^{99}\text{Mo}/^{99\text{m}}\text{Tc}$ Generator was purchased from Enviro Korea (Samyoung Unitech, Korea). ^1H -NMR spectra were recorded on a 500 MHz Avance III (Bruker, German) NMR spectrometer. Chemical shifts (δ) were reported in ppm downfield from tetra methyl silane and multiplicities were indicated by s (singlet), d (doublet), t (triplet), m (multiplet), br (broad), and bs (broad singlet). Low Resolution-MS (LRMS) were acquired on an acquired on a LTQ-Vellos ion trap spectrometer (Thermo Scientific, France). High Resolution-MS (HRMS) were acquired on a LTQ-Orbitrap Velos ion trap spectrometer (Thermo Scientific, France). Electrospray ionization positive mode mass spectra (ESI+-MS). Data were reported in the form of m/z versus intensity. Radio-thin layer chromatography (TLC) was counted using a Bio-Scan AR-2000 System imaging scanner from Bioscan (Washington, DC, USA). Instant TLC-silica gel (ITLCSG) plates were purchased from Varian, Agilent Technologies (Lake Forest City, CA, USA). All chemicals were purchased from Tokyo Chemical Industry (Japan) and Sigma-Aldrich (St. Louis, MO, USA).

3-2-2. Chemical synthesis of *S, S*-HMPAO

3-2-2-1. Dimethyl 2,2'-((2,2-dimethyl propane-1,3-diyl)bis-(azanediyl)) (2*S,2'S*)-dipropionate (**2a**)

Take 50-ml 3-necked round-bottom flask, tightly fitted with a reflux condenser and dropping funnel. Charged 2, 2-dimethylpropane-1,3-diamine 1.38 g (1 eq), acetonitrile 15mL and potassium carbonate 11.2 g (6 eq) . The above mixture of solution was taken to reflux and stirred for 30 min. Meanwhile prepare solution of Methyl (*R*) -2-chloropropanoate **1a** 5.0 g (3 eq) in 15 mL acetonitrile and transferred to dropping funnel. After reaching to reflux, reagent solution was added dropwise with vigorous stirring. After complete addition, the slurry was allowed to stirring under reflux for 66 hours. Reaction mixture was stopped and then cooled to room temperature. solid containing in reaction mixture was removed by filtration using celiate pad and concentrated in vacuo The residue was dissolved in ethyl acetate and extracted with 2 x 50ml of purified water. The organic layer was treated with Magnesium sulfate and then concentrated in vacuo. The resulting dark yellow oil residue was purified by silica gel column chromatography (Dichloromethane: Methanol) affording the title compound **2a** (2.0 g, 54%) as pale yellow oil: ¹H-NMR 500MHz (CDCl₃): δ 3.71 (m, 6H), 3.28 (q, 2H, *J*= 3.0 Hz), 2.43 (d, 2H, *J*= 6.6 Hz), 2.27 (d, 2H, *J*= 6.9 Hz), 1.73 (brs, 2H), 1.29 (s, 3H), 1.27 (s, 3H), 1.27 (s, 3H), 0.89 (s, 6H). High resolution mass spectrometry (HRMS) [M + H]⁺: calculated for C₁₃H₂₇N₂O₄ 275.19; found, 275.19.

3-2-2-2. Dimethyl 2,2'-(6,6-dimethyl-3,9-dioxo-1,11-diphenyl-2, 10-dioxa-4,8-diazaundecane-4,8-diyl) (2*S*,2'*S*)-dipropionate (3a)

2.0 g (1 eq) of dimethyl 2,2'-((2,2-dimethylpropane-1,3-diyl)-bis(azanediyl))- (2*S*,2'*S*)-dipropionate **2a** and 3.68 g (5 eq) of sodium carbonate in 20 ml tetrahydrofuran (THF) and was stirred for 10 minutes at 0°C. 2.37 mL (2.4 eq) of Benzyloxycarbonyl chloride was added dropwise to above mixture for 15 min and stirred at room temperature for 12 h. The reaction mixture was extracted ethyl acetate and purified water. The organic layer was washed 2 times with water, dried with Magnesium sulfate and then concentrated in vacuo. The resulting residue was purified by silica gel column chromatography (Hexane: Ethyl acetate) affording the title compound **3a** (4.85 g, 92%) as transparent viscous oil: ¹H-NMR 500MHz (CDCl₃): δ 7.38-7.27 (m, 10H), 5.21-5.14 (m, 1H), 5.13-5.07 (m, 2H), 5.0 (d, 1H, *J*= 6.0 Hz), 3.83-3.62 (m, 5H), 3.42 (d, 4H, *J*= 9.0 Hz), 3.34-3.06 (m, 3H), 1.62-1.34 (m, 8H), 1.11-0.93 (m, 6H). High resolution mass spectrometry (HRMS) [M + H]⁺: calculated for C₂₉H₃₈N₂O₈ 543.27; found, 543.27. [M + Na]⁺: calculated for C₂₉H₃₈N₂NaO₈ 565.25; found, 565.25.

3-2-2-3. Dibenzyl (2,2-dimethylpropane-1,3-diyl)-bis (((*S*)-1-(methoxy- (methyl)-amino)-1-oxopropan-2-yl)-carbamate) (4a)

Appropriate dimethyl 2,2'-(6,6-dimethyl-3,9-dioxo-1,11-diphenyl-2,10-dioxa-4,8-diazaundecane-4,8-diyl)(2*S*,2'*S*)-dipropionate **3a** (1.0 g, 1 eq) was dissolved in 10mL anhydrous THF in a 50 mL round-bottomed flask and cooled to -20 °C under

nitrogen. The solution was treated with *N,O*-dimethylhydroxylamine hydrochloride (0.71 g, 4 eq) and 7.4 mL (8 eq) isopropylmagnesium chloride (2 M in THF) was then added dropwisely. The resulting mixture was stirred at -20 °C for 2h then quenched with 20 mL satuated ammonium chloride solution and stirred for 30 min. The reaction mixture was extracted with ethyl acetate (3 X 30 mL). The combined organic extracts were washed with brine, dried over sodium sulfate and the solvent was removed *in vacuo*. Purification of the residue took place on a silica-gel column (hexane/ethyl acetate, 3:1) to give the desired Weinreb amide **4a** (0.95 g, 96%) as pale yellow oil: ¹H-NMR 500MHz (CDCl₃): δ 7.33-7.28 (m, 10H), 5.09 (q, 4H, *J*= 9.0 Hz), 4.60-4.42 (m, 2H), 3.72-3.69 (m, 3H), 3.35 (brs, 5H), 3.18-3.05 (m, 8H), 1.58-1.36 (m, 8H), 0.88 (brs, 6H). High resolution mass spectrometry (HRMS) [*M* + Na]⁺: calculated for C₃₁H₄₄N₄NaO₈ 623.30; found, 623.30.

3-2-2-4. Dibenzyl (2,2-dimethyl propane-1,3-diyl)-bis (((*S*)-3-oxobutan-2-yl)-carbamate) (5a)

Dibenzyl (2, 2-dimethyl propane-1, 3-diyl)-bis-(((*S*)-1-(methoxy-(methyl)-amino)-1-oxopropan-2-yl)-carbamate) **4a** (0.95 g, 1 eq) was dissolved in 12 mL anhydrous THF and cooled to -20 °C under nitrogen atmosphere. 12.5mL (20 eq) of Methyl magnesium bromide (3M in diethyl ether) was added slowly at -20 °C. The resulting solution was stirred at -20 °C for 3 h then quenched with 20 mL saturated ammonium chloride solution and stirred for 30 min. The reaction mixture was extracted with ethyl acetate (3 X 30 mL). The combined organic extracts were washed with brine, dried over sodium sulfate and the solvent was removed *in*

vacuum. Purification of the residue took place on a silica-gel column (hexane/ethyl acetate, 6:4) to give the desired product **5a** (0.68 g, 74%) as clear gummy oil: ¹H-NMR 500MHz (CDCl₃): δ 7.38-7.28 (m, 10H), 5.13-5.06 (m, 4H), 3.56-3.13 (m, 6H), 2.22-1.92 (m, 6H), 1.50 (dd, 3H, *J*= 3 & 21 Hz), 1.37 (dd, 3H, *J*=3 & 27 Hz), 1.06 (d, 3H, *J*= 15 Hz), 0.99 (d, 3H, *J*=15Hz). High resolution mass spectrometry (HRMS) [M + H]⁺: calculated for C₂₉H₃₉N₂O₆ 511.28; found, 511.27. [M + Na]⁺: calculated for C₂₉H₃₉N₂NaO₆ 533.26; found, 533.25.

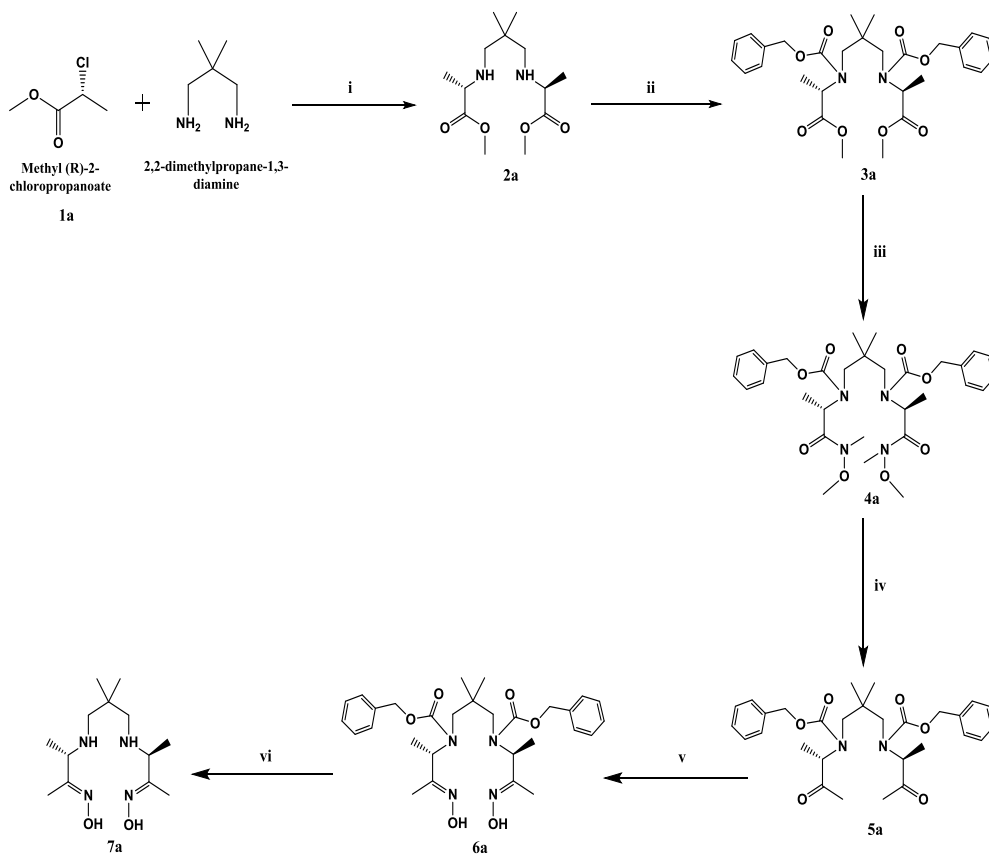
3-2-2-5. Dibenzyl (2,2-dimethylpropane-1,3-diyl)-bis(((*S,E*)-3-(hydroxyimino)-butan-2-yl)carbamate) (6a)

0.427 g of dibenzyl (2,2-dimethyl propane-1,3-diyl)-bis(((*S*)-3-oxobutan-2-yl)-carbamate) **5a** was dissolved in 4 mL ethanol. Added 0.8 g of 50% hydroxyl amine in an aqueous solution and 0.225 g of acetic acid. The reaction was heated to 50 °C and stirred for 5 hours. Cooled to room temperature and concentrated under vacuum to remove the ethanol solvent. Residue was extracted with 3mL purified water and 3 mL EA. The organic layer was washed with 3 mL Purified water, dried on magnesium sulfate and then concentrated in vacuum to give the desired compound **6a** (0.38 g, 81%) as Sticky oil. High resolution mass spectrometry (HRMS) [M + H]⁺: calculated for C₂₉H₄₁N₄O₆ 541.30; found, 541.30. [M + Na]⁺: calculated for C₂₉H₃₉N₂NaO₆ 563.28; found, 563.28.

3-2-2-6. (2*E*,2'*E*,3*S*,3'*S*)-3,3'-((2,2-dimethylpropane-1,3-diyl)-bis-(azanediyl))-bis(butan-2-one) dioxime (7a)

0.38 g of dibenzyl (2,2-dimethylpropane-1,3-diyl)-bis(((*S,E*)-3-(hydroxyimino)-butan-2-yl)carbamate) **6a** was dissolved in 4 mL of methanol and remove air using nitrogen gas ballown. Added 0.165 g of 10% Pd / C and the reaction stirring for 10 h under a hydrogen atmosphere. filtered the reaction solution through celite pad to remove Pd / C and concentrated in vacuum to give yellow oil solid . For recrystalization involved in 2-steps (**Figure 17**).In first step, dissolved that resulting compound in Dichloromethane and stirring under reflux for 2 hours. Slowly cool down to room temperature and stirred for 3 h until more amount of solid obtained. Filtered the solid on whatman filter paper.In secound step, that obtained solid was dissolved in ethyl acetate and stirring under reflux for 2 hours. Slowly cool down to room temperature and stirred for 2 h until more amount of solid obtained. filtered to give white crystalline product **7a** (0.08 g, 77%), m.p: 138-141 °C. ¹H-NMR 300MHz (CD₃OD): δ 3.23 (q, 2H, *J*= 9 Hz), 2.26 (q, 4H, *J*= 12 Hz), 1.77 (s, 6H), 1.17 (d, 6H, *J*= 6 Hz), 0.88 (d, 6H, *J*= 3Hz). High resolution mass spectrometry (HRMS) [M + H]⁺: calculated for C₁₃H₂₈N₄O₂ 273.30; found, 273.30.

Scheme 3. Chemical synthesis of *S, S* HMPAO isomer



Reagents and conditions: (i) 2, 2-dimethylpropane-1,3-diamine, potassium carbonate, acetonitrile, reflux and stirring for 66 h ; (ii) sodium carbonate, tetrahydrofuran, benzyloxycarbonyl chloride, addition at 0°C and stirring at room temperature for 10 h; (iii) anhydrous THF, *N,O*-dimethylhydroxylamine hydrochloride, isopropylmagnesium chloride (2 M in THF), stirred at -20 °C for 2 h; (iv) anhydrous THF, magnesium bromide (3M in diethyl ether), stirred at -20 °C for 3 h; (v) Ethanol, 50% hydroxyl amine solution, acetic acid, stirred for 5 h at 50°C; (vi) Methanol, 10% Pd / C under Hydrogen, stirred for 10 h at room temperature.

3-2-3. Chemical synthesis of *R, R* HMPAO

3-2-3-1. Dimethyl2,2'-((2,2-dimethylpropane-1,3-diyl)bis-(azanediyl)) (*2R,2'R*)-dipropionate (**2b**)

Take 50-ml 3-necked round-bottom flask, tightly fitted with a reflux condenser and dropping funnel. Charged 2, 2-dimethylpropane-1,3-diamine 1.51 g (1 eq), acetonitrile 20 mL and potassium carbonate 12.32 g (6 eq) . The above mixture of solution was taken to reflux and stirred for 30 min. Meanwhile prepare solution of Methyl (*S*) -2-chloropropanoate **1b** 5.5 g (3 eq) in 15 mL acetonitrile and transferred to dropping funnel. After reaching to reflux, reagent solution was added dropwise with vigorous stirring. After complete addition, the slurry was allowed to stirring under reflux for 66 hours. Reaction mixture was stopped and then cooled to room temperature. solid containing in reaction mixture was removed by filtration using celite pad and concentrated in vacuo The residue was dissolved in ethyl acetate and extracted with 2 x 50ml of purified water. The organic layer was treated with Magnesium sulfate and then concentrated in vacuo. The resulting dark yellow oil residue was purified by silica gel column chromatography (Dichloromethane: Methanol) affording the title compound **2b** (2.32 g, 58%) as pale yellow oil: ¹H-NMR 500MHz (CDCl₃): δ 3.71 (m, 6H), 3.28 (q, 2H, *J*= 3.0 Hz), 2.43 (d, 2H, *J*= 6.6 Hz), 2.27 (d, 2H, *J*= 6.9 Hz), 1.73 (brs, 2H), 1.29 (s, 3H), 1.27 (s, 3H), 1.27 (s, 3H), 0.89 (s, 6H). High resolution mass spectrometry (HRMS) [M + H]⁺: calculated for C₁₃H₂₆N₂O₄ 275.19; found, 275.19.

3-2-3-2. Dimethyl 2,2'-(6,6-dimethyl-3,9-dioxo-1,11-diphenyl-2,10-dioxa-4,8-diazaundecane-4,8-diyl) (2*R*,2'*R*)-dipropionate (3b)

2.32 g (1 eq) of dimethyl 2,2'-((2,2-dimethylpropane-1,3-diyl)-bis (azanediyl)) (2*R*,2'*R*)-dipropionate **2b** and 4.5g (5 eq) of sodium carbonate in 20 ml tetrahydrofuran (THF) and was stirred for 10 minutes at 0°C. 2.9 mL (2.4 eq) of Benzyloxycarbonyl chloride was added dropwise to above mixture for 15 min and stirred at room temperature for 12 h. The reaction mixture was extracted ethyl acetate and purified water. The organic layer was wahed 2 times with water, dried with Magnesium sulfate and then concentrated in vacuo. The resulting residue was purified by silica gel column chromatography (Hexane: Ethyl acetate) affording the title compound **3b** (5.2 g, 90%) as transparent viscous oil: ¹H-NMR 500MHz (CDCl₃): δ 7.38-7.27 (m, 10H), 5.21-5.14 (m, 1H), 5.13-5.07 (m, 2H), 5.0 (d, 1H, *J*= 6.0 Hz), 3.83-3.62 (m, 5H), 3.42 (d, 4H, *J*= 9.0 Hz), 3.34-3.06 (m, 3H), 1.62-1.34 (m, 8H), 1.11-0.93 (m, 6H). High resolution mass spectrometry (HRMS) [M + H]⁺: calculated for C₂₉H₃₈N₂O₈ 543.27; found, 543.27. [M + Na]⁺: calculated for C₂₉H₃₈N₂NaO₈ 565.25; found, 565.25.

3-2-3-3. Dibenzyl (2,2-dimethyl propane-1,3-diyl)-bis(((*R*)-1-(methoxy-(methyl) amino)-1-oxopropan-2-yl)carbamate) (4b)

Appropriate dimethyl dimethyl 2,2'-(6,6-dimethyl-3,9-dioxo-1,11-diphenyl-2,10-dioxa-4,8-diazaundecane-4,8-diyl)(2*R*,2'*R*)-dipropionate **3b** (1.2 g, 1 eq) was dissolved in 12 mL anhydrous THF in a 50 mL round-bottomed flask and cooled to

-20°C under nitrogen. The solution was treated with *N,O*-dimethylhydroxylamine hydrochloride (0.852 g, 4 eq) and 8.88 mL (8 eq) isopropylmagnesium chloride (2 M in THF) was then added dropwisely. The resulting mixture was stirred at -20 °C for 2h then quenched with 20 mL satuated ammonium chloride solution and stirred for 30 min. The reaction mixture was extracted with ethyl acetate (3 X 30 mL). The combined organic extracts were washed with brine, dried over sodium sulfate and the solvent was removed *in vacuo*. Purification of the residue took place on a silica-gel column (hexane/ethyl acetate, 3:1) to give the desired Weinreb amide **4b** (1.27 g, 98%) as pale yellow oil: ¹H-NMR 500MHz (CDCl₃): δ 7.33-7.28 (m, 10H), 5.09 (q, 4H, *J*= 9.0 Hz), 4.60-4.42 (m, 2H), 3.72-3.69 (m, 3H), 3.35 (brs, 5H), 3.18-3.05 (m, 8H), 1.58-1.36 (m, 8H), 0.88 (brs, 6H). High resolution mass spectrometry (HRMS) [M + Na]⁺: calculated for C₃₁H₄₄N₄NaO₈ 623.30; found, 623.30.

3-2-3-4. Dibenzyl(2,2-dimethylpropane-1,3-diyl)-bis-(((*R*)-3-oxobutan-2-yl) carbamate) (5b)

dibenzyl (2,2-dimethyl propane-1,3-diyl)-bis-(((*R*)-1-(methoxy-(methyl) amino)-1-oxopropan-2-yl)carbamate) **4b** (1.27 g, 1 eq) was dissolved in 16 mL anhydrous THF and cooled to -20 °C under nitrogen atmosphere. 16.7 mL (20 eq) of Methyl magnesium bromide (3M in diethyl ether) was added slowly at -20 °C. The resulting solution was stirred at -20 °C for 3 h then quenched with 20 mL saturated ammonium chloride solution and stirred for 30 min. The reaction mixture was extracted with ethyl acetate (3 X 30 mL). The combined organic extracts were washed with brine, dried over sodium sulfate and the solvent was removed *in*

vacuum. Purification of the residue took place on a silica-gel column (hexane/ethyl acetate, 6:4) to give the desired product **5b** (0.81 g, 70%) as clear gummy oil: ¹H-NMR 500MHz (CDCl₃): δ 7.38-7.28 (m, 10H), 5.13-5.06 (m, 4H), 3.56-3.13 (m, 6H), 2.22-1.92 (m, 6H), 1.50 (dd, 3H, *J*= 3 & 21 Hz), 1.37 (dd, 3H, *J*=3 & 27 Hz), 1.06 (d, 3H, *J*= 15 Hz), 0.99 (d, 3H, *J*=15Hz). High resolution mass spectrometry (HRMS) [M + H]⁺: calculated for C₂₉H₃₉N₂O₆ 511.28; found, 511.27. [M + Na]⁺: calculated for C₂₉H₃₉N₂NaO₆ 533.26; found, 533.25.

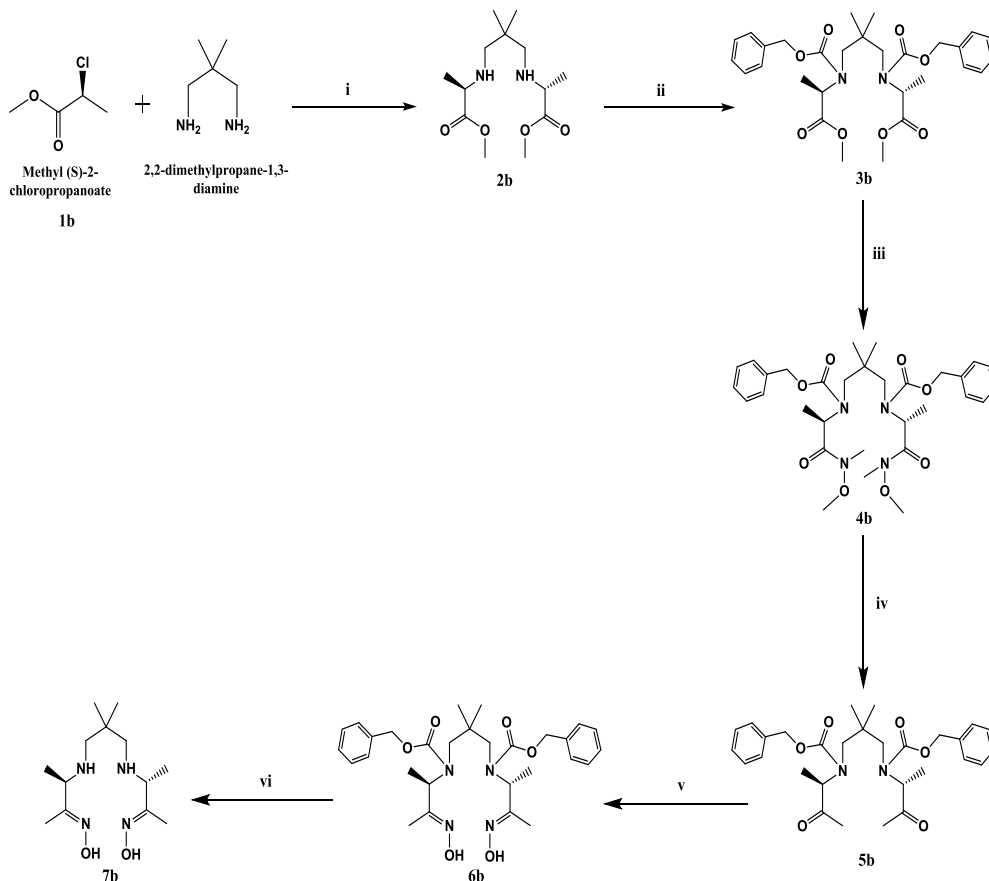
3-2-3-5. Dibenzyl (2,2-dimethylpropane-1,3-diyl)-bis(((*R,E*)-3-(hydroxyimino)butan-2-yl)carbamate) (6b)

0.726 g of dibenzyl (2,2-dimethyl propane-1,3-diyl)-bis(((*R*)-3-oxobutan-2-yl)carbamate) **5b** was dissolved in 6 mL ethanol. Added 1.36 g of 50% hydroxyl amine in an aqueous solution and 0.384 g of acetic acid. The reaction was heated to 50 °C and stirred for 5 hours. Cooled to room temperature and concentrated under vacuum to remove the ethanol solvent. Residue was extracted with 3mL purified water and 3 mL EA. The organic layer was washed with 3 mL Purified water, dried on magnesium sulfate and then concentrated in vacuum to give the desired compound **6b** (0.69 g, 92%) as Sticky oil: High resolution mass spectrometry (HRMS) [M + H]⁺: calculated for C₂₉H₄₁N₄O₆ 541.30; found, 541.30. [M + Na]⁺: calculated for C₂₉H₃₉N₂NaO₆ 563.28; found, 563.28.

3-2-3-6. (2*E*,2'*E*,3*R*,3'*R*)-3,3'-((2,2-dimethylpropane-1,3-diyl)-bis-(azanediyl)) bis(butan-2-one) dioxime (7b)

0.2 g of dibenzyl (2,2-dimethylpropane-1,3-diyl)-bis(((*R,E*)-3-(hydroxyimino)butan-2-yl)carbamate) **6b** was dissolved in 5 mL of methanol and remove air using nitrogen gas ballown. Added 0.12 g of 10% Pd / C and the reaction stirring for 10 h under a hydrogen atmosphere. filtered the reaction solution through celite pad to remove Pd /C and concentrated in vacuum to give yellow oil solid . For recrystalization involved in 2-steps (**Figure 17**).In first step, dissolved that resulting compound in Dichloromethane and stirring under reflux for 2 hours. Slowly cool down to room temperature and stirred for 3 h until more amount of solid obtained. Filtered the solid on whatman filter paper.In secound step, that abtained solid was dissolved in ethyl acetate and stirring under reflux for 2 hours. Slowly cool down to room temperature and stirred for 2 h until more amount of solid obtained. filtered to give white crystalline product **7b** (0.074 g, 80%), m.p: 135-136°C. ¹H-NMR 300MHz (CD₃OD): δ 3.23 (q, 2H, *J*= 9 Hz), 2.26 (q, 4H, *J*= 12 Hz), 1.77 (s, 6H), 1.17 (d, 6H, *J*= 6 Hz), 0.88 (d, 6H, *J*= 3Hz). High resolution mass spectrometry (HRMS) [M + H]⁺: calculated for C₁₃H₂₈N₄O₂ 273.30; found, 273.30.

Scheme 4. Chemical synthesis of *R, R* HMPAO isomer



Reagents and conditions: (i) 2, 2-dimethylpropane-1,3-diamine, potassium carbonate, acetonitrile, reflux and stirring for 66 h ; (ii) sodium carbonate, tetrahydrofuran, benzyloxycarbonyl chloride, addition at 0°C and stirring at room temperature for 10 h; (iii) anhydrous THF, *N,O*-dimethylhydroxylamine hydrochloride, isopropylmagnesium chloride (2 M in THF), stirred at -20 °C for 2 h; (iv) anhydrous THF, magnesium bromide (3M in diethyl ether), stirred at -20 °C for 3 h; (v) Ethanol, 50% hydroxyl amine solution, acetic acid, stirred for 5 h at 50°C; (vi) Methanol, 10% Pd / C under Hydrogen, stirred for 10 h at room temperature.

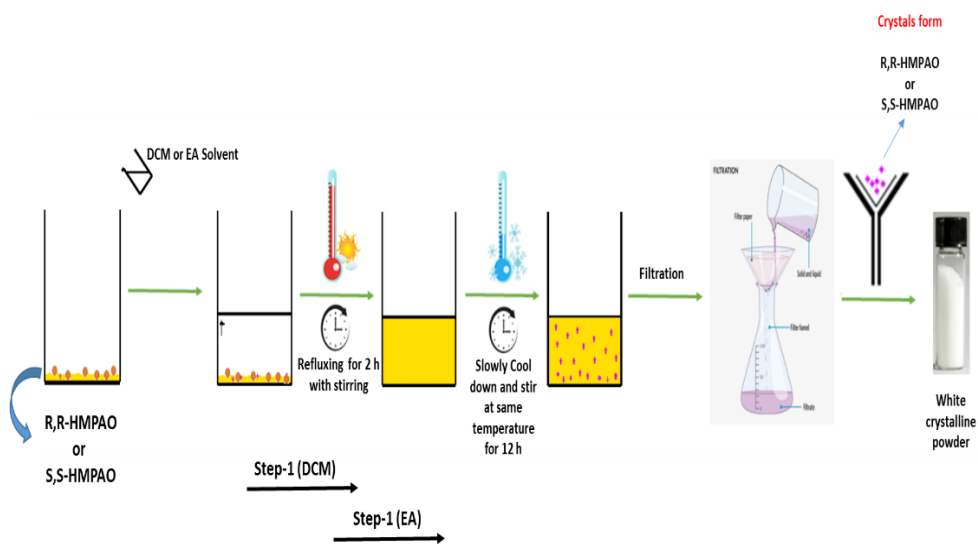


Figure 17. Recrystallization process for R, R HMPAO and S, S HMPAO isomer

3-2-4. *Meso* HMPAO Chemical synthesis

3-2-4-1. 4,8-diaza-3,6,6,9-tetra-methylundecane 3,8-diene-2, 10-diene bisoxime (2c)

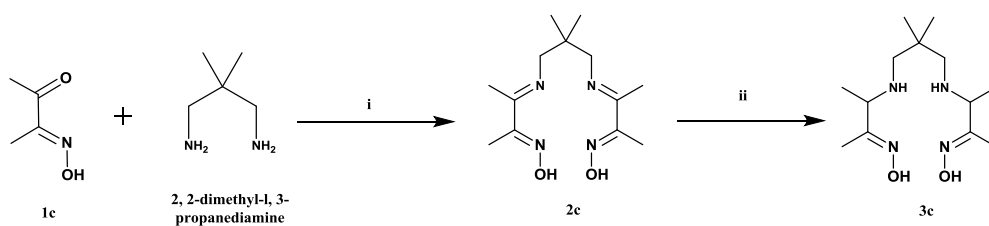
2, 3-Butanedione monoxime **1c** (4.66 g, 46.09 mmol) was dissolved in benzene (20 ml) and the solution was brought to reflux in an apparatus fitted with a Dean and Stark trap, and under a nitrogen atmosphere. To this was added a solution of 2, 2-dimethyl-1, 3-propanediamine (2.0 g, 19.5 mmol) in benzene (40 ml) over a period of 5 hr. The resulting yellow brown solution was refluxed for a further 16 h under nitrogen, then allowed to cool to room temperature. The precipitated solid was removed under suction, and washed with a little cold (-40°C) acetonitrile, giving the product as a white powder. Drying under high vacuum for 2 h gave the **2c** product: 1.38 g (60%). Low resolution mass spectrometry (LRMS) $[M + H]^+$: calculated for $C_{13}H_{25}N_4O_2$ 269.20; found, 269.25.

3-2-4-2. (*RR, SS*)-4, 8-diaza-3,6,6,9-tetra-methyl-undecane-2, 10-dione bisoxime (*dl*-HMPAO) (3c)

The above bis-imine **2c** (1.38 g, 287 mmol) was slurried in 95% aqueous ethanol (13.0 ml) at 0°C. Sodium borohydride (0.195 g, 5.15 mmol) was added in portions over 30 min, and the mixture stirred at 0°C for 2 hr. Water (10 ml) was added and the mixture was stirred well for a further 2 hr. The ethanol was removed and more water (5 ml) was added. The pH was adjusted to 11, and the resulting precipitate was removed by filtration, washed with a little water, dried giving the impure HM-

PAO: 0.65 g (47%). Double recrystallization from acetonitrile provided the diastereoisomeric mixture of HM-PAO free from major impurities: 0.5 g (33%), m.p: 119-122°C. Fractional crystallization from ethyl acetate provided the *dl*-diastereoisomer **3c**, m.p: 125-127°C. ¹H-NMR 300MHz (CD₃OD): δ 3.23 (q, 2H, *J*= 9 Hz), 2.26 (q, 4H, *J*= 12 Hz), 1.77 (s, 6H), 1.17 (d, 6H, *J*= 6 Hz), 0.88 (d, 6H, *J*= 3Hz). Low resolution mass spectrometry (LRMS) [M + H]⁺: calculated for C₁₃H₂₉N₄O₂ 273.23; found, 273.83.

Scheme 5. Chemical synthesis of *Meso*- HMPAO isomer



Reagents and conditions: (i) 2, 3-Butanedione monoxime **1c**, 2, 2-dimethyl-1, 3-propanediamine, benzene, 16 h reflux; (ii) 95% aqueous ethanol, Sodium borohydride, 0°C for 2 h

3-2-5. Kit formulation

R,R-HMPAO, *S,S*-HMPAO, *dl*-HMPAO and *Meso*-HMPAO kits were prepared for radiolabeling with ^{99m}Tc according to a previously published method. The kits were prepared in 10-mL vials containing 0.5 mg of precursor (*R,R*- or *S,S*- or *dl*-, *Meso*-HMPAO), 4.5 mg of sodium chloride (NaCl), various concentration of stannous chloride dihydrate ($\text{SnCl}_2 \cdot 2\text{H}_2\text{O}$) in 0.2N Hydrochloric acid (HCl) solution (16 μg , 12 μg , 10 μg , 8 μg , 4 μg , 2 μg , 1 μg , 0.5 μg) in each vial, 25 μL of 0.1N sodium hydroxide (NaOH) solution to adjust pH (~9.0-10.0). Vortex for 30 seconds to each step addition. The vials were sealed with aluminum cap before radiolabeling **(Figure-18)**.

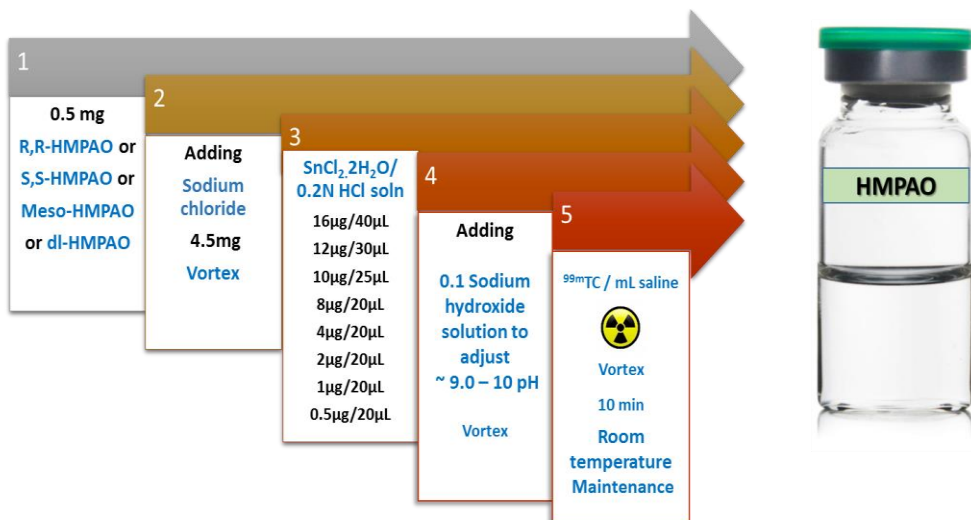


Figure 18. Flow-chart of the HMPAO kit formulation process

3-2-6. Radiolabeling

Sodium pertechnetate (^{99m}Tc) was eluted from $^{99}\text{Mo}/^{99m}\text{Tc}$ generator using normal saline solution. To label the precursor (*R,R*- or *S,S*- or *dl*- or *Meso*-HMPAO), 0.5 mL of ^{99m}Tc ($\sim 2\text{-}4\text{mCi/mL}$) was added into the each vial (**Scheme 6**). The mixture was shaken vigorously using vortex for uniform mixing of solution. The pH of the solution ranged $\sim 9\text{-}10$. The radioactive solution was maintained at room temperature for 10 min. The radiolabeling efficiency was evaluated in three different conditions (**Figure-19**) using ITLC-SG (10×100 mm) and whatman No.1 paper as a stationary phase; Methyl ethyl ketone (MEK), normal saline and 50% acetonitrile in water as a mobile phase.

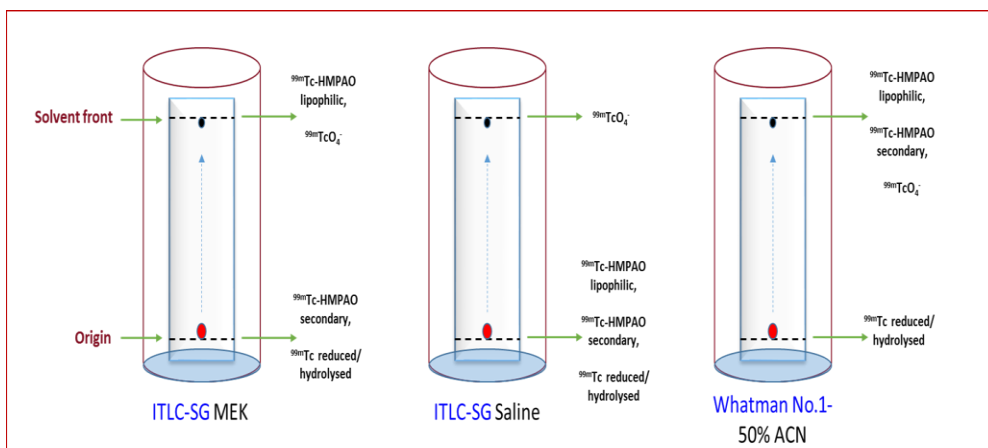


Figure 19. Radiolabeling TLC conditions of ^{99m}Tc -HMPAO isomers

3-3. Results

3-3-1. Chemical synthesis

The cold precursor *S,S*-HMPAO (**7a**) and *R,R*-HMPAO (**7b**) isomers was synthesized in new route 6 steps (**Scheme 3, 4**). New route starting from Nucleophilic substitution (S_N2) of 2,2-dimethylpropane-1,3-diamine reacting either with Methyl (*S*)-2-chloropropanoate (**1a**) or Methyl (*R*)-2-chloropropanoate (**1b**) to produce compound *R,R*-isomer **2a** or *S,S*-isomer **2b**. By reacting the above prepared compound of **2a** or **2b** with an Benzylchloroformate (Cbz), its an amine protecting group to synthesize Cbz protected tertiary amine derivative **3a** or **3b**. So that easy handling of this compound to further steps, due high Retardation Factor (R_F) value.

Compound **3a** or **3b** containing methyl ester group reacting with 2.0 M isopropyl magnesium chloride in THF (*i*-PrMgCl) (Grignard reagent) and N, O-dimethyl hydroxylamine hydrochloride to form weinreb amide derivative of **4a** or **4b**. Nucleophilic methylation of the Grignard reagent (3.0 M Methyl Magnesium chloride in Diethyl ether) on weinreb amide group **4a** or **4b** to give compound **5a** or **5b**. The oxime compound of **6a** or **6b** is produced when ketone group condensed with hydroxylamine hydrochloride (NH_2OH) in presence of acetic acid as catalyst. Finally removing amine protecting group (Cbz group) through hydrogenolysis performed under the metal catalyst 10% palladium/C and Hydrogen gas which gives *S,S*-HMPAO (**7a**) or *R,R*-HMPAO (**7b**) enantiomeric compounds.

Recrystallization process of *S,S*-HMPAO (**7a**) or *R,R*-HMPAO (**7b**) done in two steps (**Figure 17**). Repeated recrystallization of cold precursor in dichloromethane

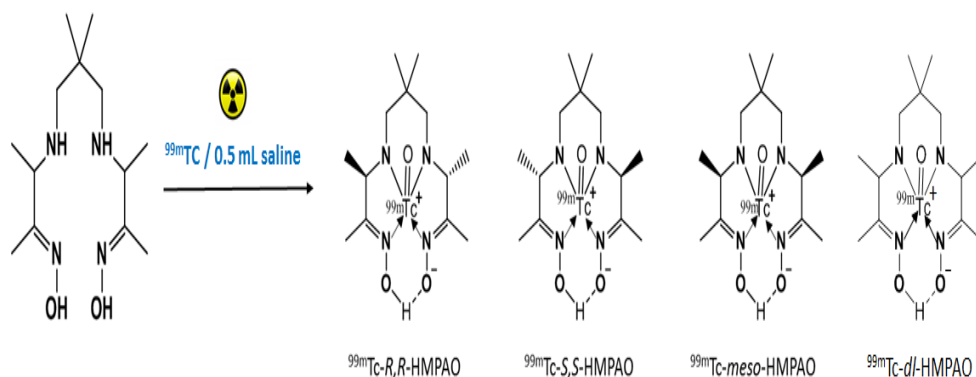
(step-1) and ethyl acetate (step-2) followed by reflux, slow cooling and finally filtration on whatmans paper forming white crystalline product. All intermediate compounds were purified by silica gel column chromatography with >50 % to 95% yields. Melting point of final *R,R*-HMPAO (m.p: 135-136°C), *S,S*-HMPAO (m.p: 138-141°C) enantiomers are checked and confirmed for desired isomeric product. All intermediates and the final compound were fully characterized by ¹H-NMR 500 MHz Avance III (Bruker, German), Low resolution and high resolution mass spectroscopy ESI⁺-MS (LTQ-Vellos, Thermo Scientific, France).

The route of HM-PAO (*meso* and *dl*) according to published method (75) (**Scheme-5**) as also synthesized for making comparative study with enantiomers (*RR*-, *SS*-HMPAO). Condensation of the starting material 2,2-dimethyl-1,3-propanediamine with two molecular equivalents of the 2,3-butanedione mono-oxime **1c** using Dean-Stark trap provides the diimine **2c** derivative in 60% yield. Reduction of this diimine groups with sodium borohydride provides HM-PAO as an equal mixture of the two diastereoisomers (*meso*- and *dl*). Repeated crystallization from acetonitrile and ethyl acetate permits the separation of the two diastereoisomers achieved the *dl*-diastereoisomer product **3c**. Melting point of final *meso*-HMPAO (m.p: 119-122°C), *dl*-HMPAO (m.p: 125-127°C °C) diastereomers are checked and confirmed for desired isomeric product

3-3-2. Radiolabeling

The amount of active substance in the single kit vial was 0.5 mg, similar to the commercially available formulation (75, 81). *R,R*-HMPAO, *S,S*-HMPAO, *dl*-HMPAO and *Meso*-HMPAO kits (containing 0.5 mg of precursor (*R,R*- or *S,S*- or *dl*, *Meso*-HMPAO), 4.5 mg of sodium chloride, various concentration of $\text{SnCl}_2 \cdot 2\text{H}_2\text{O}$ in 0.2N Hydrochloric acid solution (0.5-16 μg) in each vial, 0.1N sodium hydroxide solution) were prepared. $^{99\text{m}}\text{Tc}$ (~2.0 to 4.0 mCi) was added, kept at room temperature for 10 min (**Scheme 6**). The radiolabeling efficiency was determined by using ITLC-SG (10 \times 100 mm) and Whatman's No.1 (1 mm) paper as a stationary phase; Methyl ethyl ketone (MEK), normal saline and 50% acetonitrile in water as a mobile phase. The R_f value of $^{99\text{m}}\text{Tc}$ -HMPAO complex (primary) was found to be 1.0 by ITLC-SG/ MEK or 0.0 by ITLC-SG/ saline or 1.0 by Whatman's No.1 paper/ 50% acetonitrile in water (**Figure 19**). We found that under optimized conditions, 10 μg of $\text{SnCl}_2 \cdot 2\text{H}_2\text{O}$ provides higher radiolabeling efficiency (90.8%, 85.2% respectively) for $^{99\text{m}}\text{Tc}$ -*R,R* HMPAO (**Figure 20**) and $^{99\text{m}}\text{Tc}$ -*S,S* HMPAO (**Figure 21**) than with other $\text{SnCl}_2 \cdot 2\text{H}_2\text{O}$ concentration (**Table 10**). Based on our study, at lower $\text{SnCl}_2 \cdot 2\text{H}_2\text{O}$ concentration (8 to 0.5 μg) resulted in decreased radiolabeling efficiency of $^{99\text{m}}\text{Tc}$ -HMPAO isomers (< 5%) with an increased percentage of free $^{99\text{m}}\text{Tc}$ (> 90%). Whereas at higher $\text{SnCl}_2 \cdot 2\text{H}_2\text{O}$ concentration (12 to 16 μg) also resulted in decreased radiolabeling efficiency (60 to <80%) with an increased percentage of secondary complex (between 5 to 20%) and hydrolysed form (between 5 to 20%). Therefore, the amount of $\text{SnCl}_2 \cdot 2\text{H}_2\text{O}$ plays an important role on $^{99\text{m}}\text{Tc}$ - HMPAO (**Figure 22**). We also compared radiolabeling efficiency of

^{99m}Tc -*R,R* or *-S,S* HMPAO with ^{99m}Tc -*dl* HMPAO racemic mixture (>70 – 80%) (**Figure 23**), ^{99m}Tc -*Meso* HMPAO (>40 – 75%) (**Figure 24**) with various $\text{SnCl}_2 \cdot 2\text{H}_2\text{O}$ solution concentration (**Table 11**) and also compared with commercial available Ceretec™ *dl*-HMPAO kit ($\leq 80\%$) (**Figure 25**).



Scheme 6. Radiolabeling of *R,R*-HMPAO, *S,S*-HMPAO, *Meso*-HMPAO and *dl*-HMPAO with ^{99m}Tc

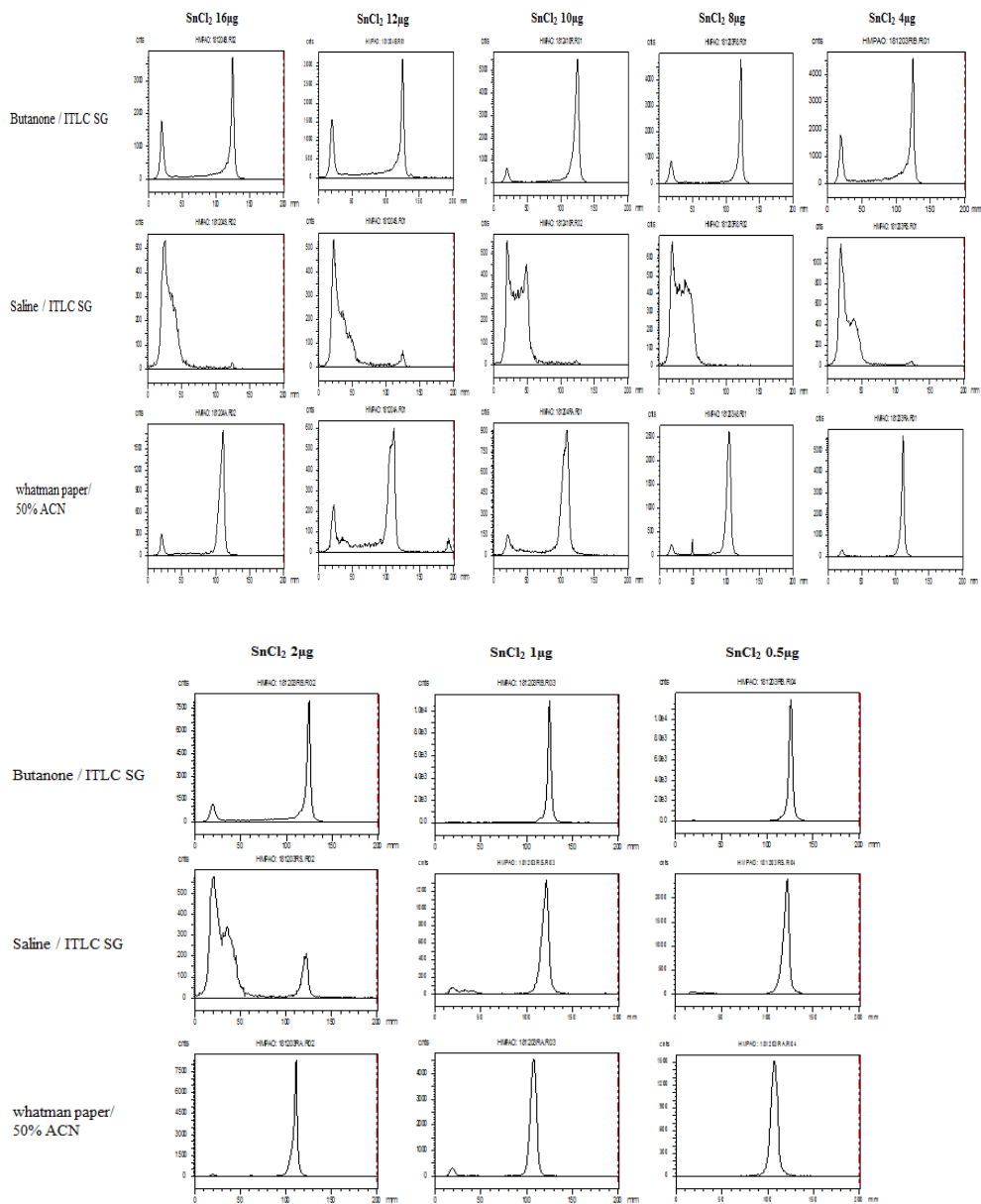


Figure 20. Radiolabeling efficiencies of ^{99m}Tc -*R,R* HMPAO with various concentration of $\text{SnCl}_2 \cdot 2\text{H}_2\text{O}$ solution (0.5-16 μg) were evaluated by ITLC-SG/Butanone, ITLC-SG/Saline and Whatman's No-1 paper/ 50% Acetonitrile in water. Radioactivity was detected by a Radio-TLC scanner.

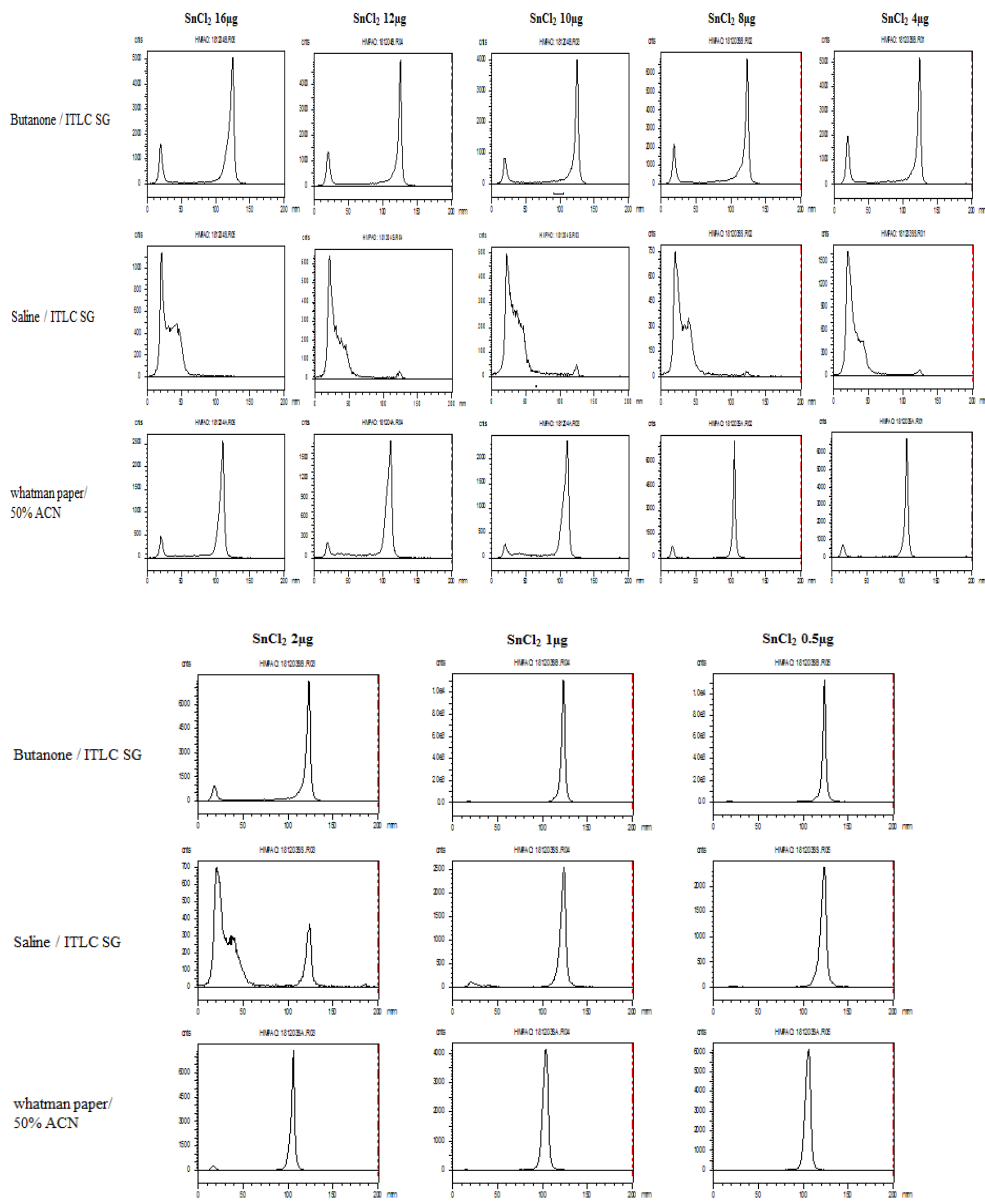


Figure 21. Radiolabeling efficiencies of $^{99m}\text{Tc-S,S}$ HMPAO with various concentration of $\text{SnCl}_2 \cdot 2\text{H}_2\text{O}$ solution (0.5-16 μg) were evaluated by ITLC-SG/Butanone, ITLC-SG/Saline and Whatman's No-1 paper/ 50% Acetonitrile in water. Radioactivity was detected by a Radio-TLC scanner

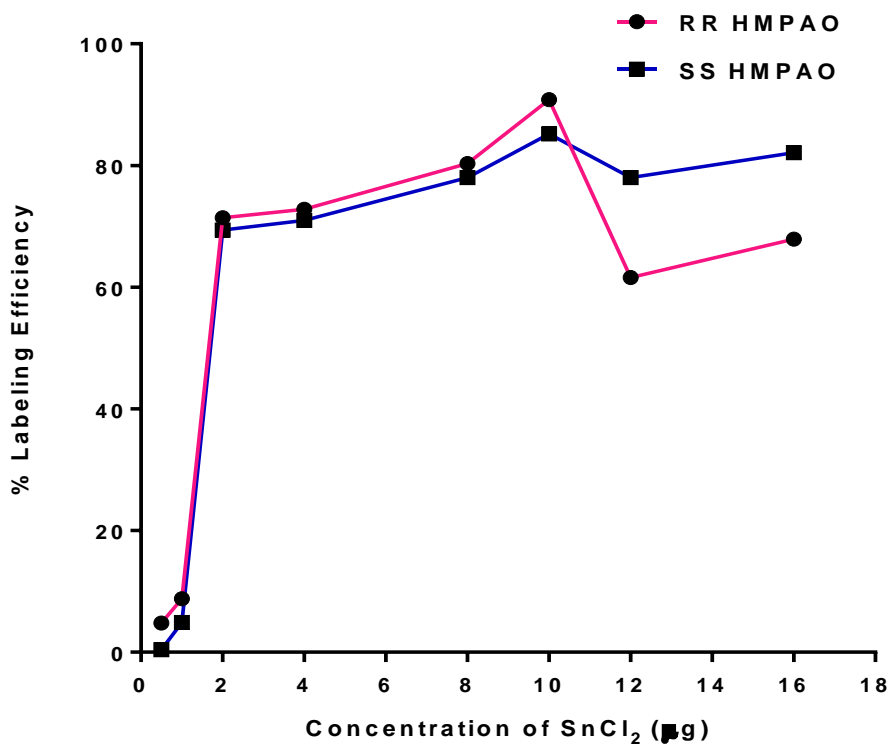


Figure 22. Labeling efficiency of ^{99m}Tc-*R,R* HMPAO and ^{99m}Tc-*S,S* HMPAO at various concentration of SnCl₂·2H₂O solution

Table 10. Radiolabeling efficiency of $^{99m}\text{Tc-R,R}$ HMPAO and $^{99m}\text{Tc-S,S}$ HMPAO

SnCl ₂ ·2H ₂ O Conc	$^{99m}\text{Tc-R,R}$ HMPAO		$^{99m}\text{Tc-S,S}$ HMPAO	
	Primary complex (%)	Secondary complex (%)	Primary complex (%)	Secondary complex (%)
16 μg	67.9	19.1	82.1	4.9
12 μg	61.6	10.4	78.0	9.2
10 μg	90.8	0.16	85.2	4.5
8 μg	80.3	11.5	78.0	6.7
4 μg	72.8	17.0	71.0	12.8
2 μg	71.4	16.2	69.4	-
1 μg	8.8	-	4.9	-
0.5 μg	4.8	-	0.4	-

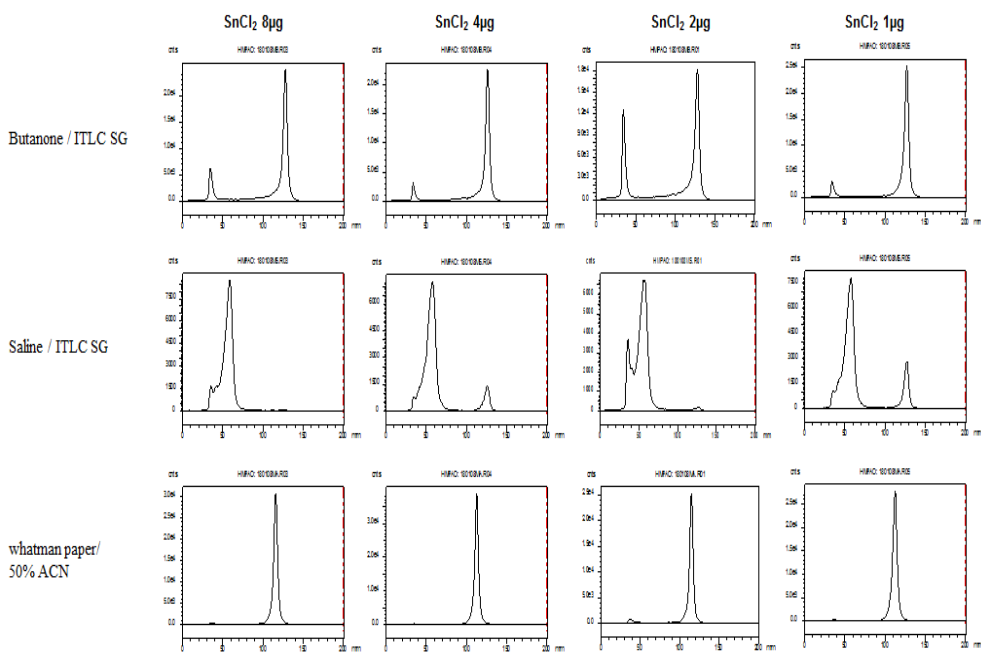


Figure 23. Radiolabeling efficiencies of ^{99m}Tc -dl HMPAO with various concentration of SnCl_2 (1.0-8.0 μg) were evaluated by ITLC-SG/Butanone, ITLC-SG/Saline and Whatman's No-1 paper/ 50% Acetonitrile in water. Radioactivity was detected by a Radio-TLC scanner

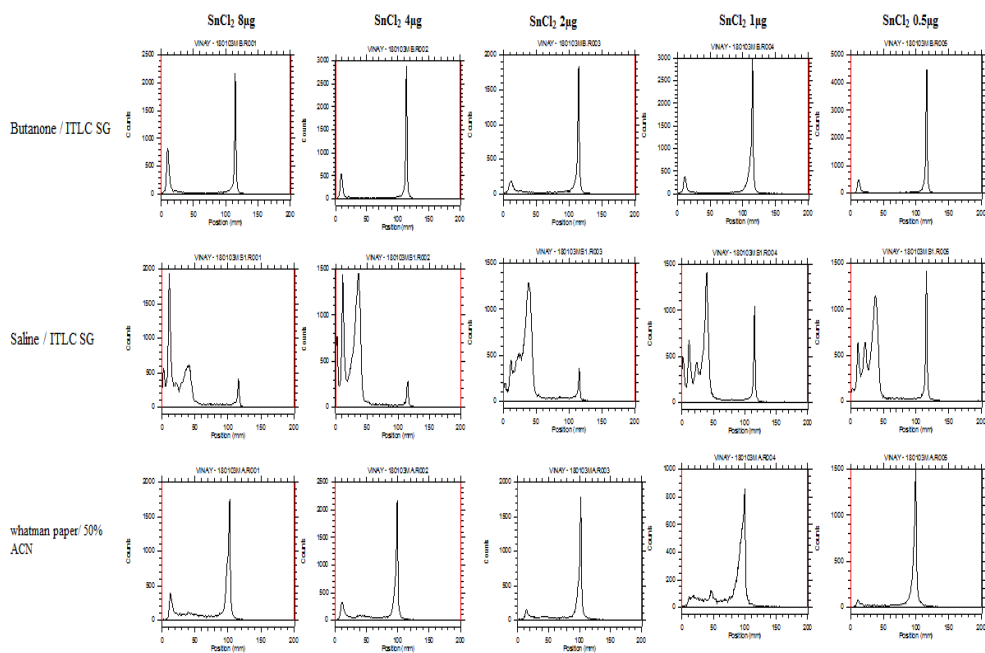


Figure 24. Radiolabeling efficiencies of $^{99m}\text{Tc-Meso}$ HMPAO with various concentration of $\text{SnCl}_2 \cdot 2\text{H}_2\text{O}$ solution (0.5-8.0 μg) were evaluated by ITLC-SG/Butanone, ITLC-SG/Saline and Whatman's No-1 paper/ 50% Acetonitrile in water. Radioactivity was detected by a Radio-TLC scanner.

Table 11. Radiolabeling efficiency of $^{99m}\text{Tc-dl}$ HMPAO and $^{99m}\text{Tc-Meso}$ HMPAO

SnCl₂·2H₂O Conc	$^{99m}\text{Tc-dl}$ HMPAO		$^{99m}\text{Tc-Meso}$ HMPAO	
	Primary complex (%)	Secondary complex (%)	Primary complex (%)	Secondary complex (%)
8 µg	83.0	14.2	72.5	9.3
4 µg	81.0	10.5	84.1	4.6
2 µg	68.0	27.9	81.8	3.7
1 µg	71.2	15.5	54.6	-
0.5 µg	-	-	42.4	-

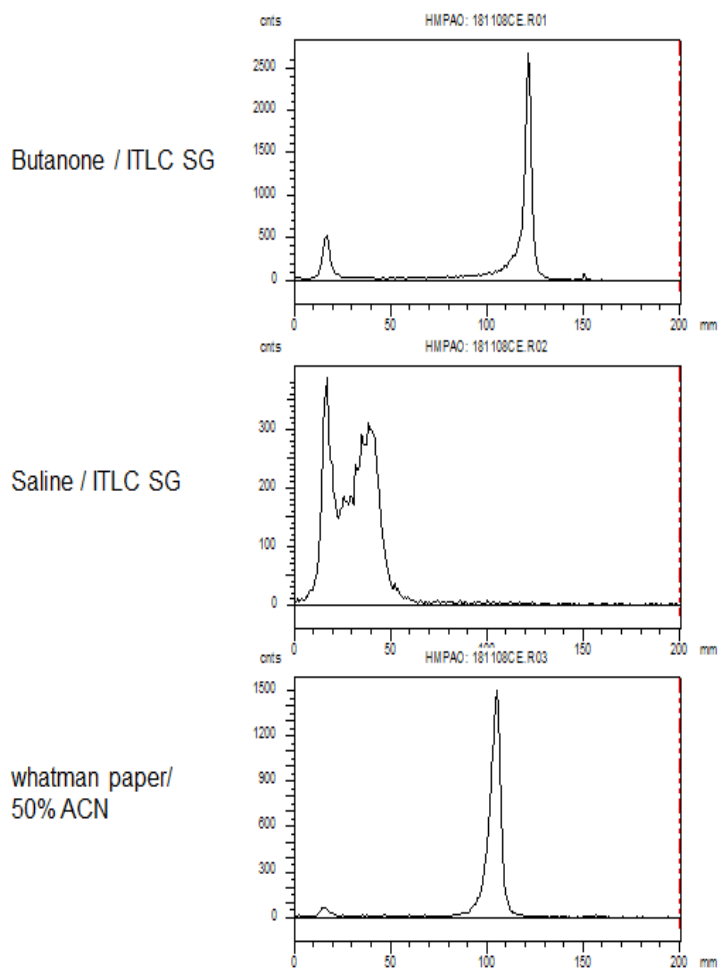


Figure 25. Radiolabeling efficiencies of $^{99m}\text{Tc-dl}$ HMPAO (Ceretek™) were evaluated by ITLC-SG/Butanone, ITLC-SG/Saline and Whatman's No-1 paper/ 50% Acetonitrile in water. Radioactivity was detected by a Radio-TLC scanner

3-4. Discussions

Technetium-99m exametazime (^{99m}Tc -HMPAO) has been introduced as a tracer for brain studies in humans as early as 1985 (73, 74) and its diagnostic utility has been very well documented (75). Currently, it is recommended by the European Association of Nuclear Medicine (EANM) and approved by FDA for brain perfusion studies using SPECT (76). It is used to diagnose abnormalities in the regional cerebral blood flow such as those occurring after a stroke (82, 83) and other cerebrovascular diseases including epilepsy (84, 85), Alzheimer's disease (82, 83) and other forms of dementia (86), transient ischemic attacks (87), migraine (88, 89) and brain tumors (90). Another application is the labelling of autologous leucocytes for infection and inflammation imaging (77).

The synthesis and radiolabeling of the active substance, ligand HMPAO have been previously reported and evaluated as a brain imaging agent (73, 75). It was originally confirmed that ^{99m}Tc -complexes of HMPAO diastereomers (*meso*- and *dl* racemate) showed different pharmacokinetics properties *in vivo*. It rapidly diffused across the BBB at normal flow rates. However, the ^{99m}Tc *dl*-HMPAO revealed superior brain uptake and retention (4.1%) compared to the ^{99m}Tc *meso*-isomer (1.7%) and stereoisomeric mixtures (1.9%) after 8 h post injection (79). The reason for higher uptake and retention of *dl*-form in brain is due to rapid intracellular conversion rate of HMPAO lipophilic to hydrophilic form. Whereas *meso* form gives 14-fold slower conversion rate than *dl*-form, resulted in decreased uptake and retention in the brain.

In addition, the later studies indicated that brain uptake of ^{99m}Tc -complexes formed from separated *d* (*R*) - and *l* (*S*)-enantiomers differed. Although ^{99m}Tc -*dl*-HMPAO have been widely studied, however less attention has paid to evaluate the efficacy and potency of enantiomers due to cumbersome, time consuming fractional crystallizations procedures for separation of *d* (*R*)-HMPAO, *l* (*S*)-HMPAO from mixture of *dl*- and *meso* -HMPAO (78) (**Figure-17**). Hence, it results in the drastic reduction of the final synthesis yield of *d*(*R*)- & *l*(*S*)-enantiomers and also still containing tracer amount of *meso* -HMPAO(80). There are some reported routes to synthesized *d* (*R*) - and *l* (*S*)-enantiomers (91). However, it has some drawbacks such as difficult in synthesizing each step with lower yields, final product cannot be recrystallized due to minor impurity and high pressure liquid chromatography (HPLC) purification for final precursor that results in changing chemical properties because of 0.1% trifluoroacetic acid (TFA) buffer as mobile phase was not suitable. According to our practical experience worked on many synthesis routes, we concluded HMPAO precursor is very sensitive and can easily decompose with acid.

To circumvent this problem, we developed new efficient route for synthesis of *S,S* - HMPAO and *R,R* -HMPAO enantiomeric compounds (**Scheme 3, 4**). All reaction steps involved in this designed scheme were straight forward with excellent yield between >50% to 95%, Final enantiomeric products with high purity and which does not contain any undesired product such as *meso*- and diastereomers as compared with other HMPAO routes. This route allows us to synthesize the final HMPAO in large scale for commercial applications. Previously published old route of HM-PAO (*meso*, *dl*) (**scheme-5**) was also synthesized for comparative

radiolabeling study with enantiomers (*RR*-, *SS*-HMPAO). In addition, the specific desired isomers which were developed from new route synthesis are confirmed with help of melting point test. The melting point is an important physical property of a compound. The melting point can be used to identify a substance and as an indication of its purity. From new route synthesis, we proved final specific enantiomers such as *SS*- (m.p: 138-141 °C), *RR*- (m.p: 135-136 °C) HMPAO melting point results shown to be matched with previously reported enantiomers synthesis in old route (91). On other side synthesized final *dl*- (m.p: 125-127 °C) and *meso*- (m.p: 119-122 °C) HMPAO isomers melting points were also matched according to published method (75).

The cold precursor *SS*-, *RR*- *dl* and *meso* -HMPAO isomers was formulated in to a kits with various concentration of SnCl₂·2H₂O (0.5 -16 μg) in each vial. Addition of ^{99m}Tc to a HMPAO kits produce ^{99m}Tc-labeled HMPAO isomers. Combination of three chromatographic systems (ITLC-SG/ MEK, ITLC-SG/saline, and whatman No.1 (1mm) /50% acetonitrile in water) was used for a complete characterization of the ^{99m}Tc-HMPAO radiochemical composition. The above TLC condition allows us to characterize the desired ^{99m}Tc-lipophilic complex, free ^{99m}Tc, reduced-hydrolyzed technetium (TcO₂) and hydrophilic secondary complex.

Over decades, there were several groups has followed same kind of radiolabeling procedure (73, 75) and results giving lower radiolabeling efficiency. The commercially available kit from Ceretec™, GE Healthcare (each vial contains 7.6 μg SnCl₂·2H₂O) give ≤ 80 % radiolabeling efficiency (**Figure 23**). Therefore we also optimized radiolabeling conditions, results with 10 μg of SnCl₂·2H₂O provides

higher radiolabeling efficiency for $^{99m}\text{Tc-R,R}$ HMPAO and $^{99m}\text{Tc-S,S}$ HMPAO than with other $\text{SnCl}_2 \cdot 2\text{H}_2\text{O}$ concentration. Based on our study, at lower $\text{SnCl}_2 \cdot 2\text{H}_2\text{O}$ concentration (8 to 0.5 μg) resulted in decreased radiolabeling efficiency of ^{99m}Tc -HMPAO isomers (< 5%) with an increased percentage of free ^{99m}Tc (> 90%). In particular, the increase of $\text{SnCl}_2 \cdot 2\text{H}_2\text{O}$ concentration from 12 to 16 μg in the kit resulted in decreased radiolabeling purity with an increased percentage of secondary complex (between 5 to 20%) and hydrolysed form (between 5 to 20%). Therefore, the amount of $\text{SnCl}_2 \cdot 2\text{H}_2\text{O}$ plays an important role on ^{99m}Tc -HMPAO. The radiochemical purity and biodistribution results were dependent on the content of $\text{SnCl}_2 \cdot 2\text{H}_2\text{O}$ in the kit formulation.

3-5. Conclusion

We successfully designed new efficient route for synthesis of *R,R*-HMPAO and *S,S*-HMPAO enantiomeric compounds. Final precursor with the high purity and which does not contain any undesired product such as meso- and diastereomers as compared with other HMPAO routes. *R,R*-HMPAO and *S,S*-HMPAO kits containing 10 μg $\text{SnCl}_2 \cdot 2\text{H}_2\text{O}$ showed higher radiolabeling efficiency (90 %) than other $\text{SnCl}_2 \cdot 2\text{H}_2\text{O}$ concentration. We also compared radiolabeling efficiency with *dl*-, *Meso*- and commercial available Ceretec™ *dl*-HMPAO kit showed good results. The radiochemical purity and biodistribution results were dependent on the content of $\text{SnCl}_2 \cdot 2\text{H}_2\text{O}$ in the kit formulation.

4. References

1. Turner J, Claringbold P, Klemp P, Cameron P, Martindale A, Glancy R, et al. ^{166}Ho -microsphere liver radiotherapy: a preclinical SPECT dosimetry study in the pig. *Nuclear medicine communications*. 1994;15(7):545-53.
2. Wang S-J, Lin W-Y, Lui W-Y, Chen M-N, Tsai Z-T, Ting G. Hepatic artery injection of Yttrium-90-lipiodol: biodistribution in rats with hepatoma. *Journal of nuclear medicine: official publication, Society of Nuclear Medicine*. 1996;37(2):332-5.
3. Wang S-J, Lin W-Y, Chen M-N, Hsieh B-T, Shen L-H, Tsai Z-T, et al. Biodistribution of rhenium-188 Lipiodol infused via the hepatic artery of rats with hepatic tumours. *European journal of nuclear medicine*. 1996;23(1):13-7.
4. Madsen MT, Park CH, Thakur ML. Dosimetry of iodine-131 ethiodol in the treatment of hepatoma. *Journal of nuclear medicine: official publication, Society of Nuclear Medicine*. 1988;29(6):1038.
5. Nakajo M, Kobayashi H, Shimabukuro K, Shirono K, Sakata H, Taguchi M, et al. Biodistribution and in vivo kinetics of iodine-131 lipiodol infused via the hepatic artery of patients with hepatic cancer. *Journal of nuclear medicine: official publication, Society of Nuclear Medicine*. 1988;29(6):1066.
6. Knapp Jr F, Beets A, Gohlke S, Zamora P, Bender H, Palmedo H, et al. Availability of rhenium-188 from the alumina-based tungsten-188/rhenium-188 generator for preparation of rhenium-188-labeled radiopharmaceuticals for cancer treatment. *Anticancer research*. 1996;17(3B):1783-95.

7. Jeong JM, Chung J-K. Therapy with ^{188}Re -labeled radiopharmaceuticals: an overview of promising results from initial clinical trials. *Cancer Biotherapy and Radiopharmaceuticals*. 2003;18(5):707-17.
8. Jeong JM, Kim YJ, Lee YS, Ko JI, Son M, Lee DS, et al. Lipiodol solution of a lipophilic agent, $(^{188}\text{Re})\text{-TDD}$, for the treatment of liver cancer. *Nucl Med Biol*. 2001;28(2):197-204.
9. Lee YS, Jeong JM, Kim YJ, Chang YS, Lee HJ, Son M, et al. Development of acetylated HDD kit for preparation of ^{188}Re -HDD/lipiodol. *Applied radiation and isotopes : including data, instrumentation and methods for use in agriculture, industry and medicine*. 2007;65(1):64-9.
10. Nakakuma K, Tashiro S, Hiraoka T, Uemura K, Konno T, Miyauchi Y, et al. Studies on anticancer treatment with an oily anticancer drug injected into the ligated feeding hepatic artery for liver cancer. *Cancer*. 1983;52(12):2193-200.
11. Paeng JC, Jeong JM, Yoon CJ, Lee YS, Suh YG, Chung JW, et al. Lipiodol solution of ^{188}Re -HDD as a new therapeutic agent for transhepatic arterial embolization in liver cancer: preclinical study in a rabbit liver cancer model. *Journal of nuclear medicine : official publication, Society of Nuclear Medicine*. 2003;44(12):2033-8.
12. Boschi A, Bolzati C, Uccelli L, Duatti A. High-yield synthesis of the terminal $^{188}\text{Re}\equiv\text{N}$ multiple bond from generator-produced $[^{188}\text{ReO}_4]^-$. *Nuclear medicine and biology*. 2003;30(4):381-7.
13. Boschi A, Uccelli L, Duatti A, Colamussi P, Cittanti C, Filice A, et al. A kit formulation for the preparation of ^{188}Re -lipiodol: preclinical studies and

preliminary therapeutic evaluation in patients with unresectable hepatocellular carcinoma. *Nuclear medicine communications*. 2004;25(7):691-9.

14. Luo T-Y, Hsieh B-T, Wang S-J, Lin W-Y, Lee T-W, Shen L-H, et al. Preparation and biodistribution of rhenium-188 ECD/Lipiodol in rats following hepatic arterial injection. *Nuclear medicine and biology*. 2004;31(5):671-7.

15. Garin E, Noiret N, Malbert C, Lepareur N, Roucoux A, Caulet-Maugendre S, et al. Development and biodistribution of 188Re-SSS lipiodol following injection into the hepatic artery of healthy pigs. *European journal of nuclear medicine and molecular imaging*. 2004;31(4):542-6.

16. Garin E, Rakotonirina H, Lejeune F, Denizot B, Roux J, Noiret N, et al. Effect of a 188 Re-SSS lipiodol/131I-lipiodol mixture, 188 Re-SSS lipiodol alone or 131I-lipiodol alone on the survival of rats with hepatocellular carcinoma. *Nuclear medicine communications*. 2006;27(4):363-9.

17. Bernal P, Raoul JL, Vidmar G, Sereegotov E, Sundram FX, Kumar A, et al. Intra-arterial rhenium-188 lipiodol in the treatment of inoperable hepatocellular carcinoma: results of an IAEA-sponsored multinational study. *International journal of radiation oncology, biology, physics*. 2007;69(5):1448-55.

18. Sundram F, Chau TC, Onkhuudai P, Bernal P, Padhy AK. Preliminary results of transarterial rhenium-188 HDD lipiodol in the treatment of inoperable primary hepatocellular carcinoma. *European journal of nuclear medicine and molecular imaging*. 2004;31(2):250-7.

19. Lee YS, Jeong JM, Kim YJ, Chung JW, Park JH, Suh YG, et al. Synthesis of ¹⁸⁸Re-labelled long chain alkyl diaminedithiol for therapy of liver cancer. *Nuclear medicine communications*. 2002;23(3):237-42.
20. Paeng JC, Jeong JM, Yoon CJ, Lee Y-S, Suh Y-G, Chung JW, et al. Lipiodol Solution of ¹⁸⁸Re-HDD as a New Therapeutic Agent for Transhepatic Arterial Embolization in Liver Cancer: Preclinical Study in a Rabbit Liver Cancer Model. *Journal of Nuclear Medicine*. 2003;44(12):2033-8.
21. Banka VK, Moon S-H, Jeong JM, Seelam SR, Lee Y-S, Kim YJ, et al. Development of 4-hexadecyl-4, 7-diaza-1, 10-decanedithiol (HDD) kit for the preparation of the liver cancer therapeutic agent Re-¹⁸⁸HDD/lipiodol. *Nuclear medicine and biology*. 2015;42(3):317-22.
22. Venook AP, Papandreou C, Furuse J, de Guevara LL. The incidence and epidemiology of hepatocellular carcinoma: a global and regional perspective. *The Oncologist*. 2010;15(Supplement 4):5-13.
23. Okuda K, Ohtsuki T, Obata H, Tomimatsu M, Okazaki N, Hasegawa H, et al. Natural history of hepatocellular carcinoma and prognosis in relation to treatment study of 850 patients. *Cancer*. 1985;56(4):918-28.
24. Nagasue N, Uchida M, Makino Y, Takemoto Y, Yamanoi A, Hayashi T, et al. Incidence and factors associated with intrahepatic recurrence following resection of hepatocellular carcinoma. *GASTROENTEROLOGY-BALTIMORE THEN PHILADELPHIA*-. 1993;105:488-.

25. Gallicchio R, Nardelli A, Mainenti P, Nappi A, Capacchione D, Simeon V, et al. Therapeutic Strategies in HCC: Radiation Modalities. *BioMed Research International*. 2016;2016:11.
26. PARK CH, SUH JH, Yoo H, Lee J, Kim D. Evaluation of intrahepatic I-131 ethiodol on a patient with hepatocellular carcinoma: therapeutic feasibility study. *Clinical nuclear medicine*. 1986;11(7):514-7.
27. Yoo H, Suh J, Lee J, Kim D, Park C, Kim B, et al. Therapeutic feasibility study and clinical trial of intrahepatic I-131-lipiodol on patients with hepatocellular carcinoma. *Korean J Nucl Med*. 1986;20:61-71.
28. Raoul J, Guyader D, Bretagne J, Heautot J, Duvauferrier R, Bourguet P, et al. Prospective randomized trial of chemoembolization versus intra-arterial injection of 131I-labeled-iodized oil in the treatment of hepatocellular carcinoma. *Hepatology*. 1997;26(5):1156-61.
29. Park C, Suh J, Yoo H, Lee J, Kim D, Lee K. Iodine-131-labeled lipiodol retention within hepatic cavernous hemangioma. *Radiology*. 1987;163(1):283-4.
30. Chua TC, Chu F, Butler SP, Quinn RJ, Glenn D, Liauw W, et al. Intra-arterial iodine-131-lipiodol for unresectable hepatocellular carcinoma. *Cancer*. 2010;116(17):4069-77.
31. Kim Y, Jeong J, Kim S, Lee D, Chung J, Lee M, et al., editors. Rhenium-188-sulfur colloid suspended in Lipiodol: a capillary-blocking radiopharmaceutical for targeting liver cancer. *JOURNAL OF NUCLEAR MEDICINE*; 1998: SOC NUCLEAR MEDICINE INC 1850 SAMUEL MORSE DR, RESTON, VA 20190-5316 USA.

32. Kumar A, Bal C, Srivastava DN, Acharya SK, Thulkar SP, Sharma S, et al. Transarterial radionuclide therapy with Re-188-HDD-lipiodol in case of unresectable hepatocellular carcinoma with extensive portal vein thrombosis. *European Journal of Radiology Extra*. 2005;56(2):55-9.
33. Kumar A, Bal C, Srivastava DN, Thulkar SP, Sharma S, Acharya SK, et al. Management of multiple intrahepatic recurrences after radiofrequency ablation of hepatocellular carcinoma with rhenium-188-HDD-lipiodol. *European journal of gastroenterology & hepatology*. 2006;18(2):219-23.
34. Kumar A, Srivastava DN, Chau TT, Long HD, Bal C, Chandra P, et al. Inoperable hepatocellular carcinoma: transarterial 188Re HDD-labeled iodized oil for treatment--prospective multicenter clinical trial. *Radiology*. 2007;243(2):509-19.
35. Lambert B, Bacher K, De Keukeleire K, Smeets P, Colle I, Jeong JM, et al. 188Re-HDD/lipiodol for treatment of hepatocellular carcinoma: a feasibility study in patients with advanced cirrhosis. *Journal of nuclear medicine : official publication, Society of Nuclear Medicine*. 2005;46(8):1326-32.
36. Lambert B, Bacher K, Defreyne L, Van Vlierberghe H, Jeong JM, Wang RF, et al. (188)Re-HDD/lipiodol therapy for hepatocellular carcinoma: an activity escalation study. *European journal of nuclear medicine and molecular imaging*. 2006;33(3):344-52.
37. Wang S-J, Lin W-Y, Chen M-N, Hsieh B-T, Shen L-H, Tsai Z-T, et al. Radiolabelling of lipiodol with generator-produced ¹⁸⁸Re for hepatic tumor therapy. *Applied radiation and isotopes*. 1996;47(3):267-71.

38. Jeong JM, Kim YJ, Lee YS, Ko JI, Son M, Lee DS, et al. Lipiodol solution of a lipophilic agent, ¹⁸⁸Re-TDD, for the treatment of liver cancer. *Nuclear medicine and biology*. 2001;28(2):197-204.
39. Lee Y-S, Jeong J, Kim Y, Chung J, Park J, Suh Y-G, et al. Synthesis of ¹⁸⁸Re-labelled long chain alkyl diaminedithiol for therapy of liver cancer. *Nuclear medicine communications*. 2002;23(3):237-42.
40. Sundram F, Jeong J, Zanzonico P, Bernal P, Chau T, Onkhuudai P. Trans-arterial rhenium-188 lipiodol in the treatment of inoperable hepatocellular carcinoma. An IAEA sponsored multi-centre phase. 2002;1:5-11.
41. Sundram F, Chau TCM, Onkhuudai P, Bernal P, Padhy AK. Preliminary results of transarterial rhenium-188 HDD lipiodol in the treatment of inoperable primary hepatocellular carcinoma. *European journal of nuclear medicine and molecular imaging*. 2004;31(2):250-7.
42. Lambert B, Bacher K, Defreyne L, Gemmel F, Van Vlierberghe H, Jeong JM, et al. ¹⁸⁸Re-HDD/lipiodol therapy for hepatocellular carcinoma: a phase I clinical trial. *Journal of Nuclear Medicine*. 2005;46(1):60-6.
43. Banka VK, Moon SH, Jeong JM, Seelam SR, Lee YS, Kim YJ, et al. Development of 4-hexadecyl-4,7-diaza-1,10-decanedithiol (HDD) kit for the preparation of the liver cancer therapeutic agent ¹⁸⁸Re-HDD/lipiodol. *Nuclear medicine and biology*. 2015;42(3):317-22.
44. Lee Y-S, Min Jeong J, Joo Kim Y, Soo Chang Y, Jeong Lee H, Son M, et al. Development of acetylated HDD kit for preparation of ¹⁸⁸Re-HDD/lipiodol. *Applied radiation and isotopes*. 2007;65(1):64-9.

45. Knapp Jr FR, Mirzadeh S. The continuing important role of radionuclide generator systems for nuclear medicine. *European journal of nuclear medicine.* 1994;21(10):1151-65.
46. Knapp Jr F, Mirzahdeh S, Beets A, Sharkey R, Griffiths G, Juweid M, et al. Curie-scale tungsten-188/rhenium-188 generators for routine clinical applications. *Technetium Chemistry and Nuclear Medicine.* 1995;4:319-84.
47. Fritzberg AR, Kasina S, Eshima D, Johnson DL. Synthesis and biological evaluation of technetium-99m MAG3 as a hippuran replacement. *Journal of nuclear medicine: official publication, Society of Nuclear Medicine.* 1986;27(1):111-6.
48. Tolia C, Sgouros S. Initial evaluation and management of CNS injury. *Emedicine com.* 2003.
49. Maas AI, Stocchetti N, Bullock R. Moderate and severe traumatic brain injury in adults. *The Lancet Neurology.* 2008;7(8):728-41.
50. Partington T, Farmery A. Intracranial pressure and cerebral blood flow. *Anaesthesia & Intensive Care Medicine.* 2014;15(4):189-94.
51. Kung HF, Blau M. Regional intracellular pH shift: a proposed new mechanism for radiopharmaceutical uptake in brain and other tissues. *Journal of nuclear medicine : official publication, Society of Nuclear Medicine.* 1980;21(2):147-52.
52. Winchell HS, Baldwin RM, Lin TH. Development of I-123-labeled amines for brain studies: localization of I-123 iodophenylalkyl amines in rat brain. *Journal of Nuclear Medicine.* 1980;21(10):940-6.

53. Tramosch KM, Kung HF, Blau M. Radioiodine-labeled N,N-dimethyl-N'-[2-hydroxy-3-alkyl-5-iodobenzyl]-1,3-propanediamines for brain perfusion imaging. *Journal of Medicinal Chemistry*. 1983;26(2):121-5.
54. Vyth A, Fennema PJ, van der Schoot JB. 201Tl-diethyldithiocarbamate: a possible radiopharmaceutical for brain imaging. *Pharmaceutisch Weekblad*. 1983;5(5):213-6.
55. Todd-Pokropek AE. Functional imaging of the brain using single photon emission computerized tomography (SPECT). *Brain topography*. 1992;5(2):119-27.
56. Kung H, Blau M. Synthesis of selenium-75 labeled tertiary diamines: new brain imaging agents. *Journal of Medicinal Chemistry*. 1980;23(10):1127-30.
57. Holman BL, Lee RG, Hill TC, Lovett RD, Lister-James J. A comparison of two cerebral perfusion tracers, N-isopropyl I-123 p-iodoamphetamine and I-123 HIPDM, in the human. *Journal of nuclear medicine : official publication, Society of Nuclear Medicine*. 1984;25(1):25-30.
58. Winchell HS, Horst WD, Braun L, Oldendorf WH, Hattner R, Parker H. N-isopropyl-[123I] p-iodoamphetamine: single-pass brain uptake and washout; binding to brain synaptosomes; and localization in dog and monkey brain. *Journal of nuclear medicine : official publication, Society of Nuclear Medicine*. 1980;21(10):947-52.
59. Moretti J, Hill TC, Holman BL. Brain imaging with radiolabeled amines and other perfusion tracers. United States: Williams and Wilkens; 1988.
60. Lee RG, Hill TC, Holman BL, Clouse ME. N-isopropyl(I-123)p-iodoamphetamine brain scans with single-photon emission tomography:

discordance with transmission computed tomography. *Radiology*. 1982;145(3):795-9.

61. Lee RG, Hill TC, Holman BL, Uren R, Clouse ME. Comparison of N-isopropyl (I-123) p-iodoamphetamine brain scans using Anger camera scintigraphy and single-photon emission tomography. *Radiology*. 1982;145(3):789-93.

62. Ell PJ, Cullum I, Donaghy M, Lui D, Jarritt PH, Harrison MJG. CEREBRAL BLOOD FLOW STUDIES WITH 123IODINE-LABELLED AMINES. *The Lancet*. 1983;321(8338):1348-52.

63. LaFrance ND, Wagner Jr HN, Whitehouse P, Corley E, Duelfer T. Decreased Accumulation of Isopropyl-iodoamphetamine (I@ 123) in Brain Tumors. *Journal of nuclear medicine : official publication, Society of Nuclear Medicine*. 1981;22:1081-3.

64. Kuhl DE, Barrio JR, Huang S-C, Selin C, Ackermann RF, Lear JL, et al. Quantifying local cerebral blood flow by N-isopropyl-p-[123I] iodoamphetamine (IMP) tomography. *Journal of nuclear medicine: official publication, Society of Nuclear Medicine*. 1982;23(3):196-203.

65. Hill TC, Magistretti PL, Holman BL, Lee RG, O'Leary DH, Uren RF, et al. Assessment of regional cerebral blood flow (rCBF) in stroke using SPECT and N-isopropyl-(I-123)-p-iodoamphetamine (IMP). *Stroke*. 1984;15(1):40-5.

66. Kung HF, Molnar M, Billings J, Wicks R, Blau M. Synthesis and biodistribution of neutral lipid-soluble Tc-99m complexes that cross the blood-brain barrier. *Journal of nuclear medicine : official publication, Society of Nuclear Medicine*. 1984;25(3):326-32.

67. Kung H, Molnar M, Billings J, Wicks R, Blau M. Synthesis and Biodistribution of Neutral Lipid-Soluble Tc-99m Complexes. *Journal of nuclear medicine : official publication, Society of Nuclear Medicine*. 1984;25:326-32.
68. Troutner DE, Volkert WA, Hoffman TJ, Holmes RA. A neutral lipophilic complex of ^{99m}Tc with a multidentate amine oxime. *The International journal of applied radiation and isotopes*. 1984;35(6):467-70.
69. Lever SZ, Burns HD, Kervitsky TM, Goldfarb HW, Woo DV, Wong DF, et al. Design, preparation, and biodistribution of a technetium-99m triaminedithiol complex to assess regional cerebral blood flow. *Journal of nuclear medicine : official publication, Society of Nuclear Medicine*. 1985;26(11):1287-94.
70. Volkert W, McKenzie E, Hoffman T, Troutner D, Holmes R. The behavior of neutral amine oxime chelates labelled with Tc at tracer level. *International journal of nuclear medicine and biology*. 1984;11(3-4):243-6.
71. Volkert W, Hoffman T, Seger R, Troutner D, Holmes R. TC-99M PROPYLENE AMINE OXIME (TC-99M PNAO)-A POTENTIAL BRAIN RADIOPHARMACEUTICAL. *EUROPEAN JOURNAL OF NUCLEAR MEDICINE*. 1984;9(11):511-6.
72. Holm S, Andersen AR, Vorstrup S, Lassen NA, Paulson OB, Holmes RA. Dynamic SPECT of the brain using a lipophilic technetium-99m complex, PnAO. *Journal of nuclear medicine : official publication, Society of Nuclear Medicine*. 1985;26(10):1129-34.

73. Nowotnik DP, Canning LR, Cumming SA, Harrison RC, Higley B, Nechvatal G, et al. Development of a ⁹⁹Tcm-labelled radiopharmaceutical for cerebral blood flow imaging. *Nucl Med Commun.* 1985;6(9):499-506.
74. Holmes RA, Chaplin SB, Royston KG, Hoffman TJ, Volkert WA, Nowotnik DP, et al. Cerebral uptake and retention of ⁹⁹Tcm-hexamethylpropyleneamine oxime (⁹⁹Tcm-HM-PAO). *Nucl Med Commun.* 1985;6(8):443-7.
75. Neirinckx RD, Canning LR, Piper IM, Nowotnik DP, Pickett RD, Holmes RA, et al. Technetium-99m d,l-HM-PAO: a new radiopharmaceutical for SPECT imaging of regional cerebral blood perfusion. *Journal of nuclear medicine : official publication, Society of Nuclear Medicine.* 1987;28(2):191-202.
76. Kapucu Ö L, Nobili F, Varrone A, Booij J, Vander Borgh T, Någren K, et al. EANM procedure guideline for brain perfusion SPECT using ^{99m}Tc-labelled radiopharmaceuticals, version 2. *European Journal of Nuclear Medicine and Molecular Imaging.* 2009;36(12):2093.
77. de Vries EFJ, Roca M, Jamar F, Israel O, Signore A. Guidelines for the labelling of leucocytes with ^{99m}Tc-HMPAO. *European Journal of Nuclear Medicine and Molecular Imaging.* 2010;37(4):842-8.
78. Canning LR, Nowotnik DP, Neirinckx RD, Piper IM. Complexes of technetium-99m with propylene amine oximes. *Google Patents;* 1988.
79. Sharp PF, Smith FW, Gemmell HG, Lyall D, Evans NT, Gvozdanovic D, et al. Technetium-99m HM-PAO stereoisomers as potential agents for imaging

regional cerebral blood flow: human volunteer studies. *Journal of nuclear medicine* : official publication, Society of Nuclear Medicine. 1986;27(2):171-7.

80. Banerjee S, Samuel G, Kothari K, Sarma HD, Mra P. On the synthesis, isolation, and radiochemical studies for the preparation of in-house kits for ^{99m}Tc-meso- and d,l-HMPAO: A few additional observations 1999. 327-38 p.

81. de Vries EF, Roca M, Jamar F, Israel O, Signore A. Guidelines for the labelling of leucocytes with ^{99m}Tc-HMPAO. *European journal of nuclear medicine and molecular imaging*. 2010;37(4):842-8.

82. Elmstahl S, Siennicki-Lantz A, Lilja B, Bjuno L. A study of regional cerebral blood flow using ^{99m}Tc-HMPAO-SPECT in elderly women with senile dementia of Alzheimer's type. *Dementia (Basel, Switzerland)*. 1994;5(6):302-9.

83. Rodriguez G, Nobili F, Copello F, Vitali P, Gianelli MV, Taddei G, et al. ^{99m}Tc-HMPAO regional cerebral blood flow and quantitative electroencephalography in Alzheimer's disease: a correlative study. *Journal of Nuclear Medicine*. 1999;40(4):522-9.

84. Rowe CC, Berkovic SF, Austin MC, Saling M, Kalnins RM, McKay WJ, et al. Visual and quantitative analysis of interictal SPECT with technetium-^{99m}-HMPAO in temporal lobe epilepsy. *Journal of nuclear medicine: official publication, Society of Nuclear Medicine*. 1991;32(9):1688-94.

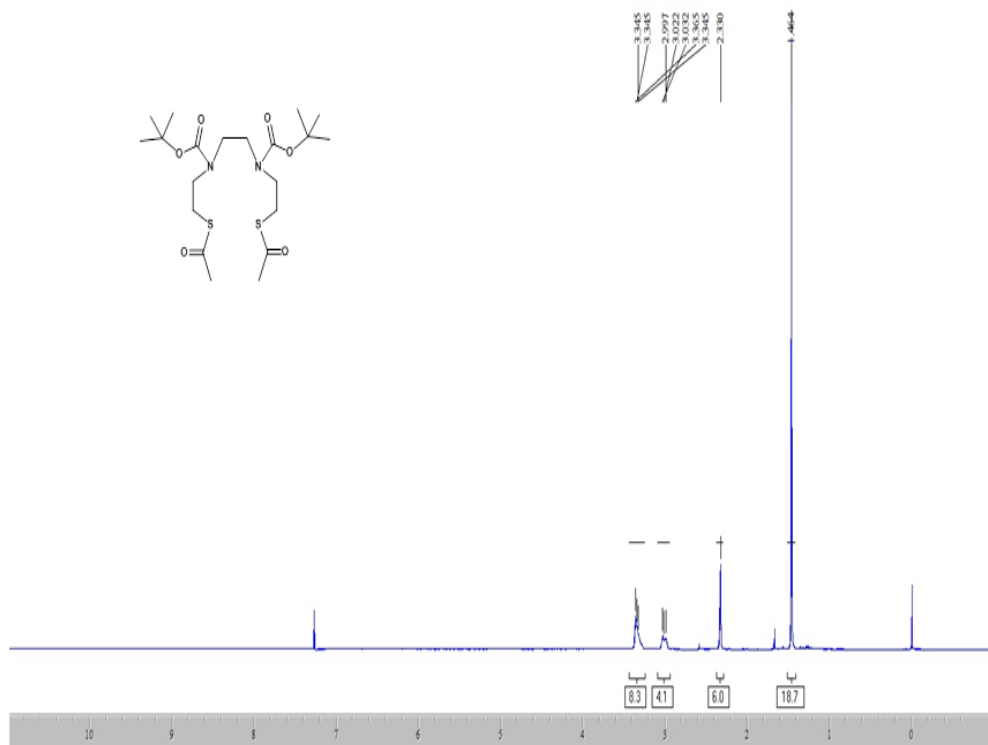
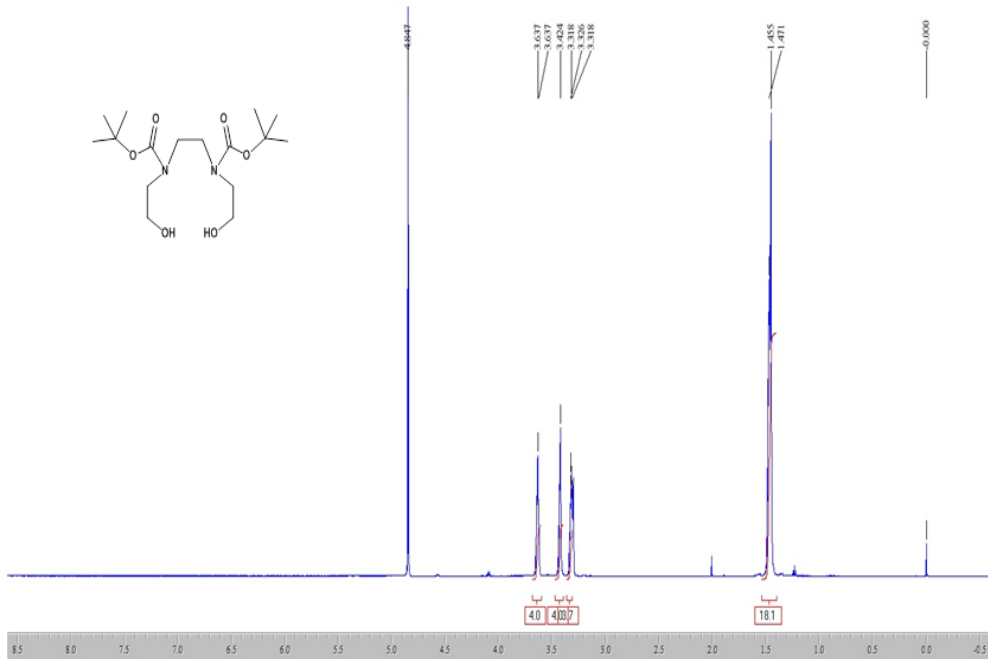
85. Harvey A, Hopkins I, SBowe J, Cook D, Shield L, Berkovic S. Frontal lobe epilepsy clinical seizure characteristics and localization with ictal ^{99m}Tc-HMPAO SPECT. *Neurology*. 1993;43(10):1966-.

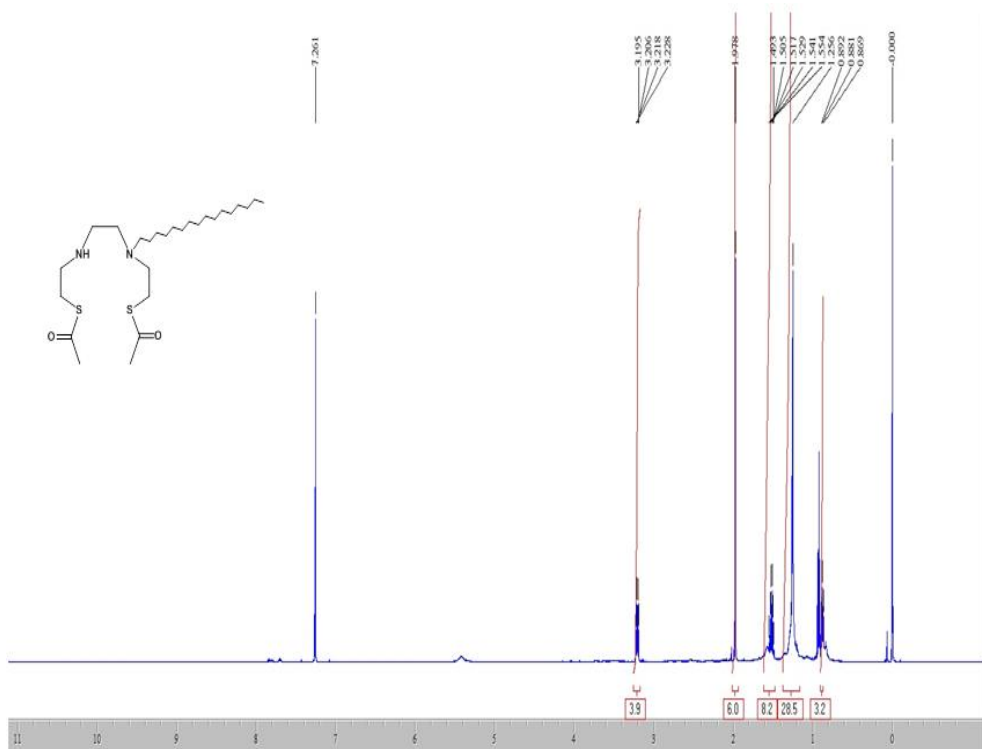
86. Talbot PR, Lloyd JJ, Snowden JS, Neary D, Testa HJ. A clinical role for 99mTc-HMPAO SPECT in the investigation of dementia? *Journal of Neurology, Neurosurgery & Psychiatry*. 1998;64(3):306-13.
87. Baird AE, Donnan GA. Increased 99mTc-HMPAO uptake in ischemic stroke. *Stroke*. 1993;24(8):1261-2.
88. Mirza M, Tutuş A, Erdoğan F, Kula M, Tomar A, Silov G, et al. Interictal SPECT with tc-99m HMPAO studies in migraine patients 1998. 190-4 p.
89. Jimenez-Hoyuela JM, Amrani-Raissouni T, Gallardo-Tur A, Moya-Espinosa F, Padilla-Parrado F. Impact of 99mTc-HMPAO brain perfusion scan in the diagnosis of hemiplegic migraine. *Clinical nuclear medicine*. 2013;38(2):e103-5.
90. Lee SH, Choi CW, Kim JH, Rhee CH, Lim SM. Increased uptake of 99mTc-HMPAO in necrotic brain tumors. *Journal of Korean medical science*. 1998;13(5):529-32.
91. Ding HJ, Huang YF, Tzeng CC, Wei LM, Yeh SJ. Synthesis of Tc-D,D-HMPAO and Tc-L,L-HMPAO and their comparison of chemical and biological properties. *Bioorganic & medicinal chemistry letters*. 1999;9(22):3199-202.

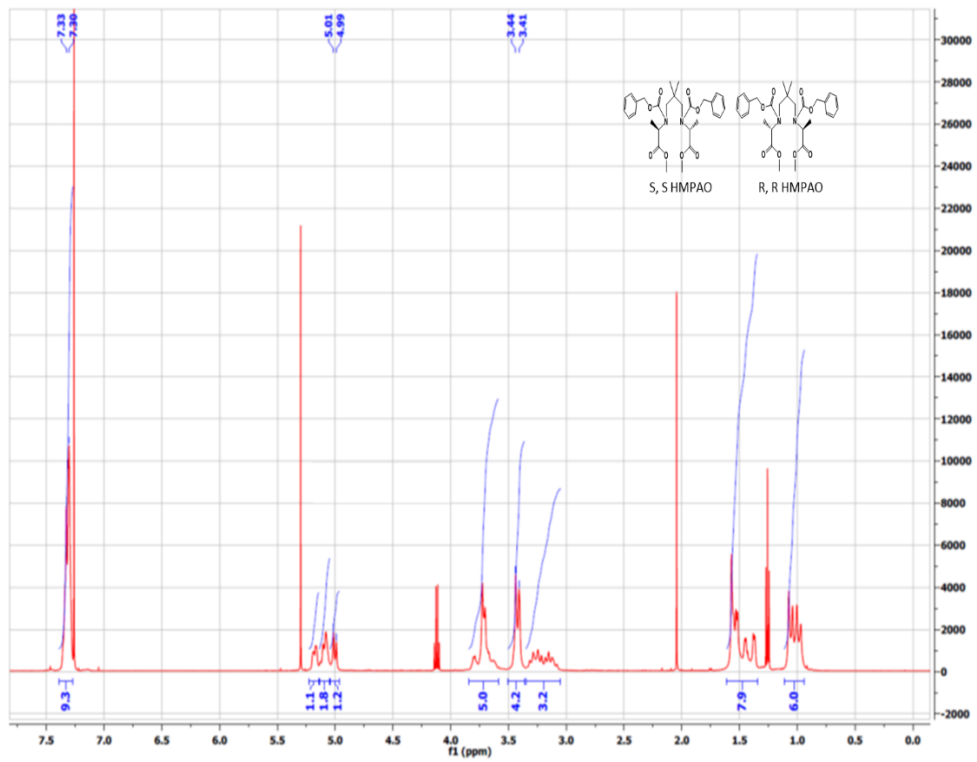
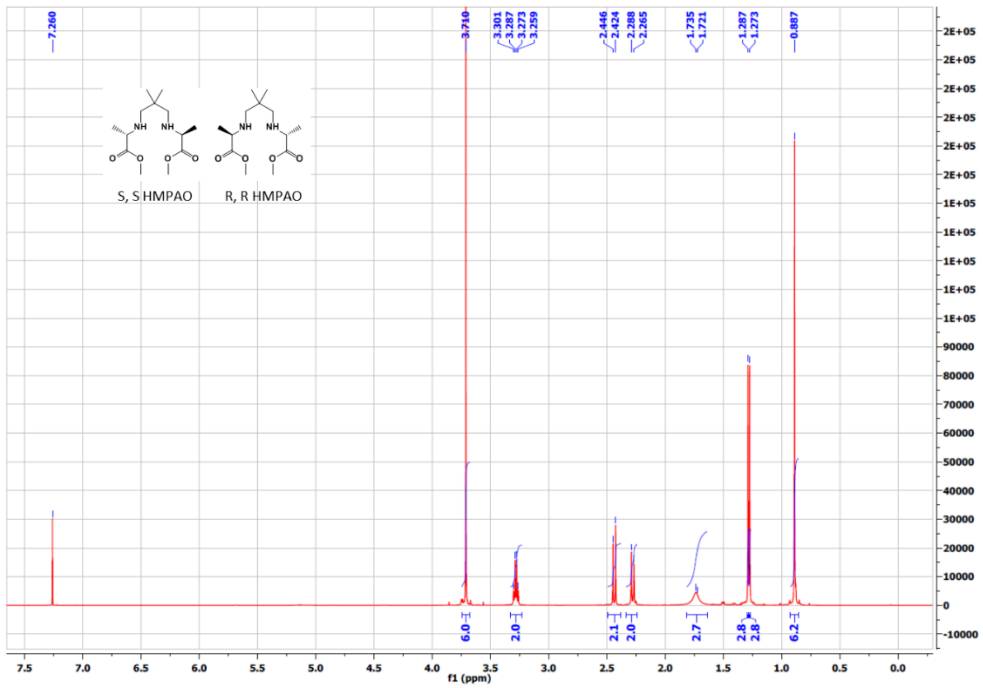
Appendix

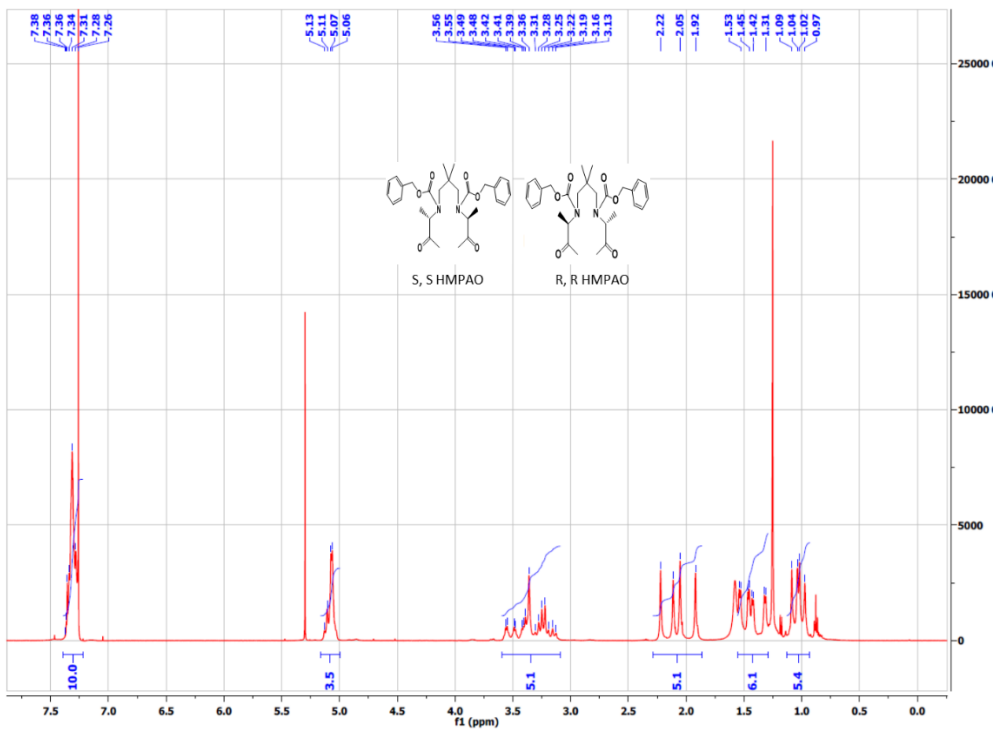
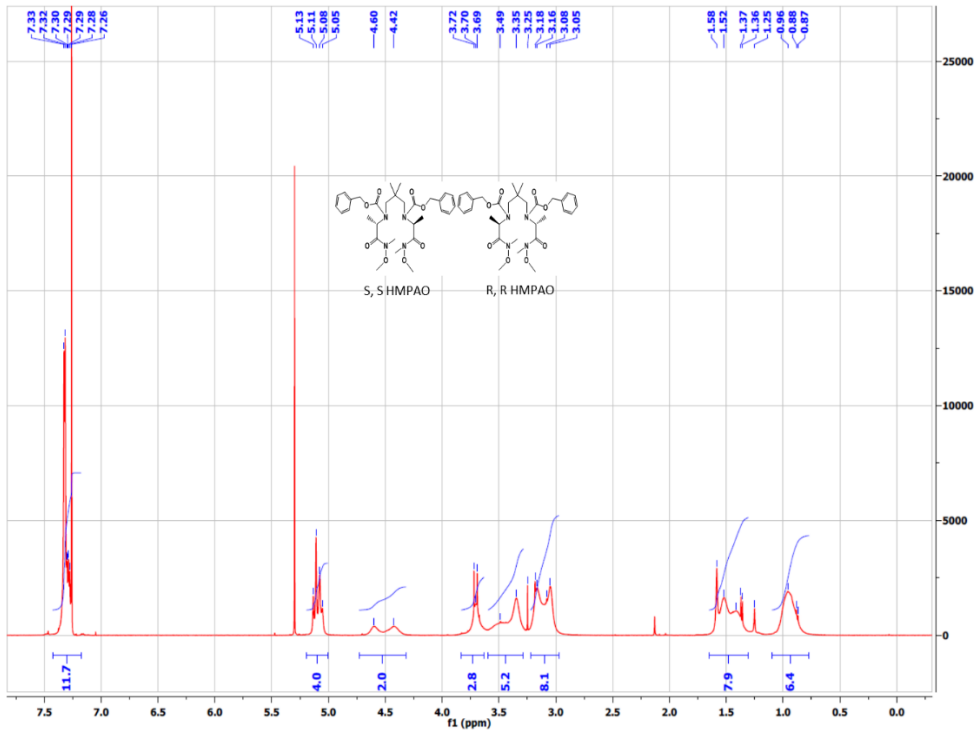
Spectral Analysis Results

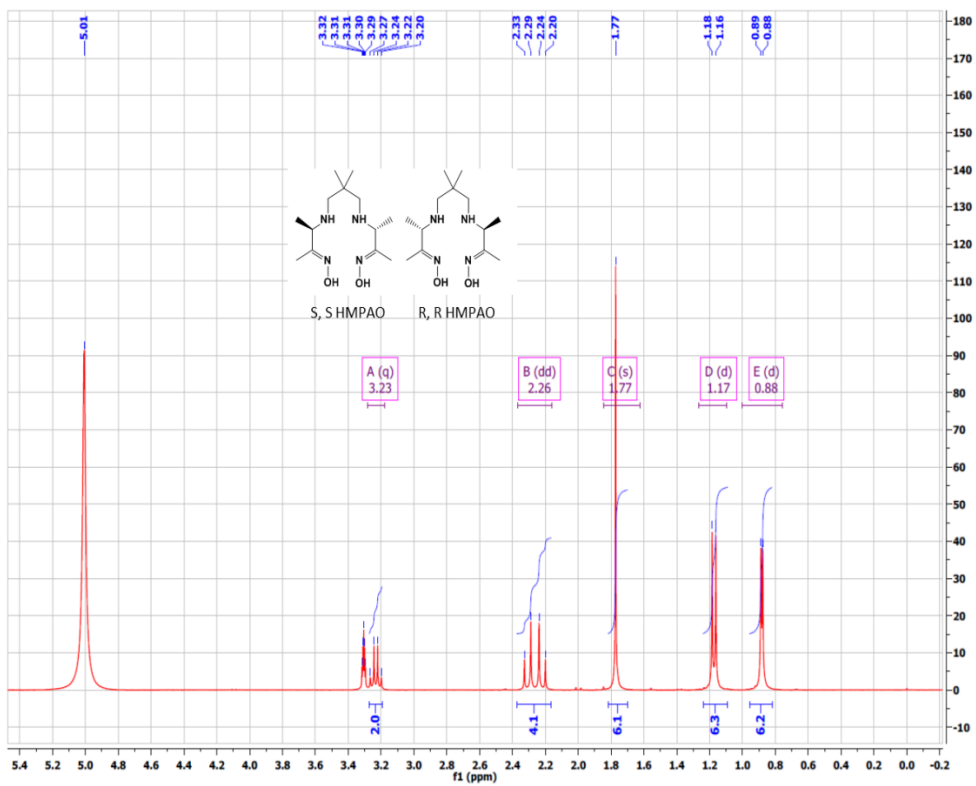
^1H NMR Spectra



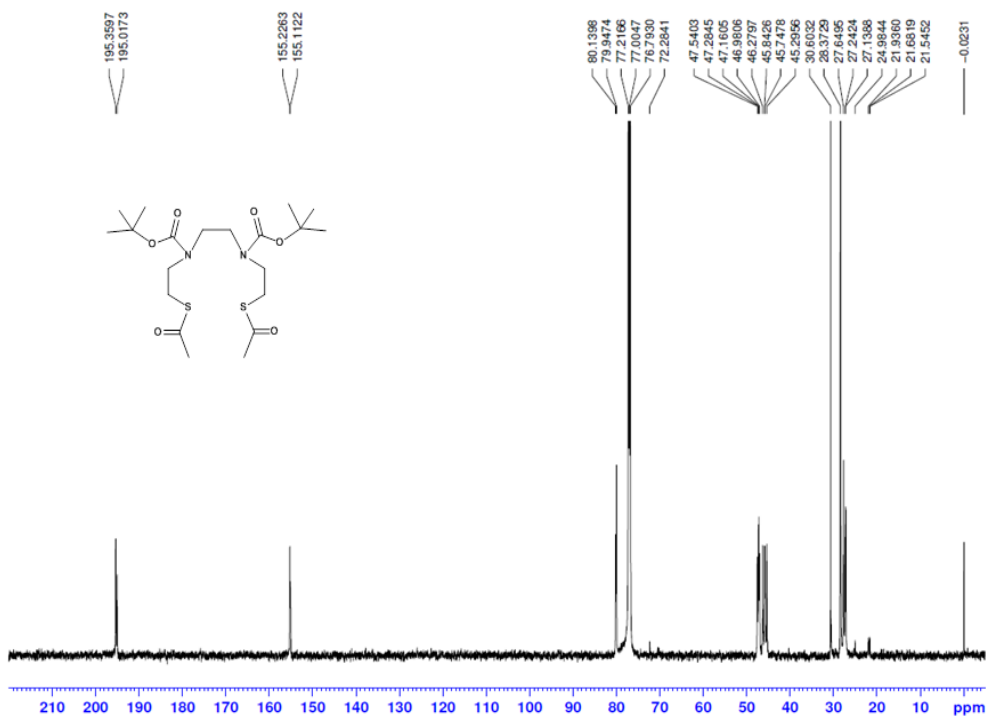
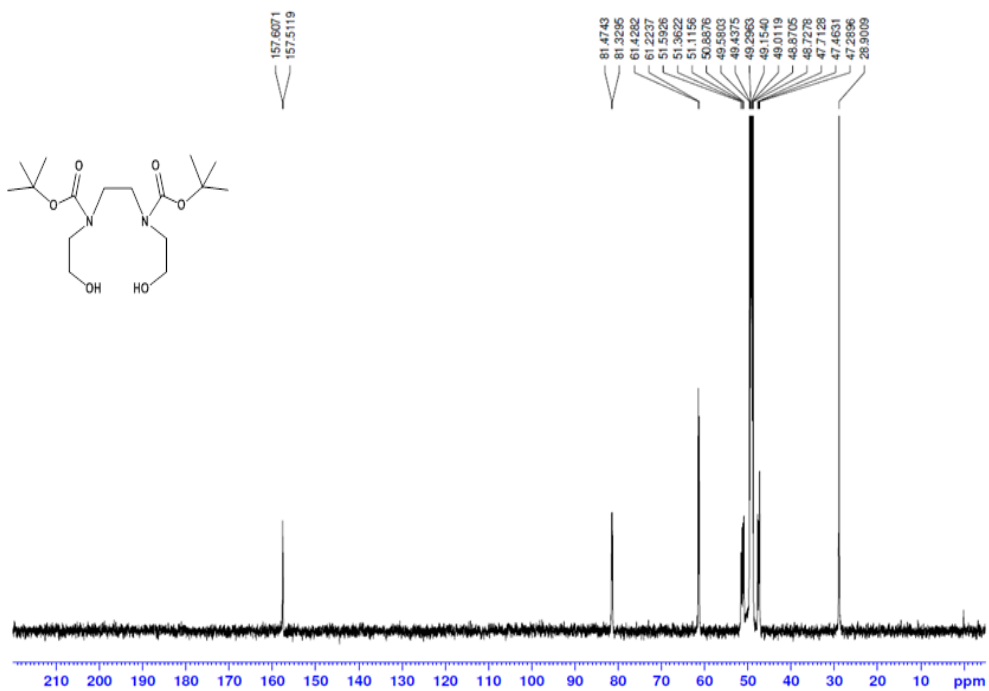


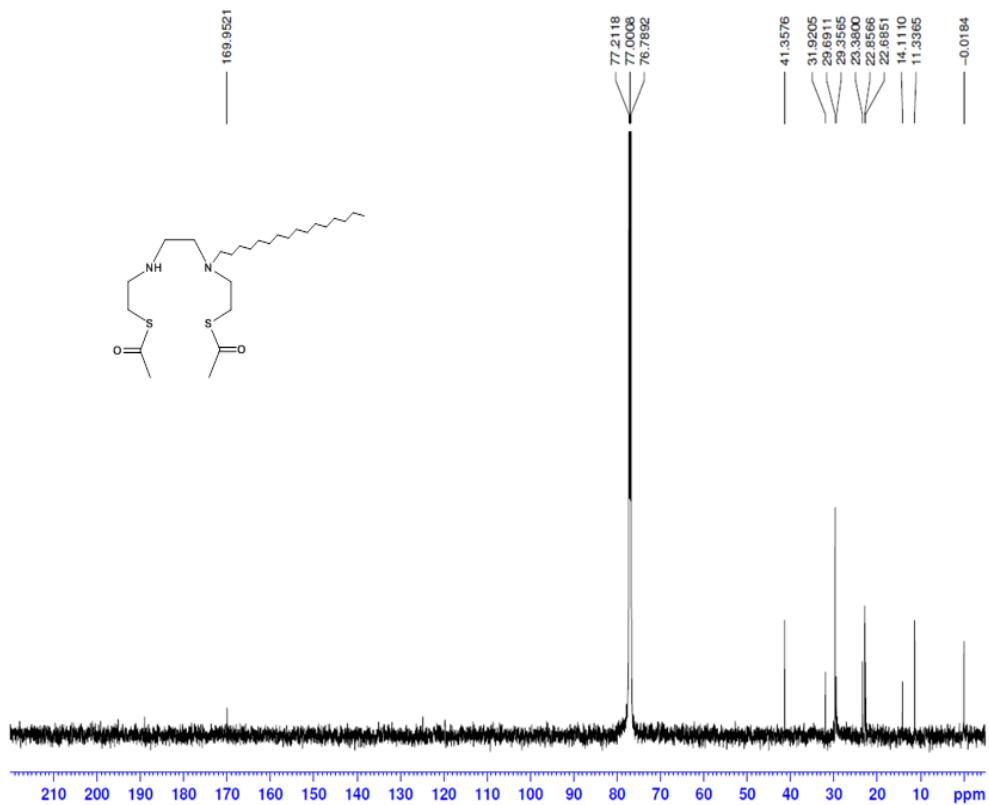




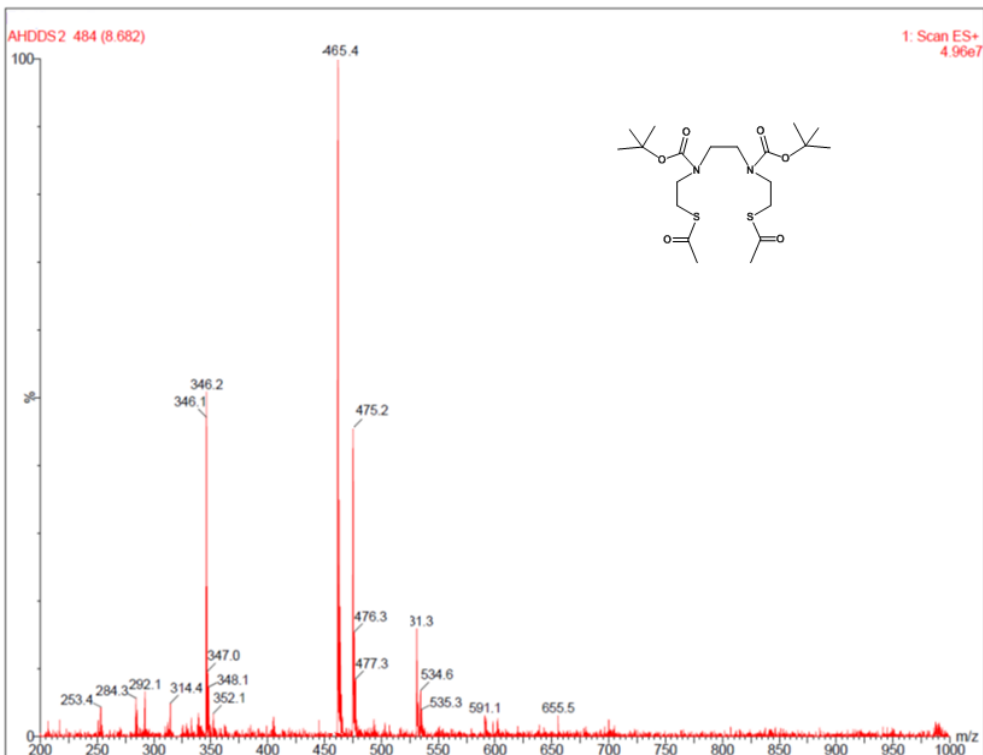
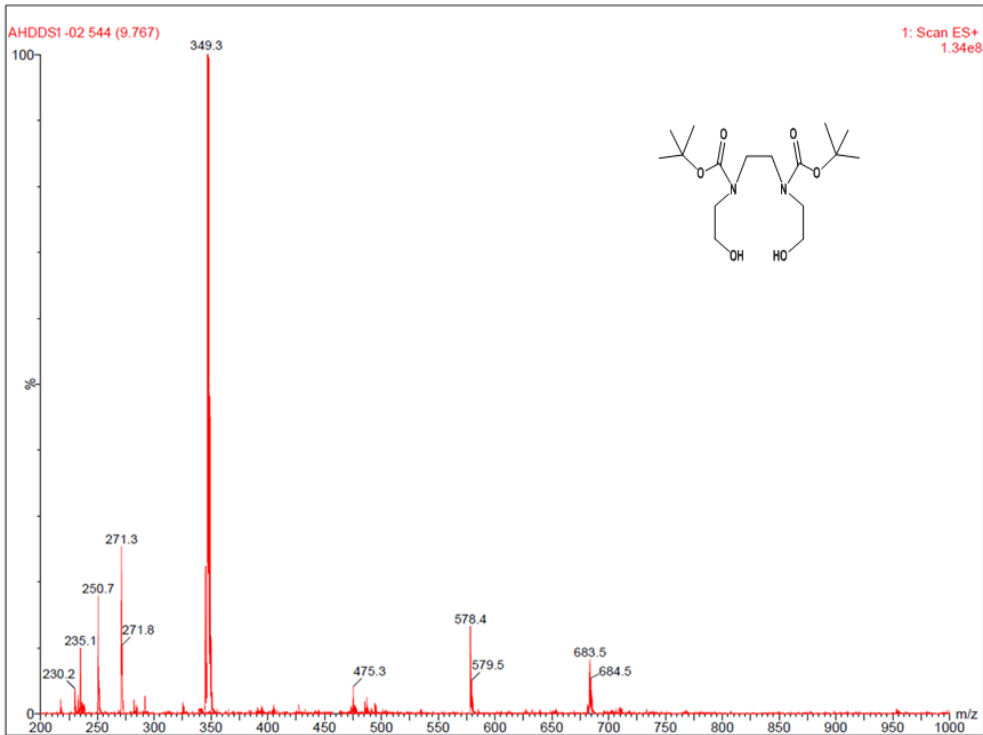


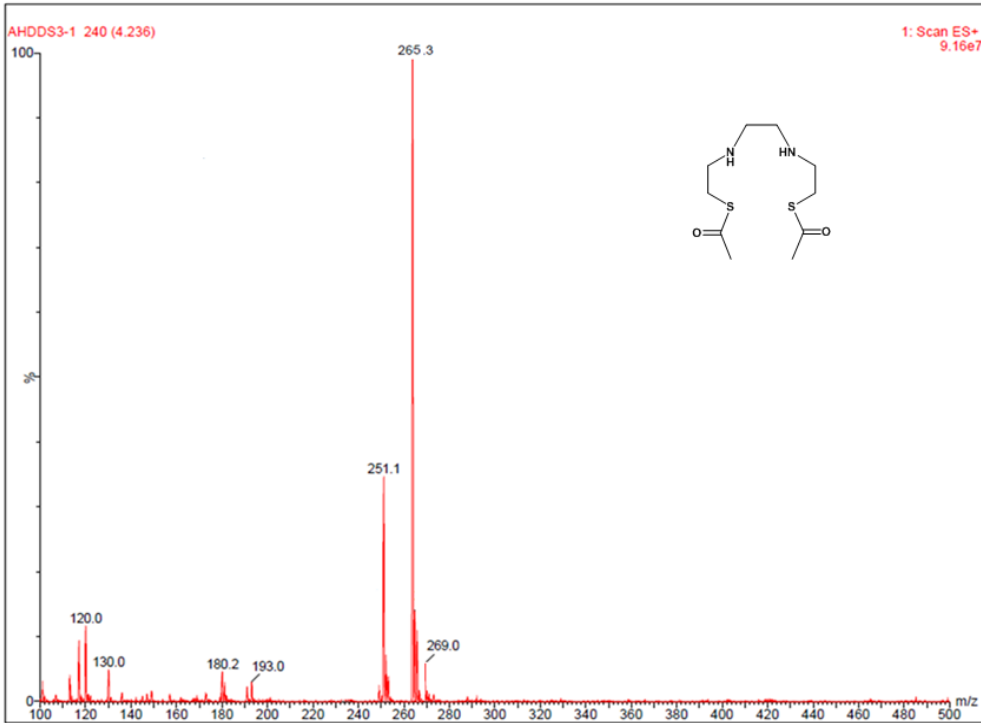
^{13}C NMR Spectra



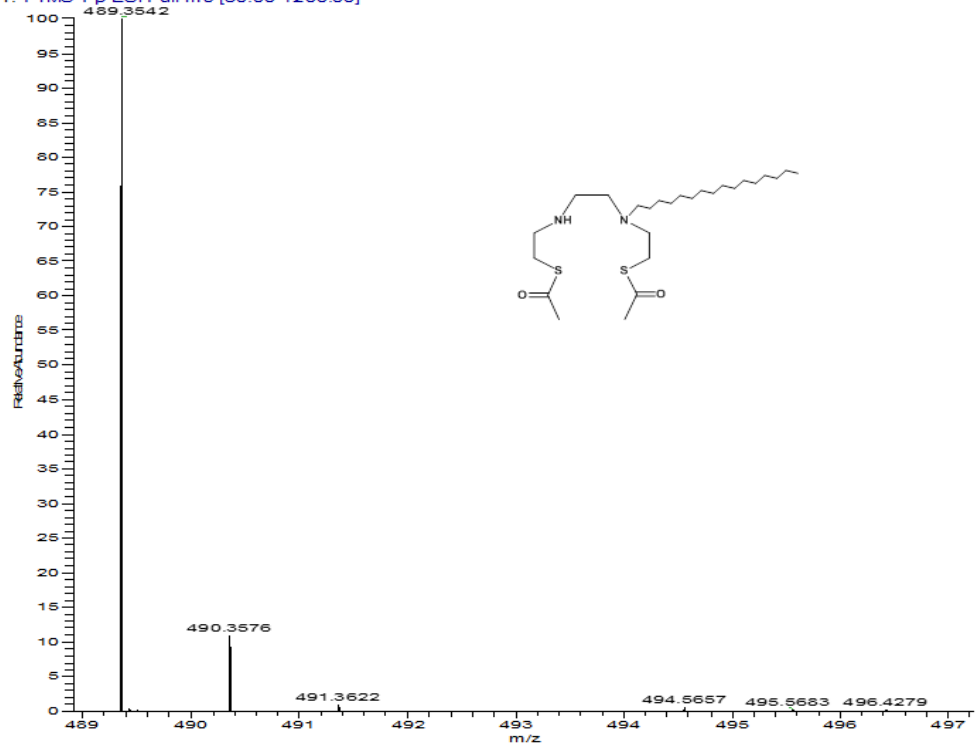


Mass Spectra

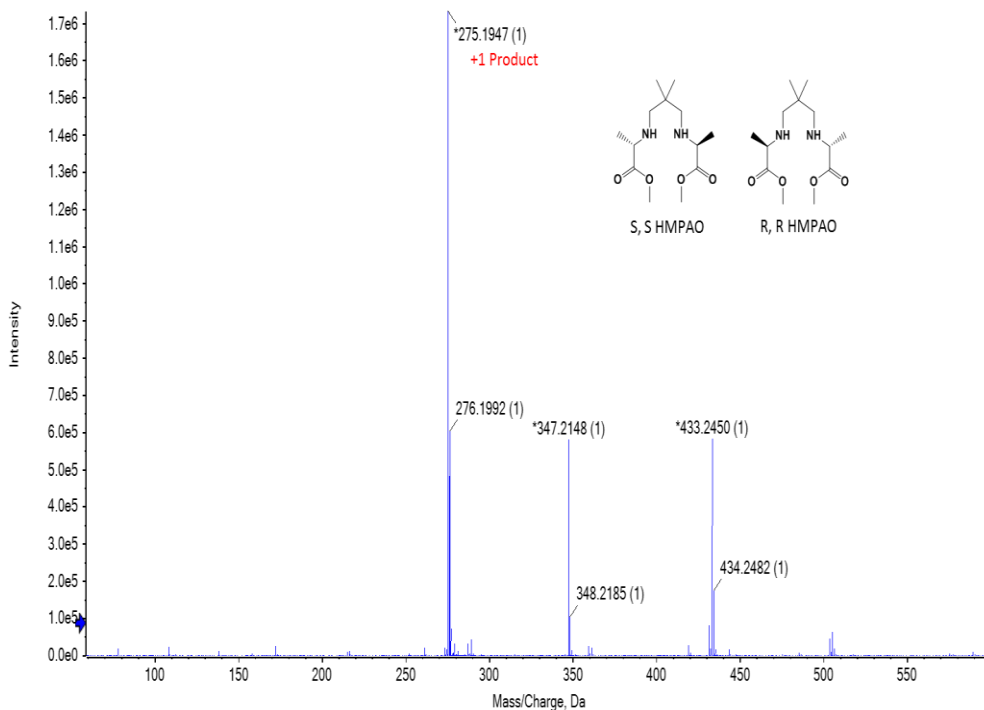




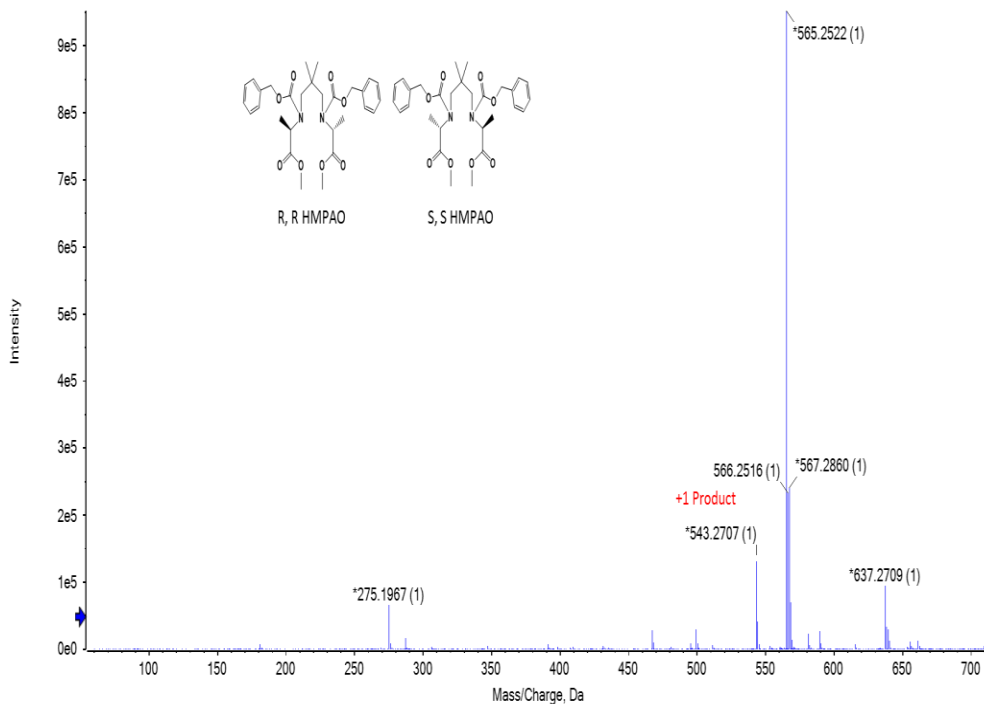
HDD_V_11_140328102404 #200-227 RT: 1.34-1.44 AV: 4 NL: 3.09E8
 T: FTMS + pESI Full ms [80.00-1200.00]



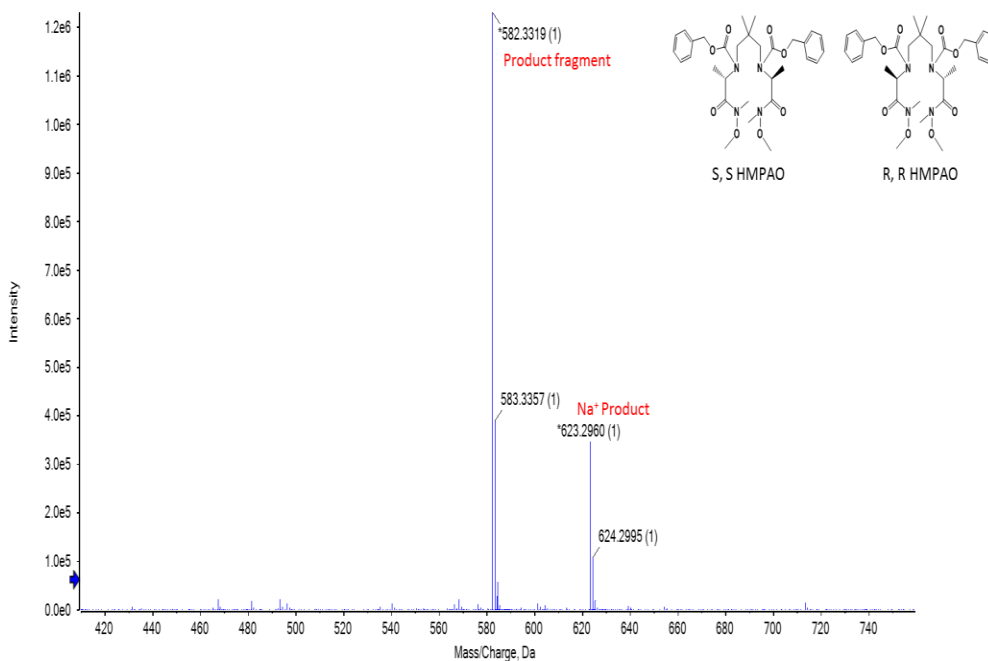
Spectrum from Pat_S1.wiff (sample 1) - Vinary_Pat_S1, Experiment 1, +TOF MS (50 - 2000) from 0.247 to 0.408 min



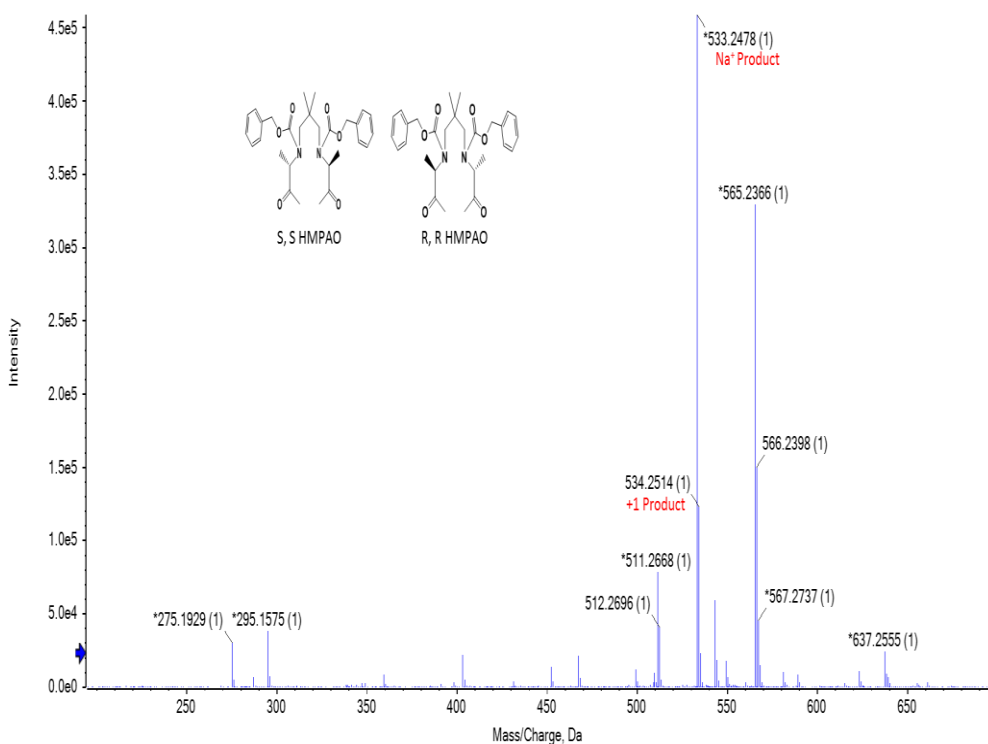
Spectrum from Pat_S2.wiff (sample 1) - Vinary_Pat_S2, Experiment 1, +TOF MS (50 - 2000) from 0.236 to 0.281 min



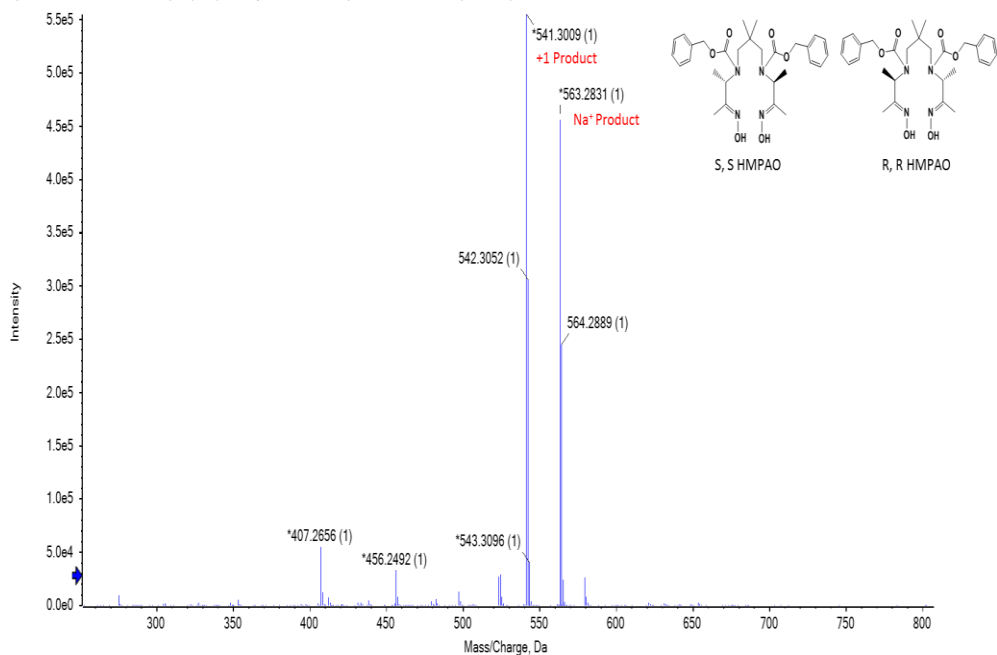
Spectrum from Pat_S3.wiff (sample 1) - Vinary_Pat_S3, Experiment 1, +TOF MS (50 - 2000) from 0.172 to 0.313 min



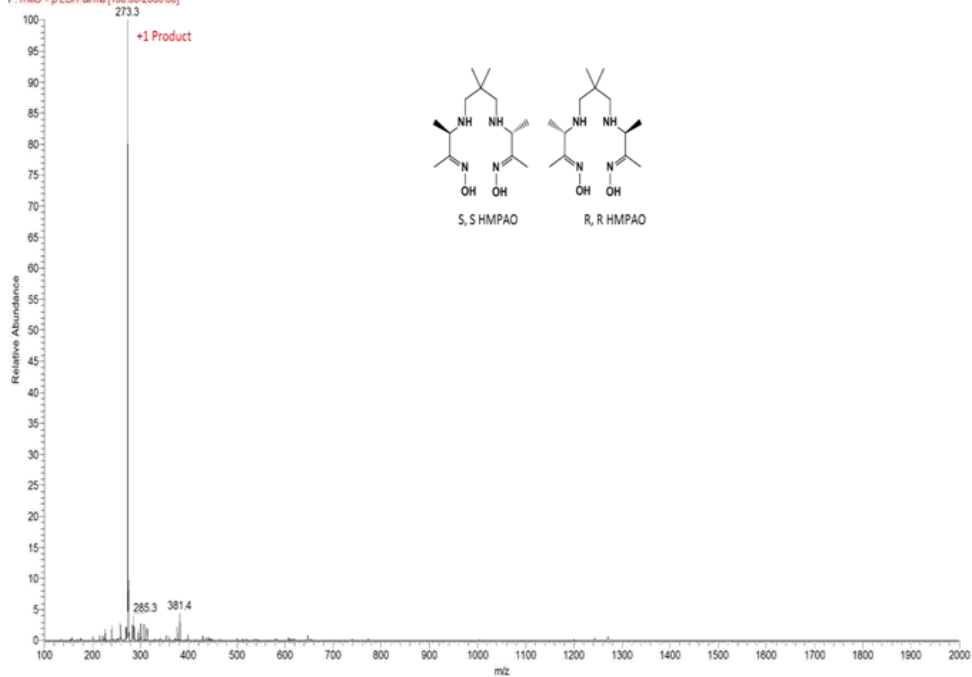
Spectrum from Pat_S4.wiff (sample 1) - Vinary_Pat_S4, Experiment 1, +TOF MS (50 - 2000) from 0.335 to 0.427 min



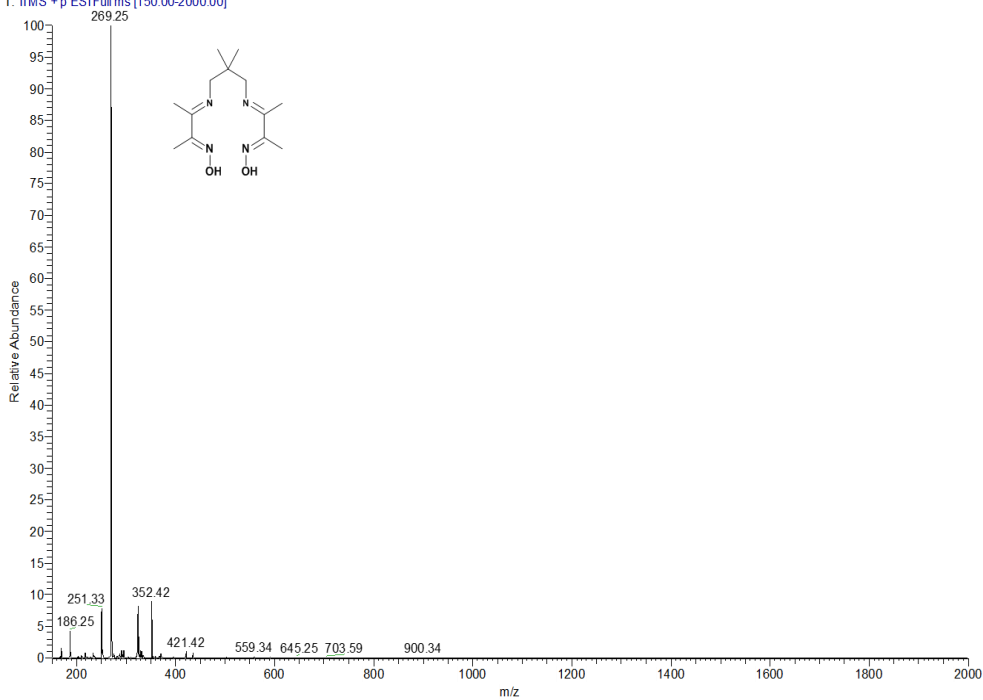
Spectrum from Pat_S5_S_4.wiff (sample 1) - Vinary_Pat_S5_S_4, Experiment 1, +TOF MS (50 - 2000) from 0.233 min



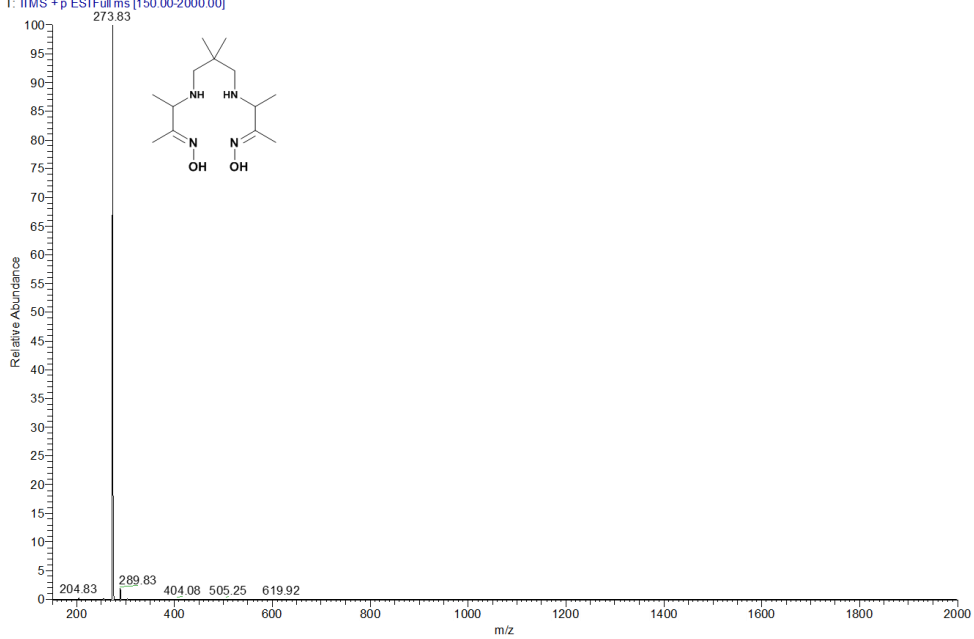
HMPRO_S_Pat_Final#21 RT: 0.24 AV: 1 NL: 6.78E5
F: (TMS + p ESI) Fullms [100.00-2000.00]



170629 Meso HMPAO S1 #91 RT: 0.28 AV: 1 NL: 3.46E5
T: ITMS + p ESI Full ms [150.00-2000.00]



170807 HMPAO Meso crystal #246 RT: 0.79 AV: 1 NL: 9.10E3
T: ITMS + p ESI Full ms [150.00-2000.00]



국 문 초 록

망간족 방사성 핵종의 친유성착체 연구

반카 비나이 쿠마르

서울대학교 의과대학원

핵의학과

테크네슘(technetium, Tc)과 레늄(rhenium, Re)은 주기율표상에서 7B 족의 전이금속에 속한다. 두 원소는 유사한 화학적성질로 인하여 리간드와 배위결합으로 결합하여 유사한 화학적 구조를 갖는 착화합물을 형성한다. 방사성핵종 테크네슘-99m 은 진단용으로 사용되며, 반면에 레늄-188 은 핵의학분야에서 진단과 치료를 동시에 하는 테라노스틱스로 사용된다. 게다가 두 방사성핵종은 높은 비방사능으로 발생기에서 쉽게 생산이 가능하다.

간암 치료용 방사성의약품인 레늄-188-4-헥사데실-2,2,9,9-테트라메틸-4,7-디아자-1,10-데칸디올 (HTDD)/리피오돌 용액제제가 성공적으로 개발되었지만, 레늄-188 을 표지하기 위한 친유성착체인 AHTDD 의 제조를 위해서는 다단계 합성과정이 필요하였다. 나는 본

연구에서 HTDD 에서 양쪽에 썸 디메틸 그룹이 없는 4-헥사데실-4,7-디아자-1,10-데칸디티오아세테이트 (AHDD)를 개발하고 AHDD 와 AHTDD 를 키트화하려고 하였다. 아세틸기가 도입된 AHDD or AHTDD 는 공기중에서 안정할 뿐만 아니라 표지 단계에서 티올에스터 결합이 쉽게 끊어져 레늄-188-HDD or 레늄-188-AHDD 를 형성한다. AHDD 는 AHTDD 보다 합성과정의 적으면서도 더 높은 표지 효율과 개선된 생체분포를 보일 수 있을 것이라 기대하였다. AHDD 의 레늄-188 표지 효율은 $98.8 \pm 0.2\%$ 로 매우 높았으며, 리피오돌로 추출한 후에도 레늄-188-HDD/리피오돌의 전체 수율이 $90.2 \pm 2.6\%$ 로 레늄-188-HTDD/리피오돌보다 높았다 ($p < 0.01$). 레늄-188-HDD 와 레늄-188-HTDD 의 생체 분포 비교 실험은 정상쥐에 약품을 정맥주사하여 수행하였다. 결과는 리피오돌의 색전효과로 인해 폐에서 방사능 섭취가 가장 높게 나타났으며, 폐의 섭취량은 레늄-188-HDD/리피오돌이 레늄-188-HTDD/리피오돌보다 높게 나타났다 ($p < 0.05$). 결론적으로 본 연구에서 새롭게 개발된 레늄-188-HDD/리피오돌은 기존의 간암 치료용 방사성의약품인 레늄-188-HTDD/리피오돌과 비교하여 보다 향상된 표지 효율이나 생체분포를 보이기 때문에 향후 간암 치료에 더 적합할 수 있다.

테크네튬-99m 엑사메타짐 (Tc-99m HMPAO)은 현재 국소뇌혈류 SPECT 영상을 위한 조영제로 사용되고 있다. HMPAO 는 d,l 및 meso 형태의

부분입체 이성질체 형태로 존재하는데, 부분입체 이성질체에 따라 생체 내에서 다른 뇌 섭취를 보였다. 후속 연구들은 각각의 d- 및 l- 광학이성질체로부터 만들어진 테크네튬-99m 복합체 또한 서로 다른 뇌 섭취를 보인다는 것을 밝혀냈다. 이러한 광학이성질체의 분리는 주로 분별 결정을 이용하지만, 합성 수율이 낮거나 시간이 많이 걸려 분리하기 힘들다는 단점이 있다. 더욱이, 분리된 최종 화합물에 여전히 meso 형태의 HMPAO 가 섞여 있을 가능성이 있다. 따라서, 나는 각각의 광학이성질체인 R,R-HMPAO 와 S,S-HMPAO 를 여섯 단계를 통해 효율적으로 합성할 수 있는 방법을 개발하였다. 우선, 친핵 치환 반응을 통해 디메틸프로판-1,3-디아민을 **1a** (S 형태) 또는 **1b** (R 형태)의 메틸-2-클로로프로피오에이트와 반응하여 **2a** (R,R-이성질체)와 **2b** (S,S-이성질체)를 만들었다. 그 후, **2a** 와 **2b** 의 아민기를 벤질 클로로포르메이트 (cbz)로 보호하였고 순차대로 와인랩 아마이드 형성하고 그리냐르시약을 이용하여 메틸레이션을 하였으며 그 후 케톤과 반응하여 옥심을 만들었다. 최종적으로 Cbz 기를 제거함으로써 원하는 S,S-HMPAO (**7a**)와 R,R-HMPAO (**7b**)를 높은 수율과 순도로 합성할 수 있었다. 이 방법으로는 최종 화합물에 meso 형태나 다른 입체 이성질체가 섞일 수 없으므로 원하는 형태의 HMPAO 만 얻을 수 있다. 테크네튬-99m 표지를 위한 키트에는 10 μ g 의 주석 이수화물을 환원제로 사용하였을 때 표지 효율이 90%로

가장 높았다. 이는 시중에 판매되고 있는 Tc-99m HMPAO 와도 표지 효율이 크게 차이 나지 않았다.

주요어 (key words):

방사성핵종, 진단과 치료, 발생기, ^{188}Re , 레늄, 간암, 리피오돌, N_2S_2 , AHDD, HDD, HTDD, 테크네튬-99m 엑사메타짐 (Tc-99m HMPAO), $^{99\text{m}}\text{Tc-d,l-HMPAO}$, 뇌 SPECT, R, R-HMPAO, S, S-HMPAO, meso-HMPAO

학번 (student number): 2012-31334